

**REGULATION OF GAG TRAFFICKING DURING RETROVIRUS ASSEMBLY AND  
BUDDING**

by

Jing Jin

B.S., Nankai University, 1997

M.S., Shanghai Institute of Biochemistry, Chinese Academy of Sciences, 2000

Submitted to the Graduate Faculty of  
Graduate School of Public Health in partial fulfillment  
of the requirements for the degree of  
Doctor of Philosophy

University of Pittsburgh

2007

UNIVERSITY OF PITTSBURGH

Graduate School of Public Health

This dissertation was presented

by

Jing Jin

It was defended on

September 21, 2007

and approved by

Ora A. Weisz, PhD, Associate Professor, Department of Medicine,  
School of Medicine, University of Pittsburgh

Linton M. Traub, PhD, Associate Professor, Department of Cell Biology and Physiology  
School of Medicine, University of Pittsburgh

Simon Barratt Boyes, PhD, Associate Professor, Department of Infectious Disease and  
Microbiology, Graduate School of Public Health, University of Pittsburgh

Tianyi Wang, PhD, Assistant Professor, Department of Infectious Disease and Microbiology,  
Graduate School of Public Health, University of Pittsburgh

**Dissertation Advisor:** Ronald C. Montelaro, PhD, Professor, Department of Molecular  
Genetics and Biochemistry, School of Medicine, University of Pittsburgh

Copyright © by Jing Jin

2007

**REGULATION OF GAG TRAFFICKING DURING RETROVIRUS ASSEMBLY AND  
BUDDING**

Jing Jin, PhD

University of Pittsburgh, 2007

Retroviral Gag polyproteins are necessary and sufficient for virus budding, but little is known about how thousands of Gag polyproteins are transported to the budding sites. The actin cytoskeleton has long been speculated to take a role in retrovirus assembly and recent studies suggest that HIV-1 assembly is regulated as early as viral RNA nuclear export, however specific mechanisms for these regulations are unknown. In contrast to numerous studies of HIV-1 Gag assembly and budding, relatively little is reported for these fundamental pathways among animal lentiviruses. In this project, we used bimolecular fluorescence complementation (BiFC) (1) to reveal intimate (<15nm) and specific associations between EIAV Gag and actin, but not tubulin; (2) to characterize and compare assembly sites and budding efficiencies of EIAV and HIV-1 Gag in both human and rodent cells when the mRNA nuclear export context is altered to be Rev-dependent or Rev-independent; (3) to reveal co-assembly of Rev-dependent and Rev-independent HIV-1 Gag and rescued assembly of Rev-independent HIV-1 Gag in human cells by *in cis* provided membrane targeting signals. The results of these studies showed that (1) multimerization of EIAV Gag was required for association with filamentous actin and this association correlated with Gag budding efficiency, suggesting that association of Gag multimers with filamentous actin is important for efficient virion production; (2) HIV-1 and EIAV Gag assembled in different cellular sites, and HIV-1 but not EIAV Gag assembly was affected by

mRNA nuclear export pathways, suggesting that alternative cellular pathways can be adapted for lentiviral Gag assembly and budding; (3) Rev-independent HIV-1 Gag was deficient in lipid raft targeting and its assembly and budding could be restored by membrane targeting signals provided *in trans* or *in cis*, suggesting that raft association is critical for HIV-1 assembly and budding and is regulated as early as nuclear export of Gag-encoding mRNA. The findings presented in these studies are significant for public health because a better understanding of the mechanism of retrovirus assembly and budding increase the potential to develop novel antiviral therapies targeting this critical step in the viral life cycle.

## TABLE OF CONTENTS

<b>PREFACE.....</b>	<b>xiv</b>
<b>1.0 INTRODUCTION.....</b>	<b>1</b>
<b>1.1 RETROVIRUSES ASSEMBLY AND BUDDING .....</b>	<b>1</b>
<b>1.1.1 General Properties of retroviruses.....</b>	<b>1</b>
<b>1.1.2 Retrovirus life cycle .....</b>	<b>4</b>
<b>1.1.3 Retrovirus assembly and budding.....</b>	<b>6</b>
<b>1.1.4 Role of Gag domains in retrovirus assembly and budding.....</b>	<b>8</b>
<b>1.1.4.1 Matrix.....</b>	<b>8</b>
<b>1.1.4.2 Capsid.....</b>	<b>10</b>
<b>1.1.4.3 Nucleocapsid .....</b>	<b>10</b>
<b>1.1.4.4 Spacer peptides.....</b>	<b>11</b>
<b>1.1.4.5 Late domains.....</b>	<b>12</b>
<b>1.1.5 Cellular factors involved in retrovirus assembly and budding .....</b>	<b>13</b>
<b>1.1.5.1 Vps proteins and retrovirus budding .....</b>	<b>13</b>
<b>1.1.5.2 Intracellular Gag trafficking during retrovirus assembly and budding</b>	<b>16</b>
<b>1.1.5.3 Endosomal trafficking and retrovirus assembly and budding .....</b>	<b>19</b>
<b>1.1.5.4 Cytoskeleton and retrovirus assembly and budding.....</b>	<b>21</b>

1.1.5.5	Connections between retroviral genomic RNA nuclear export and virion assembly.....	22
1.1.5.6	Lipid rafts on plasma membrane provide the platform for HIV assembly.....	25
1.1.5.7	Cellular factors power the energy-dependent retrovirus assembly and budding process.....	26
1.2	VISUALIZATION OF PROTEIN INTERACTIONS BY BIMOLECULAR FLUORESCENCE COMPLEMENTATION.....	26
2.0	HYPOTHESIS AND SPECIFIC AIMS.....	31
3.0	CHAPTER ONE. ASSOCIATION OF GAG MULTIMERS WITH FILAMENTOUS ACTIN DURING EQUINE INFECTIOUS ANEMIA VIRUS ASSEMBLY.....	32
3.1	PREFACE.....	32
3.2	ABSTRACT.....	33
3.3	INTRODUCTION.....	34
3.4	MATERIALS AND METHODS.....	37
3.4.1	DNA mutagenesis.....	37
3.4.2	Cell culture and transfection.....	37
3.4.3	Fluorescence microscopy.....	38
3.4.4	Flow cytometry analysis.....	38
3.4.5	Cell fractionation and immunoprecipitation.....	39
3.4.6	EIAV Gag protein expression assays.....	40
3.4.7	Immuno-gold labeling of EIAV Gag proteins and SEM.....	40

<b>3.5</b>	<b>RESULTS .....</b>	<b>41</b>
3.5.1	Intracellular association of EIAV Gag with actin .....	41
3.5.2	EIAV Gag proteins coimmunoprecipitate with filamentous actin.....	43
3.5.3	Gag domain requirements for F-actin association .....	46
3.5.4	Immuno SEM of Gag-actin association .....	49
<b>3.6</b>	<b>DISCUSSION.....</b>	<b>58</b>
3.6.1	Specificity of Gag-actin interactions .....	58
3.6.2	Gag multimerization before F-actin association.....	60
3.6.3	Roles of Gag-actin interaction.....	61
<b>4.0</b>	<b>CHAPTER TWO. DISTINCT INTRACELLULAR TRAFFICKING OF EIAV AND HIV-1 GAG DURING VIRAL ASSEMBLY AND BUDDING REVEALED BY BIMOLECULAR FLUORESCENCE COMPLEMENTATION ASSAYS .....</b>	<b>63</b>
<b>4.1</b>	<b>PREFACE .....</b>	<b>63</b>
<b>4.2</b>	<b>ABSTRACT.....</b>	<b>64</b>
<b>4.3</b>	<b>INTRODUCTION .....</b>	<b>65</b>
<b>4.4</b>	<b>MATERIALS AND METHODS .....</b>	<b>69</b>
4.4.1	DNA mutagenesis.....	69
4.4.2	Cell culture and transfection .....	69
4.4.3	Gag protein expression assays .....	70
4.4.4	Confocal microscopy .....	70
4.4.5	Flow cytometry analysis.....	70
<b>4.5</b>	<b>RESULTS .....</b>	<b>72</b>

4.5.1	Expression of Rev-dependent and Rev-independent EIAV and HIV-1 Gag-BiFC constructs .....	72
4.5.2	Demonstration of EIAV Gag assembly by BiFC assay .....	73
4.5.3	Comparison of Rev-dependent and Rev-independent EIAV and HIV-1 Gag assembly .....	74
4.5.4	Comparison of Rev-dependent and Rev-independent EIAV and HIV-1 Gag budding .....	77
4.6	DISCUSSION.....	86
4.6.1	EIAV and HIV-1 Gag use distinct trafficking routes during viral assembly/budding.....	86
4.6.2	mRNA nuclear export pathways influence Gag assembly and budding sites	89
5.0	CHAPTER THREE. LIPID RAFT ASSOCIATION OF HIV-1 GAG IS REGULATED BY THE TRAFFICKING OF GAG-ENCODING MRNA .....	92
5.1	PREFACE .....	92
5.2	ABSTRACT.....	93
5.3	INTRODUCTION .....	94
5.4	MATERIALS AND METHODS.....	97
5.4.1	DNA mutagenesis.....	97
5.4.2	Cell culture and transfection .....	97
5.4.3	Gag budding assays .....	98
5.4.4	Confocal microscopy .....	98
5.4.5	Flow cytometry analysis.....	98

5.4.6	Membrane flotation analysis .....	99
5.4.7	Immunoprecipitation.....	100
5.5	<b>RESULTS.....</b>	<b>101</b>
5.5.1	<b>Distinct Intracellular Distribution of Rev-dependent and Rev-independent HIV-1 Gag.....</b>	<b>101</b>
5.5.2	<b>Co-assembly of Rev-dependent and Rev-independent HIV-1 Gag Rescues Budding of Rev-independent HIV-1 Gag.....</b>	<b>103</b>
5.5.3	<b>Substitution of the Membrane Binding Domain Rescues Rev-independent HIV-1 Gag Assembly and Budding .....</b>	<b>106</b>
5.5.4	<b>mRNA Nuclear Export Pathway Regulates HIV-1 Gag Targeting to Lipid Raft</b>	<b>109</b>
5.6	<b>DISCUSSION.....</b>	<b>120</b>
6.0	<b>OVERALL DISCUSSION AND FUTURE DIRECTIONS.....</b>	<b>126</b>
6.1	<b>SUMMARY OF FINDINGS.....</b>	<b>126</b>
6.2	<b>PUBLIC HEALTH SIGNIFICANCE.....</b>	<b>129</b>
6.3	<b>FUTURE DIRECTION.....</b>	<b>133</b>
6.3.1	<b>Characterize and compare retroviruses assembly and budding in live cells</b>	<b>133</b>
6.3.2	<b>Explore the mechanism by which mRNA nuclear export pathway regulates HIV-1 Gag lipid rafts targeting.....</b>	<b>134</b>
6.3.3	<b>Develop BiFC based antiviral compound screening system .....</b>	<b>135</b>
	<b>BIBLIOGRAPHY .....</b>	<b>137</b>

## LIST OF TABLES

Table 1-1. Classification of Retroviruses.....	2
Table 6-1. Global AIDS epidemic .....	129

## LIST OF FIGURES

Figure 1-1. Organization of HIV-1 genome and viral particle. ....	3
Figure 1-2. Life cycle of HIV-1.....	5
Figure 1-3. Schematic representation of retroviral Gag proteins and location of retroviral L domains.....	7
Figure 1-4. Model showing the interaction network of mammalian Class E proteins and their roles in retrovirus budding.....	14
Figure 1-5. Cytoskeleton in intracellular membrane trafficking.....	18
Figure 1-6. Rev-dependent nuclear export of HIV-1 genomic mRNA.....	23
Figure 1-7. Schematic illustration of bimolecular fluorescence complementation (BiFC).....	28
Figure 3-1. Confocal association of Gag proteins with the actin cytoskeleton in EIAV-infected ED cells.....	50
Figure 3-2. BiFC analysis of Gag-actin interactions.....	51
Figure 3-3. Colocalization of Gag-Gag and Gag-actin BiFC complexes with CD63 positive compartments.....	52
Figure 3-4. Live cell imaging of BiFC complexes.....	53
Figure 3-5. Association of Gag with filamentous actin.....	54
Figure 3-6. Functions of Gag domains in F-actin association.....	55

Figure 3-7. Gag multimers interact with actin. ....	56
Figure 3-8. Immuno-SEM images of Gag complexes associated with actin filaments. ....	57
Figure 4-1. Expression and budding of Rev-dependent and Rev-independent Gag-BiFC constructs in 293T cells. ....	79
Figure 4-2. Demonstration of EIAV Gag assembly by the BiFC assay. ....	80
Figure 4-3. BiFC analysis of EIAV and HIV-1 Gag assembly in human cells. ....	81
Figure 4-4. BiFC analysis of EIAV and HIV-1 Gag assembly in NIH3T3 cells. ....	82
Figure 4-5. Demonstration of BiFC Gag complexes in assembled VLPs. ....	83
Figure 4-6. Comparison budding efficiency of Rev-dependent and Rev-independent EIAV and HIV-1 Gag in human and rodent cells. ....	84
Figure 5-1. Distinct intracellular distribution of Rev-dependent and Rev-independent HIV-1 Gag. ....	112
Figure 5-2. Co-assembly with Rev-dependent HIV-1 Gag rescued Rev-independent HIV-1 Gag budding. ....	114
Figure 5-3. Substitution of HIV-1 matrix with other membrane targeting domains rescued Rev-independent HIV-1 Gag assembly and budding in human cells. ....	116
Figure 5-4. Rev-independent HIV-1 Gag failed to associate with lipid raft in human cells. ....	118

## PREFACE

The work presented here could have never been accomplished without the help, support and encouragement of many people.

First of all, I would like to express my deep gratitude to my advisor, Dr. Ronald Montelaro for his immense patience, understanding, guidance and encouragement during the entire period of the Ph.D. work. I have truly benefited from the scientific freedom and trust that he bestowed on me over the last 3 years, which gave me the opportunity to independently develop and execute ideas. This will surely be invaluable in my development as an independent investigator in the years to come.

Next I would like to thank my co-mentor, Dr. Ora Weisz. She has taught me the attitude to life as well as to science as a female scientist. I appreciate deeply her encouragement and guidance which helped me go through all the frustrations and hard times.

I deeply thank all the members of my committee for providing me with valuable suggestions and guidance over the years. They are Dr. Ora Weisz, Dr. Linton Traub, Dr. Simon Barratt-Boyes and Dr. Tianyi Wang. The successful completion of this Ph.D. work would not have been possible without their support.

Thanks also go to many of my collaborators and outside scientists. Without help of Dr. Simon Watkins and all the members of the CBI, it would have been impossible for me to finish

this Ph.D. work. I am truly grateful to some scientists from other insitutes for their helpful discussion and valuable suggestions to my project. They are Dr. Eric Freed, Dr. Walther Mothes Dr. Volker Vogt and Dr. Eric Hunter.

I want to thank all the members of the RCM lab, especially Timothy Sturgeon for his help with flow cytometry experiments. I would like to specially thank two past lab members, Dr. Chaoping Chen and Dr. Feng Li, for their continuous help and support.

Finally I want to dedicate the work presented here to my mother, Guiqin Jin. Her truly selfless love and continuous moral support has sustained me over these years and made me overcome all difficulties placed in front me.

## 1.0 INTRODUCTION

### 1.1 RETROVIRUSES ASSEMBLY AND BUDDING

#### 1.1.1 General Properties of retroviruses

Retroviruses comprise a large and diverse family of enveloped RNA viruses defined by common taxonomic denominators that include structure, composition, and replicative properties (Coffin et al., 1997). The virions are 80-100 nm in diameter and their outer lipid envelope incorporates and displays the viral glycoproteins. The shape and location of the internal protein core are characteristic for various genera of the family (**Table 1-1**) (Coffin et al., 1997). Retroviral virions encapsulate a virus RNA genome that is linear, single-stranded, nonsegmented RNA. The hallmark of the family is the essential steps in its replication cycle: reverse transcription of the virion RNA into linear double-stranded DNA and the integration of this DNA into host genome.

Retroviruses are broadly divided into two categories – simple and complex – distinguishable by the organization of their genomes (**Table 1-1**) (Coffin et al., 1997). All retroviruses contain three major coding regions: *gag*, which encodes for the virion internal proteins that form the matrix, the capsid and the nucleoprotein structures; *pol*, which directs the synthesis of reverse transcriptase, protease and integrase enzymes; and *env*, which encodes the viral surface transmembrane envelope glycoproteins. Simple retroviruses usually only carry this

elementary information, whereas complex retroviruses code for additional regulatory nonstructural proteins derived from multiple-spliced mRNA. Retroviruses are further subdivided into seven groups defined by evolutionary relatedness (**Table 1-1**). Five of them are oncogenic retroviruses and the other two groups are the lentiviruses and the spumaviruses. Except the human T-cell leukemia virus-bovine leukemia virus (HTLV-BLV), all the oncogenic retroviruses are simple retroviruses. HTLV-BLV, lentiviruses and spumaviruses are complex retroviruses. A representative example for lentivirus is human immunodeficiency virus (HIV), the causative agent of acquired immunodeficiency syndrome (AIDS). Its genome structure and virion organization are shown in **Fig. 1-1**. The first described retroviral disease, equine infectious anemia (Vallee and Carre, 1904), is caused by equine infectious anemia virus (EIAV) that is the simplest member in lentivirus genus.

**Table 1-1. Classification of Retroviruses**

<b>Genus</b>	<b>Example</b>	<b>Virion morphology</b>	<b>Genome</b>
<b>1. Alpharetrovirus</b>	<b>Rous sarcoma virus Avian leucosis virus</b>	<b>Central, spherical core “C particles”</b>	<b>Simple</b>
<b>2. Betaretroviurs</b>	<b>Mouse mammary tumor virus</b>	<b>Eccentric, spherical core “B particles”</b>	<b>Simple</b>
<b>3. Gammaretrovirus</b>	<b>Moloney murine leukemia virus</b>	<b>Central, spherical core “C particles”</b>	<b>Simple</b>
<b>4. Deltaretrovirus</b>	<b>Human T-cell leukemia virus</b>	<b>Central, spherical core</b>	<b>Complex</b>
<b>5. Epsilonretrovirus</b>	<b>Mason-Pfizer monkey virus</b>	<b>Cylindrical core “D particles”</b>	<b>Simple</b>
<b>6. Lentivirus</b>	<b>Human immunodeficiency virus</b>	<b>Cone-shaped core</b>	<b>Complex</b>
<b>7. Spumavirus</b>	<b>Human foamy virus</b>	<b>Central, spherical core</b>	<b>Complex</b>

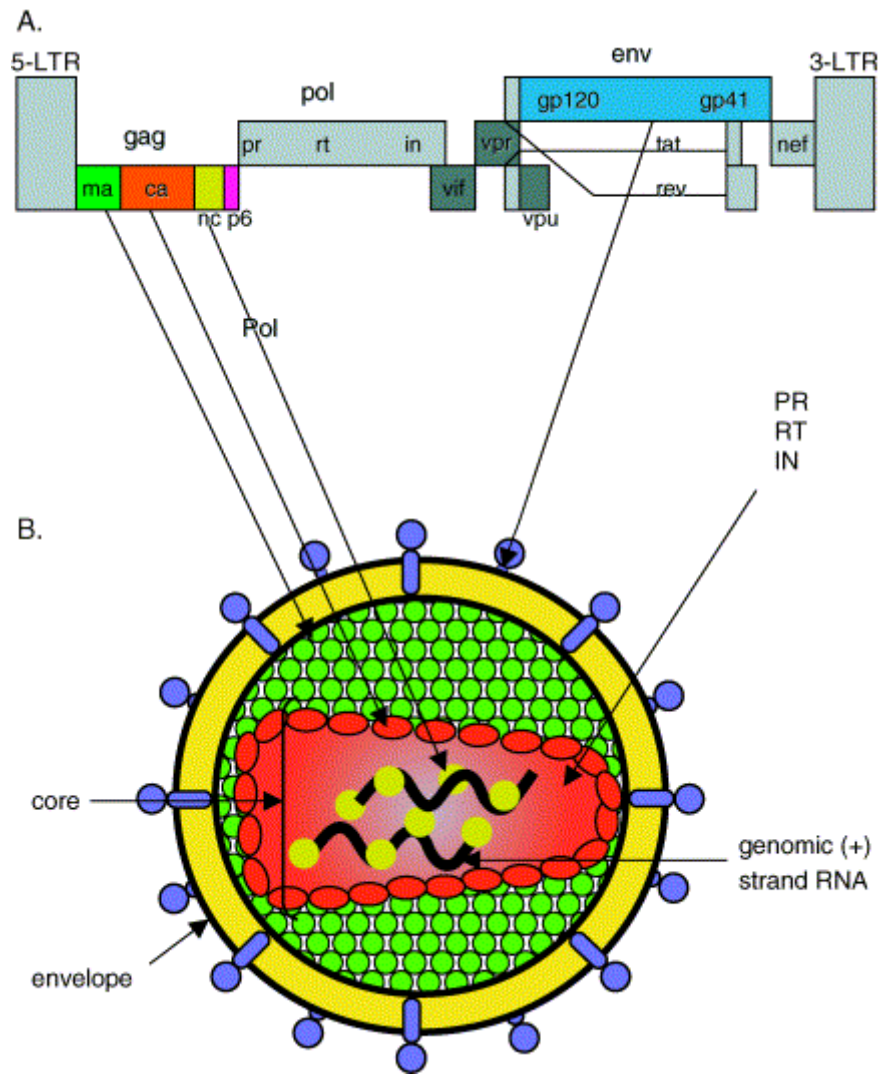


**Figure 1-1. Organization of HIV-1 genome and viral particle.**

(A) Organization of the HIV-1 proviral genome. (B) Organization of the HIV-1 mature viral particle. Reprinted with permission from Suzanne Scarlata and Carol Carter, Role of HIV-1 Gag domains in viral assembly. 2003. *Biochimica et Biophysica Acta*, 1614:62-72. Copyright 2003, Elsevier B.V.

### 1.1.2 Retrovirus life cycle

Taking HIV-1 as the example, retrovirus life cycle is shown in **Fig. 1-2**. Viruses first attach to the receptors on cell surface (step 1), then enter the host cell upon fusion between viral membrane and cell membrane (step 2). After disassembly of virus core (step 3), viral RNA is reverse transcribed into double-stranded proviral DNA that is associated with a pre-integration complex (PIC) (step 4). The PIC enters the host nucleus (step 5), leading to integration of proviral DNA into host genome (step 6). Post transcription, both spliced and unspliced viral RNA are exported from nucleus (step 7). Gag and Gag-Pol polyproteins are synthesized from unspliced viral RNA in cytosol (step 8), while Env glycoproteins are synthesized from spliced viral RNA and follow the secretory protein synthesis pathway (step 9). These newly synthesized viral structural proteins then traffic to the plasma membrane where they assemble (step 10) and bud from the host cell (step 11). Upon virus budding, viral protease mediated Gag processing leads to virus maturation (step 12), a morphological transition essential for virus infectivity.

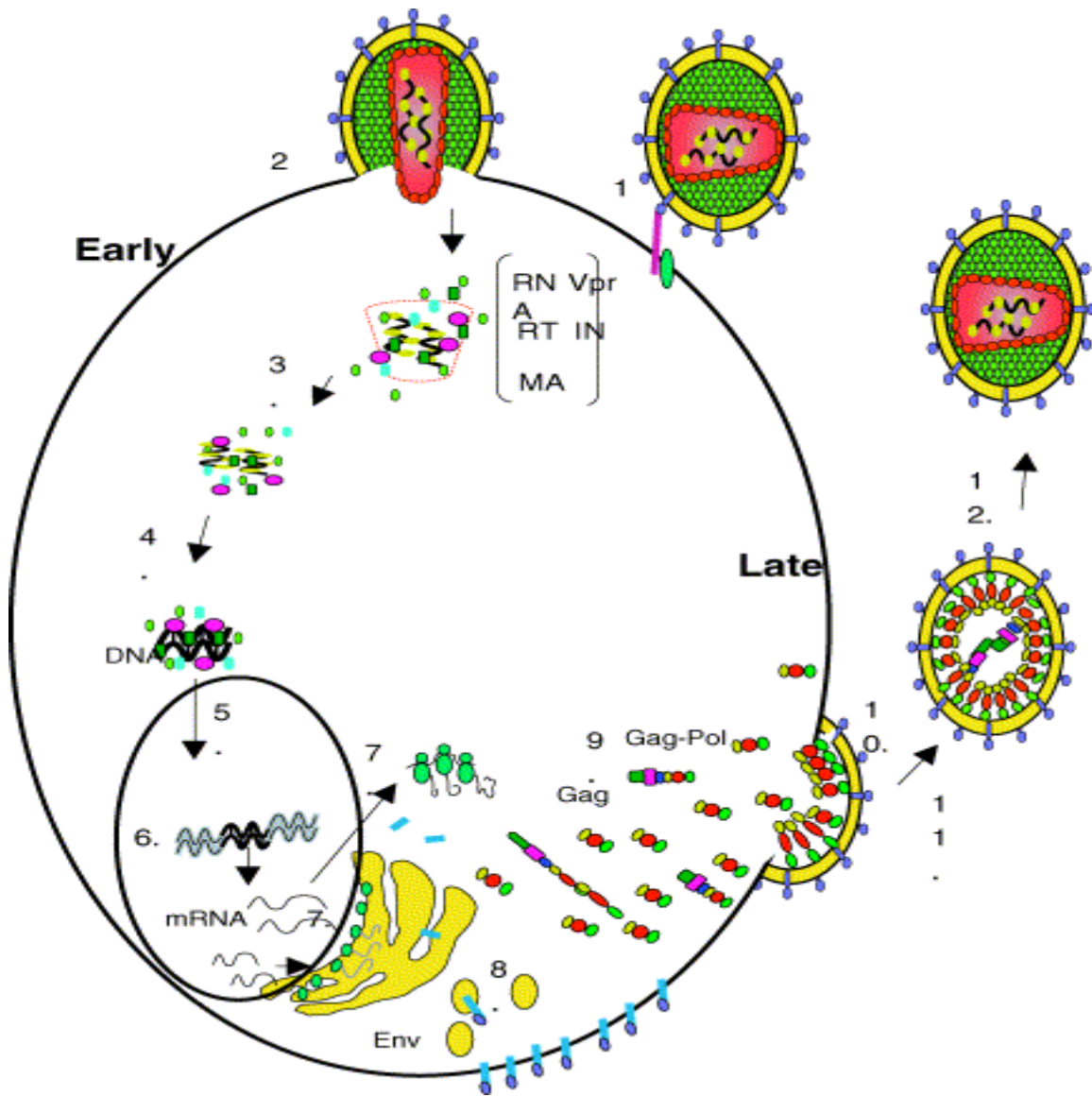


Figure 1-2. Life cycle of HIV-1.

Reprinted with permission from Suzanne Scarlata and Carol Carter, Role of HIV-1 Gag domains in viral assembly. 2003. Biochimica et Biophysica Acta, 1614:62-72. Copyright 2003, Elsevier B.V.

### 1.1.3 Retrovirus assembly and budding

Retroviral Gag polyproteins are synthesized in the cytoplasm of the infected cells and assemble into virus particles that typically bud from the plasma membrane. Although the envelope glycoproteins and the *pol*-encoded enzymes are required for the production of infectious virions, Gag expression alone is generally sufficient for the assembly and release of non-infectious, virus-like particles (VLPs). Upon virus release, cleavage of Gag precursor into matrix (MA), capsid (CA), and nucleocapsid (NC) by the viral protease leads to virus maturation. Retrovirus assembly usually takes place at either of two subcellular locations: cytosol or plasma membrane. For type C retroviruses, which include the alpharetroviruses, gammaretroviruses and lentiviruses, the assembly of electron-dense structures occurs at the plasma membrane. In contrast, for type B and D retroviruses, assembly takes place in the cytosol and the assembled intracytoplasmic particles traffic to the plasma membrane where they bud from the cell (Coffin et al., 1997).

Although expression of Gag proteins alone is generally sufficient to drive retrovirus assembly and budding, other retrovirus encoded proteins also play roles in retrovirus assembly and budding. Several lines of evidence suggest that Env glycoproteins have a role in virus trafficking and budding. In the early 1990s, it was reported that expression of HIV Env drove HIV Gag budding from the basolateral side in polarized cells, while Gag budded from both apical and basolateral sides without Env expression (Owens et al., 1991). Recently, Sandrin and Cosset reported that expression of different viral glycoproteins have different effects on retrovirus Gag protein intracellular location (Sandrin and Cosset, 2005). MLV Gag was reported to be rerouted from lysosomes to transferrin-positive endosomes in presence of MLV Env glycoproteins (Basyuk et al., 2003). For Mason Pfizer Monkey Virus (MPMV), the release of the

intracellularly assembled virus particles requires the recycling of Env glycoproteins (Sfakianos et al., 2003; Sfakianos and Hunter, 2003). Similarly, foamy viruses (FV) require expression of the envelope protein for budding of intracellular capsids from the cell (Pietschmann et al., 1999; Stanke et al., 2005).

HIV-1 encoded accessory protein Viral Protein U (Vpu) also regulates retrovirus assembly and budding by a mechanism that is not clear so far. The absence of Vpu results in an accumulation of cell-associated viral proteins and blocks progeny virus release (Klimkait et al., 1990). Vpu enhances HIV-1 particle assembly and release in most human cells, but not in simian cells, by overcoming a dominant block to HIV-1 release in human cells (Varthakavi et al., 2003). Interestingly, not only the release HIV-1 Gag, but also the release of the Gag proteins of HIV-2, visna virus, and Moloney murine leukemia virus can be enhanced by Vpu (Gottlinger et al., 1993). Recent studies suggest that Vpu enhances HIV-1 assembly and budding by preventing endocytosis of virus particles (Harila et al., 2006; Neil et al., 2006).

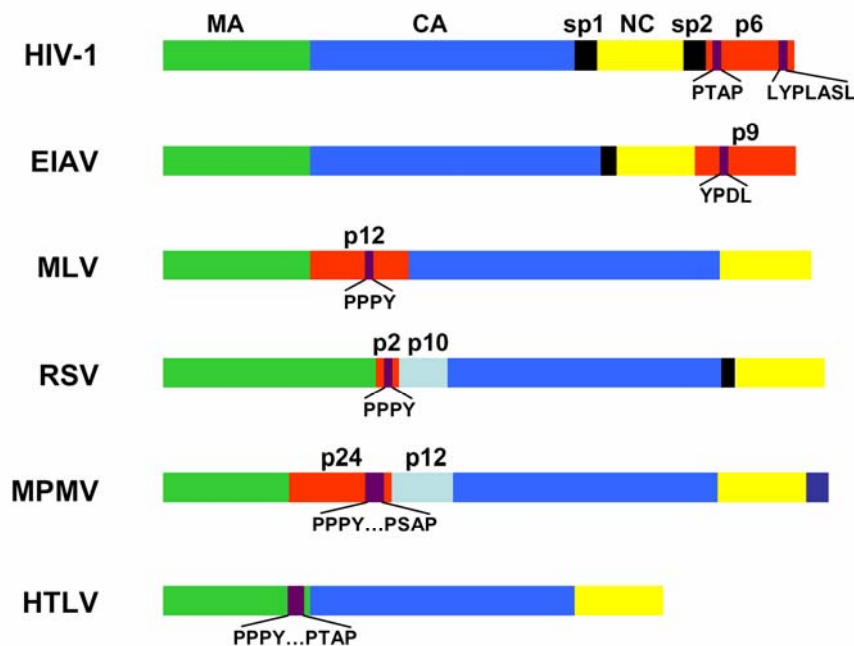


Figure 1-3. Schematic representation of retroviral Gag proteins and location of retroviral L domains.

#### **1.1.4 Role of Gag domains in retrovirus assembly and budding**

Retrovirus Gag polyprotein consists of matrix (MA), capsid (CA), and nucleocapsid (NC) proteins and small peptides (late domain and spacer peptides) (**Fig. 1-3**). These Gag domains orchestrate the major steps in virus assembly and budding (Demirov and Freed, 2004; Morita and Sundquist, 2004).

##### **1.1.4.1 Matrix**

The matrix (MA) protein plays a critical role in targeting Gag polyprotein to the host cell membrane and mediating Env glycoprotein incorporation into the virion. The membrane targeting determinant in HIV MA has been mapped to an N-terminal myristate and a region rich in basic amino acids termed the M domain (Freed, 1998; Zhou et al., 1994). The three-dimensional structure of HIV-1 MA reveals a globular head formed by four  $\alpha$ -helices and a C-terminal  $\alpha$ -helix that projects away from the core domain (Hill et al., 1996; Massiah et al., 1994). The myristic acid that is covalently attached to the N-terminal glycine residue and the highly basic patch formed by conserved positive charged residues clustered on the surface of the MA globular head both contribute to HIV-1 MA dependent membrane binding of Gag precursors (Scarlata and Carter, 2003).

Over 10 years ago, it was proposed that the membrane association of the myristoylated Gag is regulated by a so-called “myristoyl switch” mechanism whereby the myristate can adopt either an exposed or a sequestered conformation (Zhou and Resh, 1996). Recent structural studies demonstrate that HIV-1 myristoyl switch is regulated by entropic modulation of a preexisting equilibrium between the sequestered and the exposed states upon Gag multimerization (Tang et al., 2004), and specific interactions between myristoylated HIV-1 MA

and phosphatidylinositol-(4,5)-bisphosphate [PI(4,5)P<sub>2</sub>] trigger a transition of the myristate from the sequestered to the exposed conformation, therefore promoting the stable association of MA with the membrane (Saad et al., 2006). Several *in vivo* functional studies also demonstrate that Gag multimerization enhances membrane association of HIV-1 Gag polyprotein (Perez-Caballero et al., 2004; Zhou and Resh, 1996), and PI(4,5)P<sub>2</sub> plays a key role in Gag targeting to the plasma membrane (Ono et al., 2004). The PI(4,5)P<sub>2</sub> induced myristoyl switch might regulate lateral targeting of PI(4,5)P<sub>2</sub>:Gag complexes to lipid rafts, since PI(4,5)P<sub>2</sub> may preferentially associate with lipid rafts (Caroni Pico, 2001; Golub and Caroni, 2005), although this concept remains controversial (McLaughlin and Murray, 2005; van Rheene et al., 2005).

Although numerous *in vivo* studies clearly demonstrate that N-terminal myristoylation of HIV-1 Gag is critical for virus assembly and budding by mediating membrane association of Gag precursors (Bryant and Ratner, 1990; Gottlinger et al., 1989; Lindwasser and Resh, 2002; Liu et al., 1999; Ono and Freed, 1999; Spearman et al., 1997; Zhou et al., 1994), *in vitro* studies suggest that electrostatic interactions between positively charged surface of Gag multimers and negatively charged phospholipids drive the membrane association of HIV-1 Gag and that the myristoyl moiety only contributes negligibly to membrane interactions (Dalton et al., 2007; Ehrlich et al., 1992). It is noteworthy that several other retroviral Gag polyproteins are not myristoylated (eg. RSV (Dalton et al., 2007), EIAV (Hatanaka et al., 2002; Provitera et al., 2000)), indicating that membrane targeting signals other than myristoylation are used.

Retrovirus MA has been shown to recruit cellular factors to regulate Gag trafficking (see below). For example, clathrin adaptor complex AP-3 (Dong et al., 2005) and AP-1 (Camus et al., 2007) were found to interact with HIV-1 MA, and cytoskeleton regulator IQGAP1 was reported to interact with MLV MA (Leung et al., 2006).

#### **1.1.4.2 Capsid**

The capsid (CA) plays critical roles in both particle assembly and virus infectivity. In mature HIV-1 virion, capsid forms a conical core that encapsulates the viral RNA-protein complex. HIV-1 CA alone is able to assemble into particles *in vitro* (Ehrlich et al., 1992), and *in vivo* data also supports its function in HIV-1 particle assembly (Accola et al., 2000). HIV-1 CA can be divided into an N-terminal domain (NTD) and a C-terminal domain (CTD), which are connected through a flexible linker region (Berthet-Colominas et al., 1999; Momany et al., 1996).

Structural comparison between the NTD of HIV-1 CA (Gitti et al., 1996) and the N-terminal 283 residue fragment of HIV-1 Gag (Tang et al., 2002) reveals a 13-residue  $\beta$ -hairpin that is stabilized in part by a salt bridge between the terminal  $\text{NH}_2^+$  group of Pro<sup>1</sup> and the side chain carboxy group of Asp<sup>51</sup> and that is believed to be formed by refolding of the N-terminus of CA upon cleavage of CA from MA. It is thought that this change leads to the dramatic transformation of HIV-1 core structure that is essential for HIV-1 infectivity. In contrast to the NTD that is essential for formation of mature HIV-1 virion but dispensable for the assembly of immature virus particles, the CTD is crucial for Gag oligomerization, particle assembly, and core formation (Accola et al., 2000).

#### **1.1.4.3 Nucleocapsid**

The nucleocapsid (NC) is a highly basic protein and encapsulates viral RNA through its zinc fingers. HIV-1 NC contains two zinc fingers that are required for specific packaging of two copies of viral genomic RNA into the nascent viral particle through a *cis* nucleotide segment known as the Psi-site (Amarasinghe et al., 2001). However, the viral genomic RNA is completely unnecessary for efficient particle assembly in mammalian cells (Mann et al., 1983), and in absence of viral RNA, retroviruses recruit and encapsulate other cellular RNAs into assembled

virus particles (Khorchid et al., 2002; Muriaux et al., 2001; Muriaux et al., 2002). It is reasonable to assume that RNA binding helps to localize and concentrates Gag monomers to promote Gag assembly, which means that RNAs can serve as the scaffold for retroviruses assembly.

The region of NC that binds RNA is the conserved interaction (I) domain containing the zinc fingers (Feng et al., 1996; Muriaux et al., 1996) and is a functional domain required for the assembly of particles of normal density (Bennett et al., 1993; Parent et al., 1995). It was reported that HIV-1 NC can bind actin filaments in cosedimentation experiments, suggesting its role in regulating Gag trafficking by employing host cytoskeleton (Liu et al., 1999) (see below).

#### **1.1.4.4 Spacer peptides**

HIV-1 Gag polyprotein contains two spacer peptides: SP1 and SP2. SP1 has been shown to play active role in HIV-1 assembly and budding. Mutations in SP1 diminish particle release and result in the production of structurally aberrant, non-infectious virus particles (Krausslich et al., 1995; Pettit et al., 1994). The SP1 domain is predicted to exhibit  $\alpha$ -helical structure that extends across the CA-SP1 boundary and is believed essential for virus assembly (Krausslich et al., 1995; Pettit et al., 1994). Recent NMR based structural studies suggest that SP1 exists as a dynamic equilibrium of predominantly random coil and, to a smaller extent, helical states. It has been proposed that the transient coil-to-helix equilibrium functions as a 'molecular switch' that regulates Gag assembly and helps to maintain the order of CA-SP1 cleavage in Gag processing (Newman et al., 2004). During viral particle release, SP1 is removed from the C-terminus of CA prior to capsid condensation and virus maturation. It is believed that SP1 removal disrupts the  $\alpha$ -helical structure leading to capsid reorganization (Gross et al., 2000; Wieggers et al., 1998). The recently developed anti-HIV compound 3-O-(3',3'-dimethylsuccinyl)-betulinic acid (DSB)

potently and specifically inhibits human immunodeficiency virus type 1 (HIV-1) replication by delaying the cleavage of the CA-SP1 junction in Gag leading to impaired maturation of the viral core further demonstrates the critical role of SP1 in infectious HIV-1 virion production (Li et al., 2003;Li et al., ). Compared to SP1, the functional role of SP2 is largely unknown although one study suggests that it is important in the correct positioning of Gag for proteolytic processing and functions in stabilizing the dimeric form of genomic RNA (Hill et al., 2002).

#### **1.1.4.5 Late domains**

In addition to MA, CA and NC, retrovirus Gag polyprotein also contains a small protein that functions at the late stage of virus assembly and budding process (**Fig. 1-3**). In HIV-1, it is called p6 and located at the C-terminus of the Gag precursor. Budding determinants within p6 have been mapped to a highly conserved stretch of amino acids with the consensus sequence P(T/S)AP and termed viral late (L) domain (Huang et al., 1995). The L domains are required for the pinching off of the newly assembled virion from the host membrane. Even subtle mutations in this motif caused a severe defect in virus particle production (Huang et al., 1995). L domains with P(T/S)AP motifs were subsequently identified in MPMV (Gottwein et al., 2003) and HTLV (Bouamr et al., 2003).

The proline rich L domain, PPxY, was first identified in the p2 region of RSV Gag (Xiang et al., 1996). Subsequently, PPxY L domain motif was identified in MPMV (Yasuda and Hunter, 1998), MLV (Yuan et al., 1999) and HTLV (Le Blanc et al., 2002). EIAV encodes a unique L domain, YPDL (Puffer et al., 1997), and a related sequence (LYPLASL) was later found near the C-terminus of HIV-1 p6 (Strack et al., 2003).

Numerous studies indicate that retroviral L domains are often exchangeable and display positional independence (Accola et al., 2000;Li et al., 2002;Parent et al., 1995;Shehu-Xhilaga et

al., 2004;Strack et al., 2002;Strack et al., 2003). Identification of their interacting proteins support the model that L domains serve as docking sites for retrovirus budding co-factors provided by the cell that will be discussed in the next section.

## **1.1.5 Cellular factors involved in retrovirus assembly and budding**

### **1.1.5.1 Vps proteins and retrovirus budding**

A key step in the trafficking of membrane proteins and lysosomal enzymes to the lysosome (or the vacuole in yeast) is the delivery of these proteins to the late endosome prior to their fusion with the lysosome. The cargo proteins are initially delivered to early endosomal membranes where they are incorporated into vesicles (intraluminal vesicles or ILV) that bud into the lumen of the organelle. Early endosomes mature to late endosomes, or multivesicular bodies (MVBs), that accumulate ILVs (Katzmann et al., 2002). An interesting connection between MVB biogenesis and retrovirus budding is they are topologically equivalent. In both cases, budding is directed away from the cytoplasm. Numerous studies of retrovirus L domain interacting proteins indicate that retroviruses have evolved to adapt MVB machinery for their release from host cells.

Morphological characterization of vacuolar protein sorting (Vps) mutants in yeast led to the classification of a number of distinct vacuolar morphologies (Raymond et al., 1992). One of these morphological classes, “class E” was defined by the formation of an enlarged, pre-vacuolar compartment (Katzmann et al., 2002; Raymond et al., 1992). Class E Vps proteins have been thought to be cytoplasmic, multidomain proteins that transiently associate with endosomal membrane at the site where the inward invagination of cargo loaded vesicles takes place (Hurley and Emr, 2006). But a recent ultrastructure study of intracellular localization of Vps proteins suggest that majority of these proteins are associated with low affinity with the tubular-vesicular

endosomal membranes (Welsch et al., 2006). Many class E Vps proteins assemble into discrete complexes named as endosomal sorting complex required for transport (ESCRT) –I, -II or –III (Fig. 1-4) (Hurley and Emr, 2006).

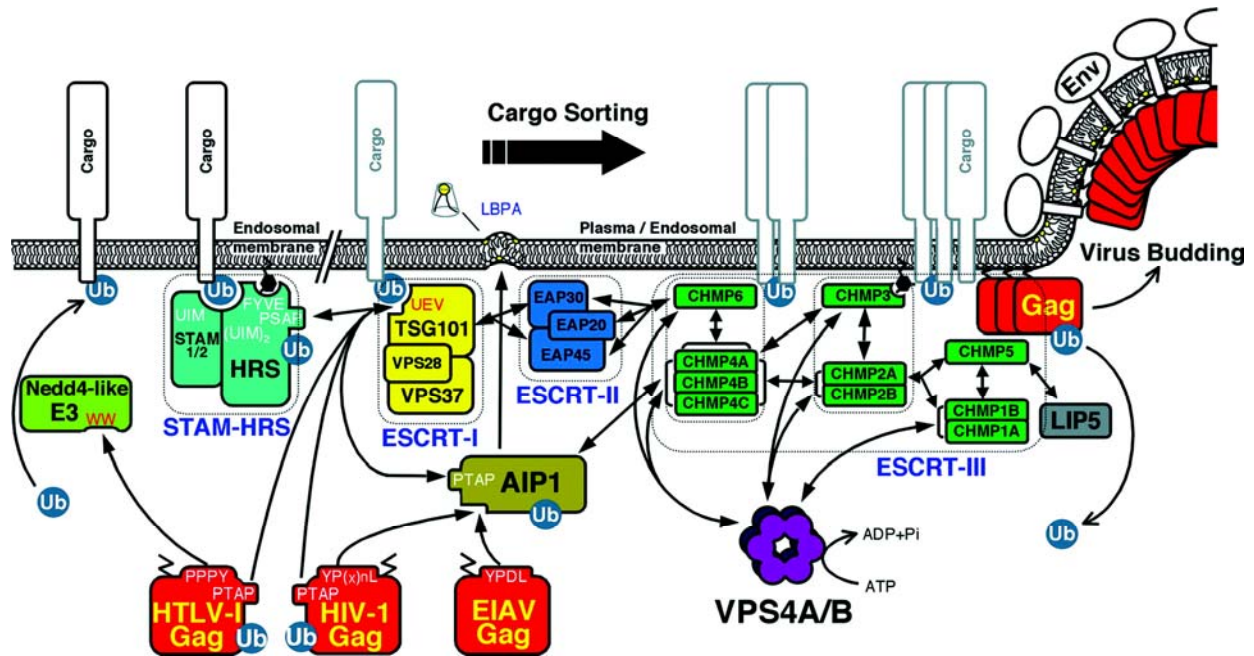


Figure 1-4. Model showing the interaction network of mammalian Class E proteins and their roles in retrovirus budding.

Reprinted with permission from Eiji Morita and Wesley I. Sundquist, Retrovirus budding. 2004. *Annu. Rev. Cell Dev. Biol.*, 20:395-425. Copyright 2004, Annual Reviews.

ESCRT-1 component Tsg101 was first identified as an HIV-1 P(T/S)AP L domain interacting protein (Garrus et al., 2001; VerPlank et al., 2001). Depletion of endogenous Tsg101 by RNAi inhibits HIV-1 virus release (Garrus et al., 2001). Overexpression of the P(T/S)AP interacting domain, N-terminal UEV domain of Tsg101 (Garrus et al., 2001; Pornillos et al., 2002) causes an inhibition of HIV-1 budding (Demirov et al., 2002). In both cases, HIV-1 virus particles are tethered to plasma membrane similar to the arrested structure induced by L domain mutations.

Alix was recently identified as the budding factor of EIAV YPxL L domain and HIV-1 secondary L domain, LYPLASL (Martin-Serrano et al., 2003; Strack et al., 2003; von Schwedler et al., 2003). SiRNA knockdown of endogenous Alix dramatically inhibits EIAV p9 mediated budding (Chen et al., 2005; Martin-Serrano et al., 2003), but has relatively little effect on HIV-1 p6 mediated budding (Martin-Serrano et al., 2003). This is consistent with the function of the secondary L domain in HIV-1 p6. Mutation of LYPLASL has a negligible effect on HIV-1 budding, in contrast to an almost complete block of virus budding induced by P(T/S)AP mutations (Fisher et al., 2007). Overexpression of Alix could rescue P(T/S)AP mutated HIV-1 budding (Fisher et al., 2007), and overexpression of the Alix fragment that interacts with LYP(x)<sub>n</sub>L motif potently inhibits HIV-1 budding (Munshi et al., 2007), indicating that p6-Alix interaction plays a role in HIV-1 budding. Alix interacts with both ESCRT-1 and ESCRT-III components (Martin-Serrano et al., 2003; Strack et al., 2003; von Schwedler et al., 2003), and its V domain is the docking sites for the LYP(x)<sub>n</sub>L L domain (Lee et al., 2007; Fisher et al., 2007), indicating its ability to serve as a connection between ESCRT complexes and a entry portal to the Vps network.

A number of studies have identified Nedd4 and related proteins as the host factors interacting with PPxY L domains. Nedd4 family members are E3 ubiquitin ligases that typically contain a N-terminal, calcium-inducible membrane binding domain, multiple centrally located WW domains, and a C-terminal HECT domain that is the enzyme activity domain (Harvey and Kumar, 1999). The PPxY sequence is the consensus binding site for WW protein recognition domains, and several groups have demonstrated that WW domains form the Nedd4 family members can bind viral PPxY late domains (Gamier et al., 1996; Bouamr et al., 2003; Yasuda et al., 2002; Kikonyogo et al., 2001). However, there are multiple Nedd4-like proteins in

mammalian cells, and there is not yet a general consensus as to which subsets actually function as late domain binding partners. Importantly, Nedd4 and its relatives mediate ubiquitin dependent down-regulation of cell surface proteins via the MVB pathway (Harvey and Kumar, 1999), and the interaction of PPxY L domains with Nedd4 family members may be functionally relevant to retrovirus budding (Demirov and Freed, 2004).

Finally, inhibition of budding by several retroviruses that harbor different L domain can be achieved by overexpression of dominant negative Vps4 AAA-ATPase that functions in the release of membrane associated ESCRT-III complexes to allow multiple rounds of sorting and budding of either intraluminal vesicle or viruses (Garrus et al., 2001; Tanzi et al., 2003), suggesting that different retroviruses budding pathways converge at the final step by utilizing host Vps machinery.

#### **1.1.5.2 Intracellular Gag trafficking during retrovirus assembly and budding**

In contrast to the final step mediated by host Vps machinery that is recruited by various retrovirus L domains, the earlier steps from Gag synthesis to membrane targeting of newly synthesized Gag polyproteins during retrovirus assembly and budding process are largely unknown even for the most extensively studied retrovirus, HIV. Multiple challenges have to be faced to elucidate these earlier steps of the dynamic, complicated, multi-step assembly and budding process. (1) The majority (~80%) of newly synthesized Gag proteins are degraded within 2 hours (Tritel and Resh, 2000). (2) Multiple assembly intermediates exist inside cells before membrane targeting of Gag polyproteins (Tritel and Resh, 2000; Dooher and Lingappa, 2004). (3) Newly synthesized Gag polyproteins are targeted to cell membrane soon after synthesis (in less than 1 hour)(Tritel and Resh, 2000; Rudner et al., 2005; Perlman and Resh, 2006). (4) Intracellular Gag proteins are highly mobile (Gomez and Hope, 2006). Therefore, it is

difficult to capture the highly dynamic trafficking of newly synthesized Gag proteins that exist in a complex containing various assembly intermediates by using traditional imaging approaches with fluorescence protein tags that mature on a time scale of hours.

Intracellular transport of Gag polyproteins can be mediated by the endosomal membrane trafficking and/or the host cytoskeleton. Given the critical function of the cytoskeleton in membrane trafficking, these two trafficking mechanisms are not independent of each other. Microtubule serves as the track for long-range transport of endosomes, while the actin cytoskeleton can either propel vesicles by forming “comet tails” on vesicle membranes or serve as the track for short-range transport of vesicles (**Fig. 1-5**).

It is well established that HIV-1 Gag buds from the plasma membrane of T lymphocytes and some epithelial cell lines (Nydegger et al., 2003; Hermida-Matsumoto and Resh, 2000; Ono et al., 2004; Demirov and Freed, 2004; Morita and Sundquist, 2004; Nguyen et al., 2003). In contrast, MVBs are apparently the sites of HIV-1 Gag accumulation and particle production in macrophages and dendritic cells (Blom J. et al., 1993; Morita and Sundquist, 2004; Nguyen et al., 2003; Pelchen-Matthews et al., 2003; Raposo et al., 2002). Based on various studies showing that HIV-1 Gag may also target to MVBs in other cell types (Nydegger et al., 2003; Ono et al., 2004; Sherer et al., 2003), MVBs are thought to be the common budding sites for HIV-1. However, recent studies appeared to contradict this model by indicating the plasma membrane as the productive sites for HIV-1 Gag assembly and budding in various cells (Welsch et al., 2007; Jouvenet et al., 2006; Deneka et al., 2007; Finzi et al., 2007), including macrophages where HIV-1 virions bud from invaginated plasma membranes (Welsch et al., 2007; Deneka et al., 2007). These recent studies are consistent with a previous dynamic imaging study of HIV-1 Gag trafficking in live cells by biarsenical labeling showing that newly synthesized Gag rapidly

concentrates in specific plasma membrane areas (~30 min) after translation (Rudner et al., 2005). However, little is known how thousands of copies of Gag molecules are transported to the plasma membrane post translation. A dynamic imaging study of HIV-1 Gag in live cells reveals a trafficking pathway through several temporal intermediates. Gag first appears diffusely distributed in the cytosol, accumulates in perinuclear clusters, passes transiently through a MVB-like compartment, and then travels to the plasma membrane (Perlman and Resh, 2006). The authors suggest that HIV-1 Gag might start its journey on endosome membranes, such that Gag “takes ride” on moving endosomes to traffic to budding sites.

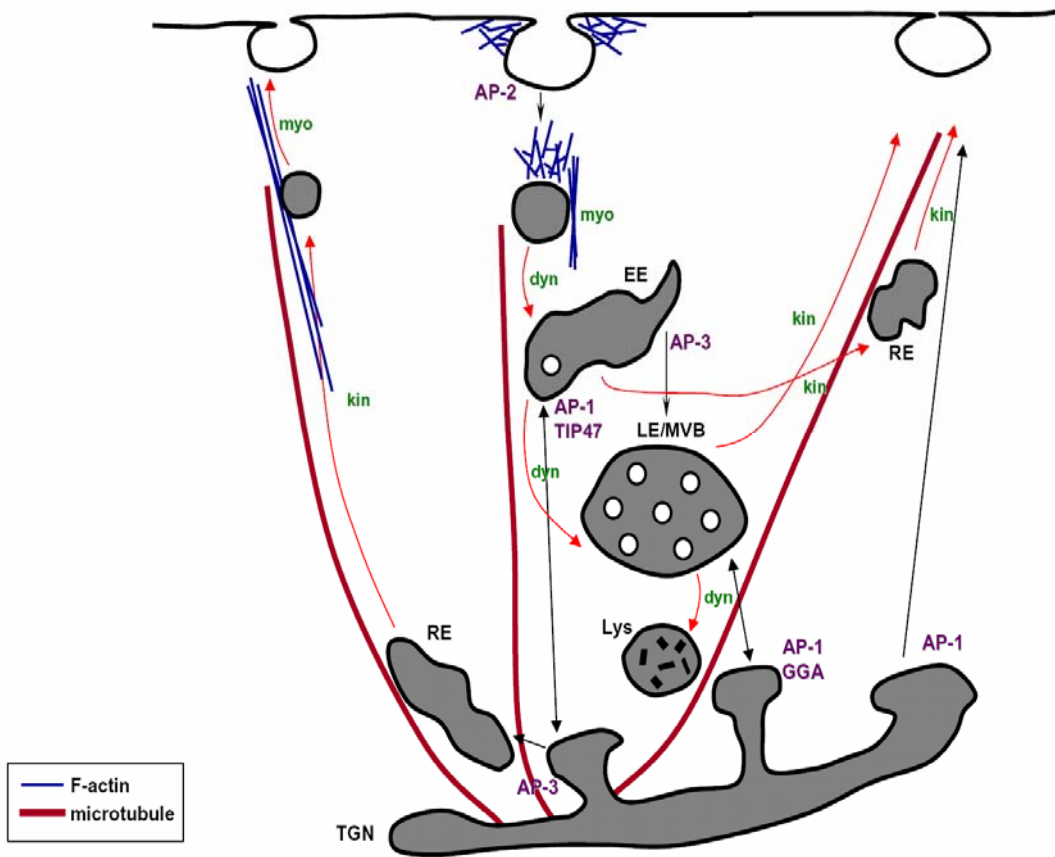


**Figure 1-5. Cytoskeleton in intracellular membrane trafficking.**

EE, early endosome; LE/MVB, late endosome/multivesicular body; RE, recycling endosome; Lys, lysosome; myo, myosin; kin, kinesin; dyn, dynein.

### 1.1.5.3 Endosomal trafficking and retrovirus assembly and budding

Multiple lines of evidence suggest that intracellular endosome trafficking might be utilized by retroviruses for transporting Gag proteins.

First, several clathrin adaptor protein (AP) complexes have been reported to be recruited by retroviruses. AP complexes mediate assembly of clathrin-coated vesicles that selectively transport designated cargo molecules between membrane-bound intracellular compartments (**Fig. 1-5**). Our lab first reported that the  $\mu 2$  subunit of AP-2 interacts with EIAV YPDL L domain and suggested it as a budding partner for EIAV (Puffer et al., 1998). Depletion of AP-2 by RNAi or overexpression of dominant negative  $\mu 2$  both inhibited EIAV budding, suggesting that AP-2 plays a role in EIAV assembly and budding. AP-3 was found to associate with the N-terminal helix of HIV-1 MA and to direct the intracellular trafficking of HIV-1 Gag, and depletion of AP3 expression inhibited HIV-1 budding (Dong et al., 2005). AP-2 was found to interact with HIV-1 Gag polyproteins at the matrix–capsid junction and to confine HIV-1 exit to distinct microdomains (Batonick et al., 2005). Recently, AP-1 was reported to facilitate HIV-1 budding through direct binding to HIV-1 MA and Tsg101 (Camus et al., 2007). However, where these AP complexes are recruited by retroviral Gag polyproteins and how they regulate Gag trafficking are not known.

Second, accumulating evidence indicates a connection between retrovirus release and the endosomal sorting signal molecule - ubiquitin (Vogt, 2000). Ubiquitin is a small, highly abundant protein that can be covalently attached to a lysine residue in target proteins post-translationally. It can also be linked to other ubiquitin moieties on target proteins to form polyubiquitin chains. The poly-ubiquitin chains generally serve as a signal for protein degradation in the proteasome, while a monoubiquitin tag directs membrane-associated proteins

for internalization and/or sorting into the endosomal pathway (Mukhopadhyay and Riezman, 2007).

Retroviruses have long been known to contain ubiquitin, and monoubiquitylated Gag (Chertova et al., 2006; Heidecker et al., 2004; Ott et al., 1998; Putterman et al., 1990). Treatment of virus-producing cells with proteasome inhibitors to deplete free ubiquitin by inducing the accumulation of polyubiquitin complex inhibits virus release of some (but not all) retroviruses (Accola et al., 2000; Patnaik et al., 2000; Patnaik et al., 2002; Schubert et al., 2000). A correlation exists between the endocytic function of ubiquitin and HIV-1 particle release. Expression of ubiquitin mutants that are deficient in ubiquitin-mediated endocytosis leads to a reduction of VLP production (Strack et al., 2002). Retroviral Gag interacts with components of the ubiquitylation machinery (Alroy et al., 2005; Bouamr et al., 2003; Gamier et al., 1996; Kikonyogo et al., 2001; Yasuda et al., 2002). However the precise role of ubiquitin in retrovirus assembly and budding and functional relevance of Gag ubiquitination remains unclear.

Third, annexin 2 was identified as a HIV Gag binding partner in macrophages, and the annexin 2-Gag binding was specific for productively infected macrophages (Ryzhova et al., 2006). Annexin 2 locates on endosomes (Emans et al., 1993) and has been implicated in MVB formation, probably mediated by its binding with actin (Futter and White, 2007). Annexin 2 depletion is associated with a significant decline in the infectivity of released virions that correlates with incomplete Gag processing and inefficient incorporation of CD63 (Ryzhova et al., 2006), suggesting that interaction with annexin 2 directs HIV-1 Gag to correct membrane domains for assembly and budding.

A recent study showing that HIV-1 virions are efficiently released when Gag is rationally targeted to the PM, but not when targeted to endosomes, challenges the model that HIV-1 Gag

utilizes endosome trafficking pathways (Jouvenet et al., 2006). In contrast to HIV-1, Mason-Pfizer monkey virus (M-PMV) is clearly demonstrated to utilize endosome trafficking pathways for Gag assembly and budding. This D-type retrovirus specifically targets Gag precursor proteins to the pericentriolar region of the cytoplasm in a microtubule dependent process mediated by the dynein/dynactin motor complex. The Gag molecules are concentrated in pericentriolar microdomains, where they assemble to form immature capsids (Sfakianos et al., 2003). Then Env glycoproteins endocytosed from the plasma membrane interacts with Gag at the pericentriolar microdomains and transport the immature capsids out *via* Rab11 dependent pericentriolar recycling endosomes (Sfakianos and Hunter, 2003).

#### **1.1.5.4 Cytoskeleton and retrovirus assembly and budding**

The importance of the integrity and dynamics of host cell cytoskeletal structures for efficient HIV-1 replication has long been suggested (Sasaki et al., 1995). However, the detailed mechanisms by which retroviruses exploit cytoskeletal dynamics are not known. Recent studies suggest that the host cell cytoskeleton is involved in retrovirus entry (Lehmann et al., 2005; Iyengar et al., 1998; Jimenez-Baranda et al., 2007; Pontow et al., 2004; Komano et al., 2004), transport of virion components (Tang et al., 1999; Rey et al., 1996; Sasaki et al., 2004; Leung et al., 2006; Kim et al., 1998), retrovirus release (Jolly et al., 2007; Sasaki et al., 2004), as well as retrovirus transmission through virological synapse (McDonald et al., 2003; Jolly et al., 2004; Jolly et al., 2007). In addition, the export of HIV genomic RNA to the cytosol seems to require nuclear actin (Hofmann et al., 2001), and synthesized Gag protein tethers viral RNA to actin filaments close to the MTOC (Poole et al., 2005).

Numerous studies suggest that retroviruses exploit actin cytoskeleton for intracellular Gag transport (Chen et al., 2004; Edbauer and Naso, 1983; Ott et al., 1996; Ott et al., 2000;

Sasaki et al., 1995; Liu et al., 1999). Perturbation of the actin cytoskeleton affects the assembly and budding of several retroviruses (Sasaki et al., 1995; Chen et al., 2004; Maldarelli et al., 1987; Audoly et al., 2005). Actin and actin-binding proteins have been identified within highly purified HIV-1 virions (Ott et al., 1996; Ott et al., 2000; Chertova et al., 2006; Ott, 2002). Assembly and budding of several retroviruses at actin-rich sites has been reported (Maldarelli et al., 1987; Mortara and Koch, 1986). Gag polyproteins are present in the same fractions as actin filaments in cell fractionation analysis (Chen et al., 2004; Rey et al., 1996). Furthermore, both *in vitro* translated HIV-1 Gag polyprotein (Rey et al., 1996) and purified nucleocapsids of HIV-1 virions (Liu et al., 1999) co-sediment on density gradients with polymerized actin filaments. However, the mechanism by which retroviruses utilize actin cytoskeleton for Gag trafficking is unknown.

Microtubule filaments might also serve as the track for retroviral Gag trafficking. HIV-1, SIV, MLV, and M-PMV Gag all recruit microtubule based motor protein KIF-4 (Tang et al., 1999; Kim et al., 1998). However, it is unclear whether the Gag assembly intermediates before membrane binding or Gag molecules associated with vesicles recruit KIF-4 for intracellular trafficking. In addition, transport of M-PMV Gag precursors to the pericentriolar region of the cytoplasm is mediated by the dynein/dynactin motor complex (Sfakianos et al., 2003).

#### **1.1.5.5 Connections between retroviral genomic RNA nuclear export and virion assembly**

Retroviral Gag polyproteins are synthesized from an unspliced full-length viral genomic mRNA that requires specific regulatory factors for nuclear export. The HIV-1 genome contains a *cis*-acting RNA element known as the Rev-response element (RRE) that binds to a viral *trans*-acting protein. Rev binds to the nuclear exporter Crm1 protein which in turn binds to Ran, a small GTPase that shuttles between the nucleus and the cytoplasm (**Fig. 1-6**). Some simple retroviruses, such as Mason-Pfizer monkey virus (M-PMV) and avian leukosis virus (ALV),

contain *cis*-acting RNA export elements (constitutive transport elements or CTE) that do not require viral *trans*-acting factors. CTE mediated gRNA nuclear export takes the host cell mRNA nuclear export pathway by interacting directly with cellular export factors Tap-Nxt1 complex (also known as NXF1/NXT complex) (Swanson and Malim, 2006)(**Fig. 1-6**).

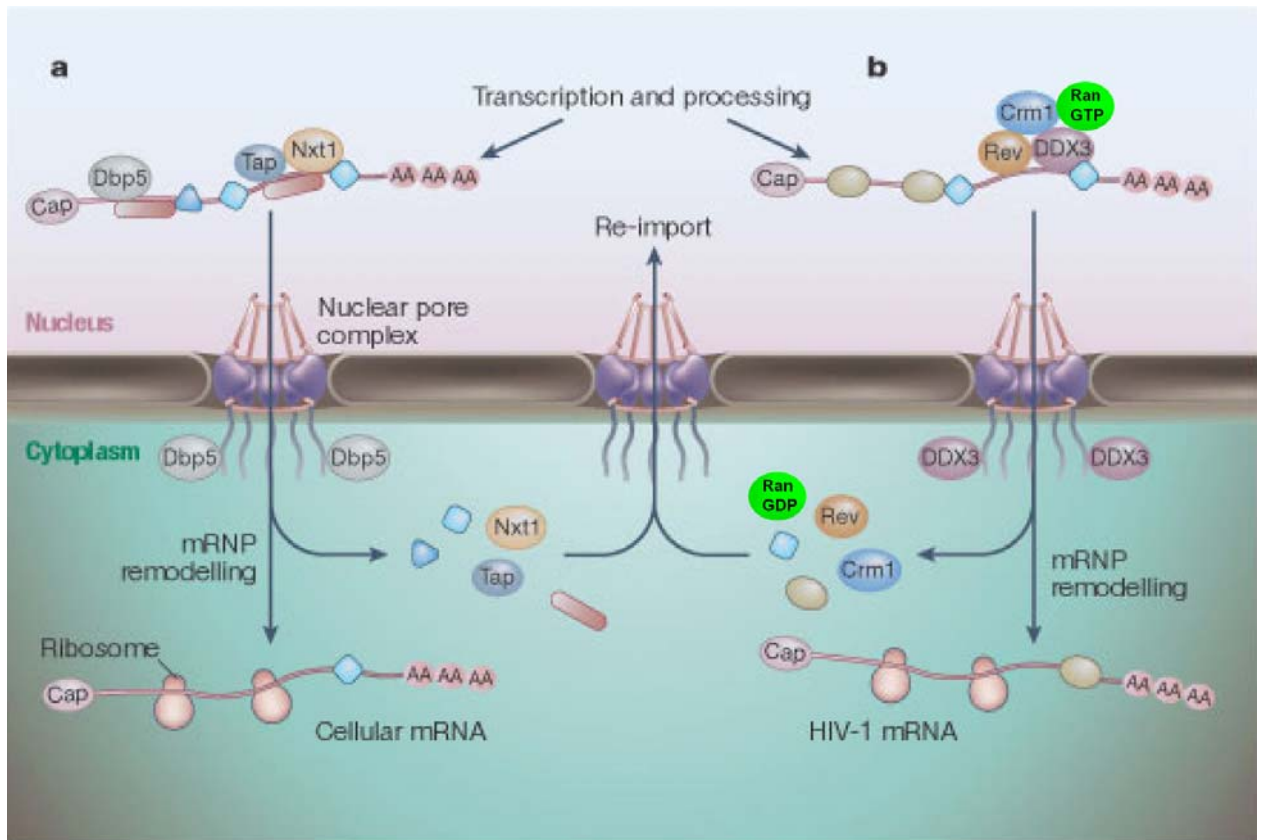


**Figure 1-6. Rev-dependent nuclear export of HIV-1 genomic mRNA.**

a, Transcription and processing of cellular mRNAs give rise to export-competent mRNA-protein (mRNP) complexes that include the export factors Tap-Nxt1 complex (also known as NXF1-Nxt1). b, HIV-1 genomic mRNAs are bound to a distinct export factor, the RanGTP-dependent Crm1 that is recruited by viral accessory protein, Rev. Adapted from Figure 1 in Nature 433, 26-27 (Cullen, 2005).

Swanson *et al* (Swanson et al., 2004) recently demonstrated that altering the RNA nuclear export element used by HIV-1 *gag-pol* mRNA from the RRE to the M-PMV CTE resulted in efficient trafficking and assembly of Gag at cellular membranes in murine cells, which are notable for their inability to support HIV-1 assembly and budding (Mariani et al., 2000; Bieniasz and Cullen, 2000; Swanson et al., 2004). Similarly, a deficiency of assembly of ALV Gag proteins synthesized in mammalian cells could be overcome by replacement of the ALV CTE-mediated mRNA nuclear export pathway with the HIV-1 Rev-RRE-mediated mRNA nuclear export pathway (Nasioulas et al., 1995). These results support the model that RNA export pathway selection during Gag expression and assembly can affect the cytosolic fate or function of the retroviral Gag polyproteins. However, the mechanisms by which trafficking pathways of mRNA regulate the intracellular fate of the proteins synthesized from this mRNA are unknown.

Interestingly, Swanson *et al* also demonstrated that the Gag location and budding efficiency in human cells are different between Rev-dependent HIV-1 Gag and codon-optimized HIV-1 Gag that is synthesized from mRNA exported from the nucleus by Tap-Nxt1 in a Rev-independent manner (Swanson and Malim, 2006). Because it is much easier to manipulate Rev-independent HIV-1 Gag than Rev-dependent Gag, most of the HIV-1 Gag trafficking studies have been performed using Rev-independent constructs (Sherer et al., 2003; Rudner et al., 2005; Derdowski et al., 2004; Perlman and Resh, 2006; Jouvenet et al., 2006; Gomez and Hope, 2006; Nydegger et al., 2003; Ono and Freed, 2004). This technical detail might be one of the reasons for some conflicting reports about the specificity of HIV-1 Gag assembly sites reported by different groups, MVB versus plasma membrane. Therefore, it should be important to repeat

some of the live cell imaging studies mentioned above using Rev-dependent HIV-1 Gag constructs.

#### **1.1.5.6 Lipid rafts on plasma membrane provide the platform for HIV assembly**

Lipid rafts are membrane microdomains that are highly enriched in sphingolipids and cholesterol (Simons and Toomre, 2000; Simons and Vaz, 2004). Clustering of separate rafts exposes raft associated proteins to a new membrane environment and facilitates raft protein interactions, and this dynamic feature enables rafts to serve as concentrating platforms for signal transduction and protein trafficking (Simons and Toomre, 2000; Kusumi et al., 2004). Lipid rafts have been implicated in the assembly and release of several families of enveloped viruses including orthomyxoviruses, paramyxoviruses, filoviruses, and retroviruses (Ono and Freed, 2005; Schmitt and Lamb, 2005; Suomalainen, 2002; Briggs et al., 2003). Multiple lines of evidence suggest that lipid rafts play a critical role in HIV-1 assembly and budding: (1) The HIV-1 lipid bilayer has long been known to be enriched (relative to the host cell plasma membrane) in sphingolipids and cholesterol (Brugger et al., 2006; Aloia et al., 1993); (2) HIV-1 Gag was found to associate with rafts in detergent-resistant membrane (DRM) binding assays that isolate lipid rafts biochemically based on their insolubility in a number of nonionic detergents (e.g., Triton X-100) at low temperature (Nguyen and Hildreth, 2000; Ono and Freed, 2001; Ding et al., 2003; Lindwasser and Resh, 2001); (3) Gag proteins colocalize or “co-patch” with raft markers (Ono and Freed, 2001; Nguyen and Hildreth, 2000); and (4) Higher-order Gag assembly and particle production of HIV-1 is inhibited by cholesterol depletion (Ono and Freed, 2001; Brugger et al., 2006; Ono et al., 2007). Together, these studies suggest that HIV-1 Gag assembly and budding depend on Gag targeting to lipid rafts. However, the mechanism of raft targeting is unknown.

### **1.1.5.7 Cellular factors power the energy-dependent retrovirus assembly and budding process**

Retroviral assembly and budding are energy-dependent multi-step processes (Tritel and Resh, 2001; Doohar and Lingappa, 2004; Tritel and Resh, 2000). Recent structural studies indicate HIV-1 Gag monomer assumes a folded conformation, with its N-terminal matrix domain near its C-terminal nucleocapsid domain (Batonick et al., 2005; Datta et al., 2007). Since Gag is a rod-shaped molecule in the assembled immature virion, these findings imply that Gag undergoes a major conformational change upon virus assembly. It is reasonable to propose that chaperone proteins might be recruited by HIV-1 Gag during the Gag assembly process, and this is supported by several studies. First, certain heat shock proteins (Hsp60, Hsp70, and Hsc70) were reported to associate with HIV-1 virions (Gurer et al., 2002). Second, M-PMV Gag polyprotein associates with the TRiC chaperonin complex and this association depends on ATP hydrolysis (Hong et al., 2001). Third, HIV-1 Gag recruits the cellular adenosine triphosphatase ABCE1 (also termed HP68) to an assembly intermediate and dissociation of ABCE1 from Gag correlates closely with Gag processing during virion maturation (Doohar and Lingappa, 2004; Zimmerman et al., 2002; Doohar et al., 2007).

## **1.2 VISUALIZATION OF PROTEIN INTERACTIONS BY BIMOLECULAR FLUORESCENCE COMPLEMENTATION**

Selective interactions with different co-factors can enable a single protein to have different functions. Retrovirus assembly and budding is a multi-step process mediated by temporally and

spatially regulated protein interactions between viral proteins and between viral protein and host factors.

Numerous approaches have been used to study protein interactions. Many of the biochemical experimental approaches, such as co-precipitation and co-purification can detect protein interactions but require isolation of proteins from their normal environment. In contrast, other approaches, such as genetic analysis of compensatory mutations can detect protein interactions indirectly in their normal environment by measuring consequences of protein interactions. A combination of genetic and biochemical approaches can be used to identify thousands of potential proteins interactions, but not to define the cell specificity and the subcellular location of these protein interactions.

Visualization of protein complexes in living cells directly enables characterization of protein interactions in their normal environment. Two major methods have been developed to visualize protein interactions in living cells. One is fluorescence resonance energy transfer (FRET), and the other is bimolecular fluorescence complementation (BiFC). The former technique is based on measuring changes in the fluorescence intensities or the lifetimes of two fluorophores when they are brought sufficiently close together compared to those parameters in individual proteins (Jares-Erijman and Jovin, 2003;Jares-Erijman and Jovin, 2006;Miyawaki, 2003). And the latter is based on the formation of a fluorescent complex by non-fluorescent fragments of fluorescent proteins. The complemenation of these fragments is facilitated by the interaction between the proteins fused to these fragments (Hu et al., 2002;Hu and Kerppola, 2003) (**Fig. 1-7**).

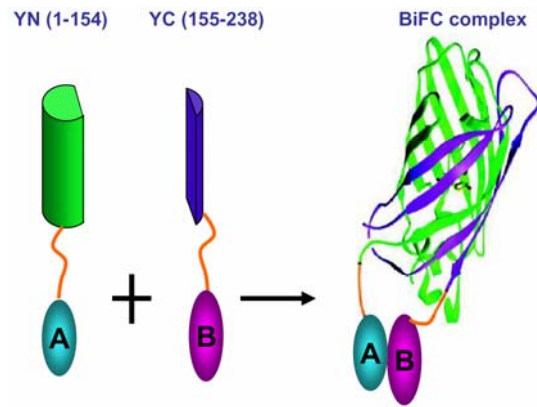


**Figure 1-7. Schematic illustration of bimolecular fluorescence complementation (BiFC).**

The BiFC technique is based on the formation of a bimolecular fluorescent complex when two non-fluorescent fragments of yellow fluorescent protein are brought together by an interaction between proteins (A and B) that are fused to the fragments.

Many proteins, like  $\beta$ -galactosidase (Rossi et al., 1997;Ullmann et al., 1996), ubiquitin (Johnsson and Varshavsky, 1994;Miller et al., 2005) and dihydrofolate reductase (Pelletier et al., 1998), can be divided into fragments that can complement with each other to produce a functional complex. Complementation assays that use fragments of different proteins have different properties, like enzyme activity or ubiquitin specific protease activation. BiFC has the advantage that a complex can be directly visualized in living cells without the needs for staining with exogenous molecules, because the complemented fragments are derived from fluorescence proteins (Hu et al., 2002;Hu and Kerppola, 2003;Magliery et al., 2005).

BiFC assays allow the visualization of protein interactions *in vivo* with minimal perturbation of the normal cellular environment, so it is generally applicable for visualizing protein interaction in live cells. The formation of a fluorescent complex does not require that the interacting protein partners position the fragments in a specific orientation, as long as the fragments can be brought in a close proximity (less than 10 nm) (Hu et al., 2002). Although

some studies reported that the formation of BiFC complex is reversible under some condition (Anderie and Schmid, 2007;Demidov et al., 2006;Magliery et al., 2005), Hu *et al* reported that the BiFC complex formation is essentially irreversible (Hu et al., 2002). Thus, the interacting partners do not need to form a complex with a long half-life time in order to form BiFC complexes. This property allows the BiFC assay to visualize transient protein interactions (Nyfeler et al., 2005). With the identification of numerous green fluorescence protein variants with altered spectral and photophysical characteristics (Shaner et al., 2005;Zhang et al., 2002), the BiFC assay can be used to visualize multiple protein complexes simultaneously in the same cell. The BiFC complexes that are formed of fragments from different fluorescence proteins have spectra that differ from those of BiFC complexes formed of fragments from the same fluorescence protein (Grinberg et al., 2004;Hu and Kerppola, 2003;Shyu et al., 2006).

The BiFC technique has been used to study interactions among a wide range of proteins in many cell types and organisms. It has been applied to study interactions among transcription factors (Grinberg et al., 2004;Hu and Kerppola, 2003;Rajaram and Kerppola, 2004), to identify enzyme-substrate interactions (de Virgilio et al., 2004;der Lehr et al., 2003;Niu et al., 2005;Remy et al., 2004), to visualize the subcellular localization of protein complexes (Grinberg et al., 2004;Hu et al., 2002;Hynes et al., 2004a;Hynes et al., 2004b;Niu et al., 2005), to visualize protein interactions in signal transduction networks (Hynes et al., 2004a;Hynes et al., 2004b;Remy et al., 2004), to study post-translational modifications (Fang and Kerppola, 2004;Nyfeler et al., 2005), to study macromolecular complexes and molecular scaffolds (Rackham and Brown, 2004;Stains et al., 2005), to visualize assembly of virus structural proteins (Avitabile et al., 2007;Boyko et al., 2006;Jin et al., 2007;Lee et al., 2007b) and to screen protein interactions (Ding et al., 2006;Remy and Michnick, 2004a;Remy and Michnick, 2004b).

Retrovirus assembly and budding process is a highly dynamic, multi-step process mediated by temporally and spatially regulated host-virus interactions. With the advantage to directly visualize protein interactions with high sensitivity, the BiFC technique is highly suitable to study numerous protein interactions during retrovirus assembly and budding process.

## **2.0 HYPOTHESIS AND SPECIFIC AIMS**

Previous studies suggest linkages between retrovirus Gag assembly and budding and the host cell cytoskeleton dynamics as well as the viral gRNA nuclear export pathway. I hypothesize that the host cell actin cytoskeleton might be utilized for retrovirus Gag trafficking. And I hypothesize further that alternative trafficking pathways might be adapted for different retroviruses and for Gag synthesized from mRNA exported from nucleus via different pathways.

To test these hypotheses, I propose to address three specific aims:

**(1) To characterize the Gag-actin interaction sites and the determinants for this interaction;**

**(2) To characterize and compare assembly sites and budding efficiencies of EIAV and HIV-1 Gag;**

**(3) To explore the mechanism by which HIV-1 Gag assembly and budding is regulated by nuclear export pathway taken by viral genomic RNA.**

**3.0 CHAPTER ONE. ASSOCIATION OF GAG MULTIMERS WITH  
FILAMENTOUS ACTIN DURING EQUINE INFECTIOUS ANEMIA VIRUS  
ASSEMBLY**

**3.1 PREFACE**

This chapter is adapted from a published study (Jing Jin<sup>1,4</sup>, Chaoping Chen<sup>5</sup>, Marc Rubin<sup>3</sup>, Liangqun Huang<sup>5</sup>, Timothy Sturgeon<sup>1</sup>, Kelly M. Weixel<sup>2</sup>, Donna B. Stolz<sup>3</sup>, Simon C. Watkins<sup>3</sup>, James R. Bamburg<sup>5</sup>, Ora A. Weisz<sup>2,3</sup>, and Ronald C. Montelaro<sup>1</sup>. *Curr HIV Res.* 2007 May;5(3):315-23.).

<sup>1</sup>Department of Molecular Genetics and Biochemistry, <sup>2</sup>Department of Medicine, Renal-Electrolyte Division, <sup>3</sup>Department of Cell Biology and Physiology, School of Medicine, University of Pittsburgh, Pittsburgh, Pennsylvania

<sup>4</sup>Department of Infectious Disease and Microbiology, Graduate School of Public Health, University of Pittsburgh, Pittsburgh, Pennsylvania

<sup>5</sup>Department of Biochemistry and Molecular Biology, Colorado State University, Fort Collins, Colorado

Work described in this chapter is in fulfillment of specific aim 1.

### 3.2 ABSTRACT

A role for the actin cytoskeleton in retrovirus assembly has long been speculated. However, specific mechanisms by which actin facilitates the assembly process remain elusive. We previously demonstrated differential effects of experimentally modified actin dynamics on virion production of equine infectious anemia virus (EIAV), a lentivirus related to HIV-1, suggesting an involvement of actin dynamics in retrovirus production. In the current study, we used bimolecular fluorescence complementation (BiFC) to reveal intimate (<15nm) and specific associations between EIAV Gag and actin, but not tubulin. Specific interaction between Gag and filamentous actin was also demonstrated by co-immunoprecipitation experiments combined with the actin severing protein gelsolin to solubilize F-actin. Deletion of capsid (CA) or nucleocapsid (NC) genes reduced Gag association with F-actin by 40% and 95%, respectively. Interestingly, GCN4, a leucine zipper motif, could substitute for the NC domain in mediating F-actin association. Furthermore, deficiency of the  $\Delta$ NC Gag in F-actin interaction was restored upon co-expression of Gag constructs containing both CA and NC or the GCN4, suggesting a requirement for Gag polyprotein multimerization prior to F-actin association. The observed Gag-F-actin association appeared to correlate with viral budding, as enhanced budding of the  $\Delta$ NC mutant was evident upon restoration of F-actin association. Intracellular association of Gag complexes with F-actin was also detected by immunoscanning electron microscopy of Triton-extracted EIAV-infected cells. Together, these data suggest that Gag multimers induced by CA and NC domains interact with F-actin and that this association is important for efficient virion production.

### 3.3 INTRODUCTION

Retrovirus assembly and budding is a highly concerted process mediated by specific interactions between viral Gag polyproteins and various host cellular cofactors. The Gag polyprotein is the primary viral determinant for virion production as expression of the Gag polyproteins alone is essential and sufficient to produce virus-like particles (VLPs) in transfected cells (Scarlatà and Carter, 2003). The Gag polyprotein comprises matrix (MA), capsid (CA), nucleocapsid (NC) and late domains, and is cleaved into individual proteins that form virion cores upon virus maturation. These domains perform cooperative roles during retrovirus assembly and budding. For example, the myristoylation signal in the N-terminus of MA is essential for targeting HIV-1 Gag polyprotein to the plasma membrane (Bryant and Ratner, 1990; Bryant et al., 1989; Spearman et al., 1994). CA is required for the dimerization of homologous Gag polyproteins during assembly (Alfadhli et al., 2005; Gamble et al., 1997; Mayo et al., 2003). NC is essential for Gag multimerization and other viral functions including genomic RNA packaging, reverse transcription, integration, and incorporation of Vpr protein into virions (Buckman et al., 2003; Burniston et al., 1999; Johnson et al., 2002; Rein et al., 1998; Takahashi et al., 2001). The L-domains of various retroviruses specifically interact with components involved in steps along the endocytic pathway, including the formation of endosomes (Alroy et al., 2005; Chen et al., 2005; Puffer et al., 1998) and MVBs (Garrus et al., 2001; Strack et al., 2003; VerPlank et al., 2001; von Schwedler et al., 2003), indicating that retroviruses have adapted cellular membrane trafficking machinery for their assembly and budding.

The Gag polyprotein is synthesized from full length genomic RNA on free cytoplasmic ribosomes in infected cells. However, retroviruses predominantly bud from membrane structures, including the plasma membrane in T lymphocytes and epithelial cell lines (Finzi et al.,

2007;Jouvenet et al., 2006;Ono et al., 2004;Ono and Freed, 2001) and multivesicular bodies (MVBs) in primary macrophages (Pelchen-Matthews et al., 2003). It remains largely undefined how thousands of copies of Gag polyproteins are transported from the site of synthesis to assembly and budding sites on target membranes. Our previous studies demonstrate that stabilization of filamentous actin inhibited virion production of equine infectious anemia virus (EIAV) in infected cells (Chen et al., 2004) and we speculated that the actin cytoskeleton is involved in transporting Gag polyproteins within the cytoplasm of infected cells.

There is considerable evidence in the literature consistent with this idea (Chen et al., 2004;Edbauer and Naso, 1983;Liu et al., 1999;Ott et al., 1996;Ott et al., 2000;Sasaki et al., 1995). Perturbation of the actin cytoskeleton affects the assembly and budding of several retroviruses (Audoly et al., 2005;Chen et al., 2004;Maldarelli et al., 1987;Sasaki et al., 1995). Actin and actin-binding proteins have been identified within highly purified HIV-1 virions (Chertova et al., 2006;Ott et al., 1996;Ott et al., 2000;Ott, 2002). Assembly and budding of several retroviruses at actin-rich sites has been reported (Maldarelli et al., 1987;Mortara and Koch, 1986). Cell fractionation analysis using mild detergents such as Triton X-100 demonstrates that Gag polyproteins are present in detergent-insoluble fractions, which also contain actin filaments (Chen et al., 2004;Rey et al., 1996). Furthermore, both *in vitro* translated HIV-1 Gag polyprotein (Rey et al., 1996) and purified nucleocapsids of HIV-1 virions (Liu et al., 1999) co-sediment with polymerized actin filaments. However, to date these observations have not been considered conclusive due to concerns about the possibility that the observed association may be the result of nonspecific interactions between cationic NC Gag protein and anionic actin or the result of the formation of insoluble Gag complexes that copurify with filamentous actin. Here, we sought to examine the nature of the EIAV Gag-actin interaction

using a combination of approaches including high resolution imaging techniques and biochemical analyses. The results of these studies for the first time reveal a highly specific intracellular interaction between multimeric Gag complexes and F-actin that appears to contribute to efficient virion production.

## 3.4 MATERIALS AND METHODS

### 3.4.1 DNA mutagenesis

Overlapping PCR was used to construct Gag mutations and fusion proteins as previously described (Chen et al., 2001b). For bimolecular fluorescence complementation (BiFC) assays, sequences encoding the N (1-173, VN)- or C (155-238, VC)- fragments of venus fluorescence protein (template generously provided by Dr. Atsushi Miyawaki, RIKEN Brain Science Institute, Saitama, JAPAN) were fused to the N-terminus of actin and tubulin via a 6-alanine linker or to the C-terminus of Gag MA domain with two flanking 6-alanine linkers. Individual domains of the Gag polyprotein were deleted to generate  $\Delta CA$ ,  $\Delta NC$  and  $\Delta p9$ , respectively. A DNA fragment encoding the GCN4 leucine zipper sequence was *in vitro* synthesized by PCR, and the resulting fragment was introduced into the EIAV Gag expression vector to replace the NC domain in the GCN4 construct. To make HA-tagged Gag polyproteins, the YPYDVPDY epitope from influenza virus HA protein was inserted into the C-terminus of MA or p9 protein, respectively. All plasmids were isolated with Qiagen Midiprep Kit (Qiagen, Valencia, CA), and the specific mutations were confirmed by DNA sequencing.

### 3.4.2 Cell culture and transfection

Equine dermal (ED) cells (ATCC cat. no. CCL 57, Rockville, MD), Green monkey kidney Cos-7 cells, and fetal equine kidney (FEK) cells were cultured in MEM medium as described (Chen et

al., 2001b). For fluorescence studies (**Figs. 1&2**), Fugene 6 (Roche, Indianapolis, IN) was employed to transfect cells following the recommended procedures by manufacturer. For domain mapping and complementation assays (Fig. **3-6**), GenePorter II (Gene Therapy Systems, San Diego, CA) was used.

### **3.4.3 Fluorescence microscopy**

For confocal imaging, transfected cells grown on coverslips were fixed and permeabilized with 2% paraformaldehyde and 0.1% Triton X-100 in PBS. Images were then captured sequentially using a Leica TCS-SL microscope and processed with Metamorph software (**Fig. 3-2, panels A-E**). Images of gelsolin-mediated F-actin severing and complementation BiFC (**Figs. 3-5&3-7**) or live BiFC (**Fig. 3-4**) were captured with a Nikon Diaphot inverted phase/epifluorescence microscope.

### **3.4.4 Flow cytometry analysis**

Cos-7 cells grown on 6-well plates were transfected with BiFC constructs using FuGene 6 transfection reagent. At 24 h post transfection, cells were detached with PBS containing 2.5 mM EDTA and resuspended in PBS solution. A minimum of 50,000 gated live events were acquired on a FACSCalibur (Becton Dickinson) flow cytometer and analyzed with FlowJo batch analysis software (Treestar).

### 3.4.5 Cell fractionation and immunoprecipitation

Separation of Triton X-100 soluble and insoluble fractions has been described previously (Chen et al., 2004). Gelsolin was purified as described previously (Larson et al., 2005; Pope et al., 1997). For gelsolin-mediated fractionation, cells (about  $5 \times 10^6$ ) were collected by centrifugation at 500 xG for 5 min and resuspended with 200  $\mu$ l of extraction buffer (0.5% Triton X-100, HEPES 20mM, NaCl 110 mM, KCl 25mM, KOAC 25mM, MgCl<sub>2</sub> 4mM, 1x protease inhibitor cocktail, EGTA 1mM, pH7.4) for 5 min at ambient temperature. The mixture was centrifuged at 500 xG for 5 min, and the recovered supernatant was designated as the S1 fraction. The pellet was further incubated for 5 min in 200  $\mu$ l of severing buffer (HEPES 20mM, NaCl 110 mM, KCl 25mM, KOAC 25mM, MgCl<sub>2</sub> 4mM, 1x protease inhibitor cocktail, CaCl<sub>2</sub> 2mM, pH 7.4) containing 0.2-1  $\mu$ M of *in vitro* purified gelsolin. The gelsolin-treated mixture was centrifuged at 1000 xG for 5-7 min, and the resulting supernatant (S2) collected. The pellet was then solubilized in 200  $\mu$ l lysis buffer (25 mM Tris-HCl, pH 8.0, 150 mM NaCl, 1% deoxycholic acid, 1% Triton X-100, 1x protease inhibitor cocktail), centrifuged at 20,800 xg for 2 min to remove cell nuclei. The resulting supernatant was designated as the S3 fraction. Each fraction (normalized to equal amounts of Gag proteins) was mixed with 5  $\mu$ l of anti-HA agarose beads (Sigma, St. Louis, MO) and incubated at 4°C overnight on an end-to-end shaker. The anti-HA beads were washed with 200  $\mu$ l of the corresponding buffer for three times. Proteins bound to the beads were eluted with low pH buffer (Pierce, Rockford, IL) for further analysis.

### **3.4.6 EIAV Gag protein expression assays**

Virus-like particles (VLPs) released into culture medium were pelleted (20,800 xG, 3 h, 4°C) and resuspended in 1x PBS solution. Detection of EIAV-specific Gag polyproteins and HA-tagged fusion proteins were described previously (Chen et al., 2004;Chen et al., 2005).

### **3.4.7 Immuno-gold labeling of EIAV Gag proteins and SEM**

Uninfected and infected ED cells were extracted with 0.75% of Triton-X-100 before fixation with 2% paraformaldehyde. Purified rabbit IgG against EIAV CA (1:50) and goat anti-rabbit antibody (1:25) conjugated to 15nm gold particles (Amersham, Piscataway, NJ) were used to immuno-label Gag proteins. Cells were then fixed in 2.5% glutaraldehyde and processed for SEM observation using a JEOL JEM-6335F field emission gun scanning electron microscope (JEOL, Peabody, MA, USA). Field emission backscattered electron and standard scanning electron digitized images were taken in tandem to identify areas of gold labeling on the cell surfaces.

## 3.5 RESULTS

### 3.5.1 Intracellular association of EIAV Gag with actin

We previously reported that perturbation of the actin cytoskeleton altered the efficiency of EIAV production (Chen et al., 2004). To determine whether Gag association with filamentous actin was responsible for these effects we initially examined Gag-actin interactions by confocal microscopy in equine dermal (ED) cells infected with EIAV. Both intact and Triton X-100 extracted cells were labeled with antibodies specific for EIAV Gag proteins (Fig. 3-1, panels A&E) and with fluorescent phalloidin for F-actin (Fig. 3-1, panels B&F). A subpopulation of Gag protein co-localized with F-actin in both intact (Fig. 3-1, panels C, D&I) and detergent-extracted cells (Fig. 3-1, panels G, H&J). However the prevalence of filamentous actin throughout the cytoplasm limited our ability to draw definitive conclusions from these colocalization assays. Therefore, we sought to confirm the observed intracellular association between Gag and actin using more specific approaches.

The bimolecular fluorescence complementation (BiFC) assay is a powerful tool to visualize specific protein interactions in the cellular environment (Hu et al., 2002; Kerppola, 2006; Nyfeler et al., 2005). In this technique, the amino- and carboxy-terminal fragments of fluorescent proteins are individually fused to proteins of interest that are co-expressed in pairs. Interaction between the fusion protein pairs then facilitates association of the fluorescent protein fragments (within a distance less than 15 nm) (Hu et al., 2002) to produce a stable fluorescent complex. To test the interaction between EIAV Gag and actin by BiFC methods, we generated a

panel of constructs with Gag and actin proteins fused to fragments of the yellow fluorescent protein variant “Venus” (VN and VC, respectively)(Shyu et al., 2006). Cos-7 cells expressing the VN-actin/VC-actin pair (Fig. 3-2 B) demonstrated a fluorescence pattern similar to that observed in YFP-actin transfected cells (Fig. 3-2, panel A), indicating that the actin-Venus fusion proteins were efficiently incorporated into filaments. Importantly, positive BiFC signal was readily detected in cells expressing the Gag/actin pair (Fig. 3-2, panel C), indicative of a close association of Gag and actin in transfected cells. To confirm the specificity of the observed Gag-actin interactions, we also examined Gag interactions with tubulin, another abundant cytoskeletal protein that mediates numerous cellular processes, including pathogen transport. Unlike the Gag/actin pair, transfection of the Gag/tubulin pair produced only background levels of fluorescence (Fig. 3-2, panel D). The biological activity of these tubulin fusion constructs was verified in cells expressing the tubulin/tubulin BiFC pair, in which BiFC signals demonstrated a normal cellular microtubule organization (Fig. 3-2, panel E). We also observed Gag-Gag interaction-mediated BiFC in cells expressing the VN-Gag/VC-Gag pair (Fig. 3-3, panel A). Late endosomes of the same cell were also labeled with CD63 antibody (Fig. 3-3, panel B) and the Gag-Gag BiFC signals appeared to colocalize with the CD63-positive compartments (Fig. 3-3, panel C). A subset of the Gag-actin BiFC complexes also overlapped with CD63 staining (Fig. 3-3, panel F).

To complement the qualitative BiFC interaction assays described above, we next sought to obtain quantitative information about Gag-actin interaction by flow cytometry analysis of cells transfected with various BiFC pairs (Fig. 3-2, panels F-J). Transfection with only the VC-actin served as a control to measure the background level of cellular autofluorescence in our assay (Fig. 3-2, panel F). Approximately 9% of cells transfected with the actin/actin BiFC pair

exhibited positive fluorescence as a result of BiFC mediated by actin-actin interactions (**Fig. 3-2, panel G**). Similarly, about 8% of cells transfected with the Gag-actin pair were positive for BiFC (**Fig. 3-2, panel H**). In contrast, less than 1% and 2% of cells transfected with the Gag/tubulin and the actin/tubulin pairs, respectively, displayed fluorescence above background levels (**Fig. 3-2, panels I&J**).

We next compared Gag-actin and Gag-Gag BiFC signals in living cells. In Cos-7 cells expressing the VN-actin and VC-Gag pair, about 90% of the observed BiFC complexes remained stationary when imaged at a 5 sec interval over periods of 5-10 min (data not shown). However, about 10% of BiFC complexes migrated rapidly in the cytoplasm with movement towards both the cell surface and the nucleus (**Fig. 3-4, panel A**). Panel 2C-F displays snapshots of a BiFC particle that travels from a juxtannuclear region towards the cell periphery. Similarly, in cells expressing the Gag-Gag BiFC pair, about 10% positive BiFC signals actively migrated in the cytoplasm (**Fig. 3-4, panel G**). Panel 2H-L demonstrates two BiFC complexes that migrated rapidly over a 20 sec time interval. The BiFC complexes did not migrate at a constant velocity; instead, rapid movement usually followed a period of restricted local motion of the complex. Some BiFC complexes traveled very rapidly; during the 1 sec exposures they appeared as comet-like streaks (**Fig. 3-4, panels D, I&J**) with an estimated velocity of up to 0.5-1  $\mu\text{m/s}$ .

### **3.5.2 EIAV Gag proteins coimmunoprecipitate with filamentous actin**

We and others previously reported that about 50% of intracellular Gag polyproteins are associated with insoluble filamentous actin (F-actin) recovered after treatment of cells with Triton X-100 in EIAV-infected ED cells (Chen et al., 2004). Although our BiFC results demonstrated close interaction between Gag and actin inside cells, we could not determine

whether actin monomers or filaments are recruited by Gag by this assay. To examine whether the Triton X-100-insoluble fraction contains Gag-actin complexes, we developed an in vitro actin-severing protocol using purified gelsolin, a Ca<sup>++</sup>-dependent F-actin severing protein. Our rationale was that actin filaments shortened by gelsolin activity would become soluble, along with any actin-associated Gag. The F-actin severing activity of purified gelsolin was verified using equine dermal (ED) cells expressing eGFP-actin (**Fig. 3-5, panels A-F**). Fluorescently-labeled filamentous actin in these cells is resistant to Triton X-100 washes (**Fig. 3-5, panel D**). Upon brief (2-5 min) incubation with 500 nM gelsolin at ambient temperature, the majority of the GFP-actin filaments disappeared, presumably as shortened actin fragments dissolved into the reaction buffer (**Fig. 3-5, panel F**). The observed disappearance of fluorescent actin was specific for gelsolin treatment, as incubation of cells with severing reaction buffer alone had no significant influence on the fluorescent intensity of actin filaments over a period of 20 min (data not shown).

Using the gelsolin severing assay, we next fractionated EIAV-infected fetal equine kidney (FEK) cells to obtain Triton X-100 soluble (S1), gelsolin-soluble (S2) and lysis buffer-soluble (S3) fractions (**Fig. 3-5, panel G**). The S1 is equivalent to the Triton X-100 soluble fraction described previously (Chen et al., 2004). The S2 contains gelsolin-dissolved F-actin and associated proteins, and the S3 contains residual insoluble proteins. Thus, the sum of S2 and S3 is roughly equivalent to the previously described Triton X-100-insoluble fraction (Chen et al., 2004). Separation of the S2 and S3 fractions allowed us to differentiate the Gag polyproteins associated with F-actin from the Triton X-100 insoluble Gag aggregates formed during the process of virion assembly. For these studies, we employed FEK cells chronically infected with EIAVuk(MA-HA) virus, a proviral construct modified to contain an influenza virus HA epitope

tag in the C-terminal region of the MA domain of Gag polyprotein. The EIAVuk(MA-HA) virus was shown in preliminary experiments to replicate as efficiently as the wild type EIAVuk in experimentally infected FEK cells (data not shown). Western blotting analysis of equal volume of the S1-S3 fractions from the virus infected cells demonstrated the presence of Gag protein in all three fractions. The S2 fraction contained about 10-15% of total Gag (the S1 about 50% and the S3 about 35-40%) (data not shown), suggesting a subpopulation of Gag was released from the insoluble fraction. No Gag protein was detected when gelsolin was eliminated from the severing buffer (data not shown).

To examine whether Gag and actin co-exist as complexes in the three fractions, we next immunoprecipitated HA-Gag and associated proteins by adding anti-HA antibodies coupled to agarose to each fraction normalized to equal amounts of Gag proteins (**Fig. 3-5, panel H**, right half). The immunoprecipitated proteins recovered from the beads were then examined by Western blotting. As shown in **Fig. 3-5, panel H** (right half), only the HA-tagged Gag proteins were specifically recovered in the precipitate from each fraction; mature capsid proteins were not detected due to the lack of an HA tag (**Fig. 3-5, panel H**, right top). Treatment of the same blot with anti- $\beta$ -actin antibody revealed actin in the S2 fraction, evidently as a co-immunoprecipitate with HA-Gag (**Fig. 3-5, panel H**, right bottom). In contrast, co-immunoprecipitation of actin with Gag proteins in either the S1 or the S3 fraction was not observed under these conditions. Taken together, these data demonstrate the specific association of Gag proteins with F-actin in the detergent insoluble complexes.

### 3.5.3 Gag domain requirements for F-actin association

Previous study shows that purified HIV-1 nucleocapsid proteins (and Gag polyproteins) bind to *in vitro* polymerized actin filaments in a co-sedimentation assay (Liu et al., 1999; Rey et al., 1996). However, it remains unclear whether this binding is due to nonspecific electrostatic interactions or instead mediated by a specific interaction between the two proteins. Here, we sought to examine the Gag-actin interactions using a panel of EIAV Gag expression vectors lacking individual domains (**Fig. 3-6, panel A**) Western blots of lysates from ED cells transfected with the individual Gag constructs demonstrated expression of each of the mutant Gag polyproteins at their expected molecular mass (**Fig. 3-6, panel B**). Approximately equal amounts of the wild-type Gag polyprotein were present in the Triton-soluble and -insoluble fractions of the cell lysate, as reported previously (Chen et al., 2004). Deletion of CA in the Gag construct reduced the level of insoluble Gag to about 40% of the wild type level (**Fig. 3-6, panel B**). Deletion of NC resulted in a 95% loss in Gag associated with the insoluble fraction. In contrast, deletion of p9 enhanced F-actin association by 60% compared to wild type Gag. These results indicate that the NC region of the polyprotein is the primary determinant for F-actin association, but that other Gag protein domains can influence the interaction, both positively and negatively. To further define the role of NC in mediating F-actin association, we constructed a chimeric expression vector with the NC domain replaced by the leucine zipper motif of a yeast transcription factor (GCN4). The same motif was used to replace HIV-1 NC in the minimal Gag construct (Accola et al., 2000). Interestingly, the GCN4 Gag showed wild type levels of F-actin association (**Fig. 3-6, panel B**), suggesting that the oligomer-inducing function rather than the specific sequence, of the NC domain plays a role in F-actin association.

To define the role of CA in F-actin association, we performed complementation analysis to test ability of Gag polyproteins to rescue  $\Delta$ NC deficiency in F-actin association. The distribution of the  $\Delta$ NC-HA between Triton-soluble and -insoluble fractions generated from transfected cells was examined by Western blotting with anti-HA antibody. The percentage of insoluble HA-tagged  $\Delta$ NC as in the total detected  $\Delta$ NC-HA was calculated to reflect F-actin association efficiency of the HA-tagged  $\Delta$ NC. Less than 5% of the  $\Delta$ NC-HA was insoluble in cells cotransfected with  $\Delta$ NC-HA and  $\Delta$ NC at a 1:1 mass ratio. In marked contrast, co-expression of  $\Delta$ NC-HA with wild type Gag produced ~30% insoluble  $\Delta$ NC-HA (**Fig. 3-6, panel C**). This data indicates that the wild type Gag rescued F-actin association of  $\Delta$ NC-HA, presumably through homolog dimerization mediated by the CA proteins of the two constructs. Co-expression of the  $\Delta$ NC-HA construct with the  $\Delta$ CA construct failed to rescue the association of HA- $\Delta$ NC with F-actin (<5% insoluble) (**Fig. 3-6, panel C**), supporting a role for the CA domain in complementation. Interestingly, co-expression of the  $\Delta$ p9 construct rescued F-actin association of HA-tagged  $\Delta$ NC to yield ~50% insoluble protein, a level that was reproducibly higher than the ~30% observed upon complementation with the wild type Gag construct. The  $\Delta$ p9 construct itself also displayed an enhanced F-actin association (**Fig. 3-6, panel B**), perhaps indicating an inhibitory role for the late domain in F-actin association or an enhanced activity of F-actin dissociation (Chen et al., 2004). Taken together, these data suggested that association with F-actin requires both CA-mediated dimerization and NC-mediated oligomerization of Gag polyproteins.

While the preceding complementation experiments examined the determinants of Gag association with F-actin, these studies did not address the correlation between Gag multimer-F-actin association and virion production. To investigate this correlation, we measured virus-like

particle-associated HA- $\Delta$ NC in the supernatants of the co-transfected ED cells. As presented in **Fig. 3-6, panel C**, virion production was positively correlated with F-actin association efficiency. Co-transfection of the HA- $\Delta$ NC with the  $\Delta$ NC or  $\Delta$ CA constructs produced limited amounts of VLP, while co-transfection with wild type Gag, the  $\Delta$ p9 and the GCN4 Gag constructs enhanced virion production of the HA- $\Delta$ NC by an average of about 3 fold.

We then examined whether the  $\Delta$ NC mutant interacts with actin using BiFC. In cells co-transfected with the  $\Delta$ NC-VN/VC-actin pair, we only observed low levels of diffuse fluorescence (**Fig. 3-7, panel A**). In contrast, with co-expression of wild type Gag, the  $\Delta$ NC-VN/VC-actin pair displayed a punctate staining pattern (**Fig. 3-7, panel B**) reminiscent of that observed in cells expressing the Gag-VN/VC-actin pair (**Fig. 3-7, panel D**). Co-expression of EIAV Gag-hCA, a chimeric Gag in which the EIAV CA domain is replaced by the HIV CA domain, failed to rescue actin association of  $\Delta$ NC (**Fig. 3-7, panel C**).

In the preceding BiFC assays (**Fig. 3-7, panels A-D**), we employed plasmids DNA mass ratios different from those in the complementation assays based on Gag solubility (**Fig. 3-7**). We next sought to verify the CA-mediated rescue of the  $\Delta$ NC deficiency by repeating the insolubility complementation assay using the plasmid ratios employed in the BiFC, The results presented in **Fig. 3-7, panel E** demonstrated effective complementation under these transfection conditions. Taken together, our data suggested that Gag multimers induced by CA- and NC- function are the functional units that interact with actin filaments.

### 3.5.4 Immuno SEM of Gag-actin association

To obtain higher resolution images of EIAV Gag-actin complexes, we utilized immuno-scanning electron microscopy to visualize Gag proteins associated with F-actin in Triton X-100-extracted ED cells (**Fig. 3-8**). In these studies, the ultrastructure of the insoluble actin cytoskeleton and Gag polyproteins stained with gold-labeled antibody in the same field were examined using scanning EM. Superimposition of the two images revealed extensive labeling of Gag polyproteins associated with the actin filament network (**Fig. 3-7, panel A**) that was absent in uninfected cells (**Fig. 3-8, panel B**). Examples of representative EIAV Gag complexes associated with actin filaments are shown in **Fig. 3-8, panel C**. The size of Gag complexes associated with actin filaments varied from 20 to 70 nm in diameter. As typical mature retrovirus virion cores are about 120 nm in diameter (Briggs et al., 2003b; Briggs et al., 2004; Roberts and Oroszlan, 1989), this suggests that Gag-actin interactions occur prior to the completion of Gag assembly.

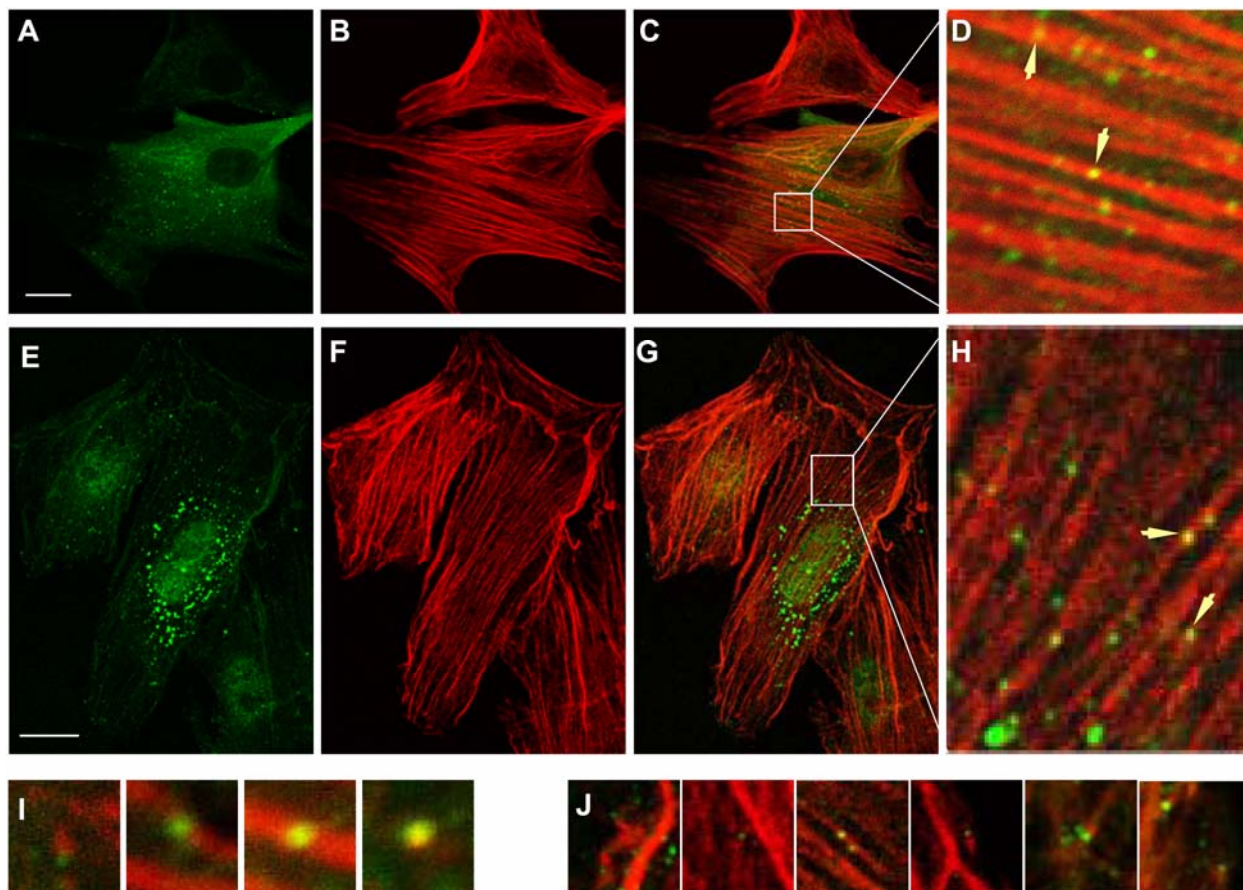


**Figure 3-1. Confocal association of Gag proteins with the actin cytoskeleton in EIAV-infected ED cells.**

Intact (A-D, I) and Triton X-100 extracted (E-H, J) ED cells infected with EIAV were stained using a rabbit anti-EIAV antibody to detect Gag polyprotein (A, E) and Alexa phalloidin 647 to label filamentous actin (B, F). Proximate localization of Gag proteins with F-actin is demonstrated in panels C and G, and the indicated regions of these panels are enlarged in D and H. More examples of overlays from intact (I) and extracted (J) cells are shown in the bottom panel. Bars: 10 $\mu$ m.

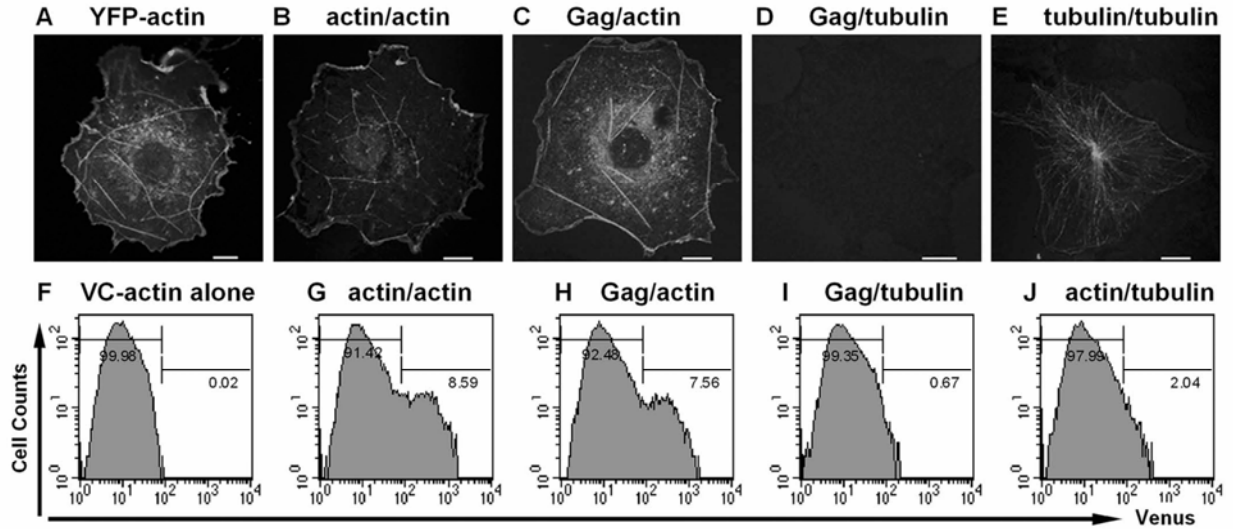


**Figure 3-2. BiFC analysis of Gag-actin interactions.**

Cos-7 cells grown on glass coverslips were transfected with the indicated plasmids using Fugene 6. At 24 h post transfection, cells were fixed with 2% paraformaldehyde and imaged with a Leica TCS-SL confocal microscope. Fluorescence signals in panel B-E represent positive BiFC activity resulting from formation of the Venus fluorescent complex induced by protein-protein interaction. To quantify BiFC activity, Cos-7 cells were transfected with the indicated plasmid pairs. At 24 h post transfection, about 100,000 transfected cells were collected and analyzed by FACS. Cells displaying higher than background fluorescence as a percentage of total population were calculated to reflect BiFC activity.

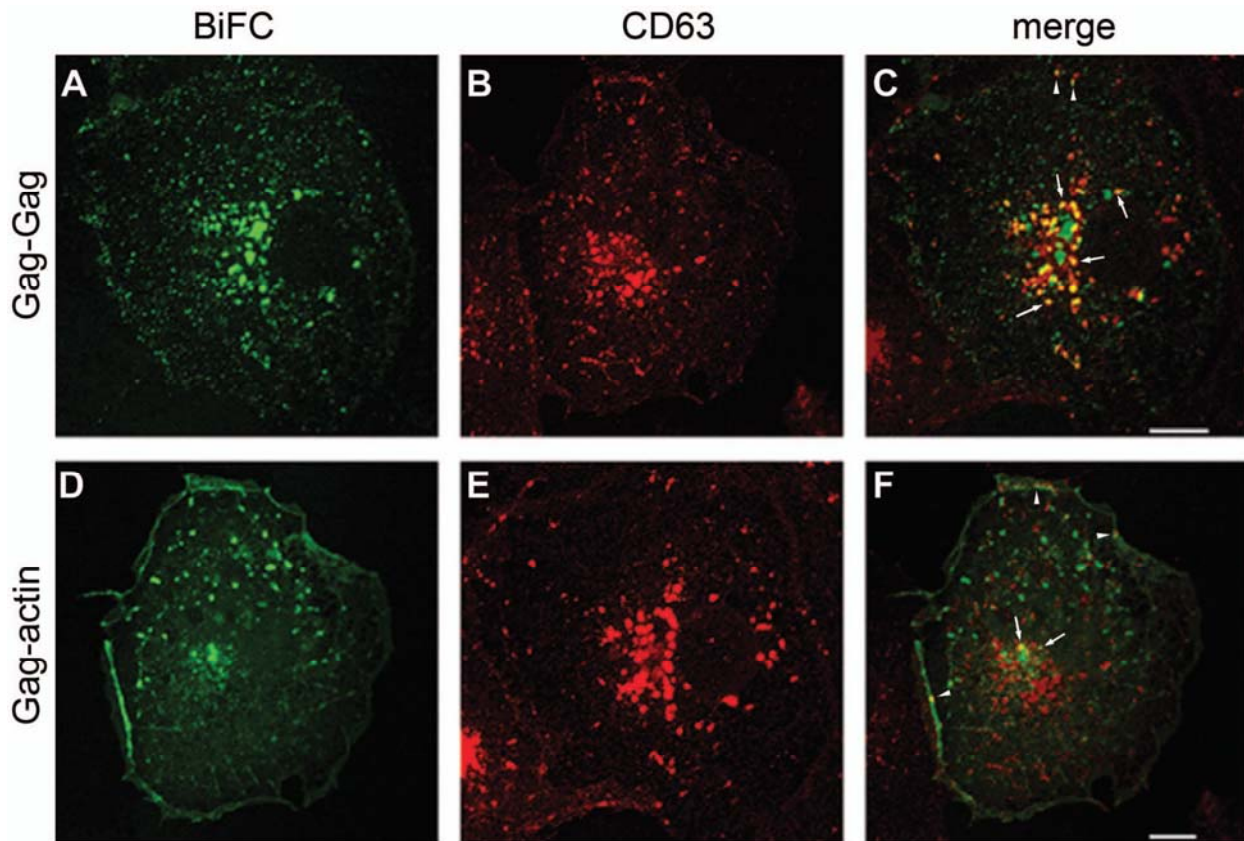


**Figure 3-3. Colocalization of Gag-Gag and Gag-actin BiFC complexes with CD63 positive compartments.**

Transfected Cos-7 cells expressing the VN-Gag/VC-Gag pair (A-C) or VN-Gag/VC-actin pair (D-F) were fixed and permeabilized at 24 h post transfection. Mouse anti-LAMP-3 antibody and Alexa Fluor®647 goat anti-mouse were used as primary and secondary antibodies to visualize CD63-positive subcellular compartments in transfected cells (B&E). Overlay of two images of the same field revealed colocalization of Gag-Gag BiFC complexes(C) or Gag-actin BiFC complexes (F) with CD63 at both perinuclear (arrows) and peripheral regions of cells (arrowheads). Bars: 10  $\mu$ m.

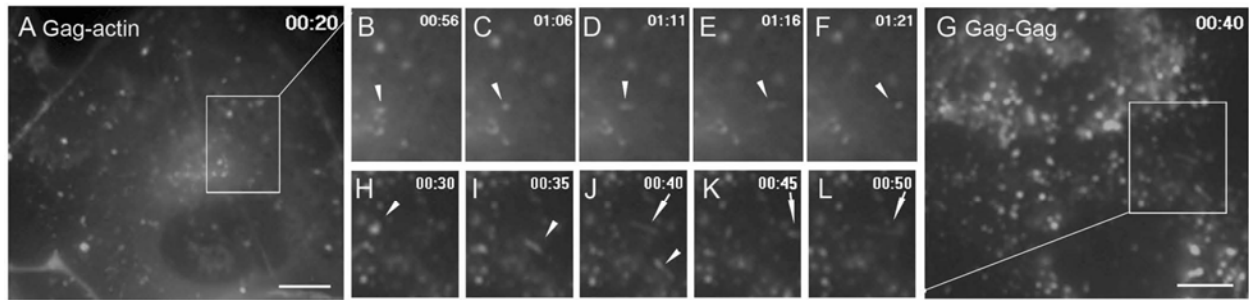


**Figure 3-4. Live cell imaging of BiFC complexes.**

Cos-7 cells grown on glass-bottom petri dishes were transfected with the VN-Gag/VC-actin (**A-F**) or VN-Gag/Gag-VC (**G-L**) pairs. At 15-24h post transfection, cells were imaged by a Nikon Diaphot inverted epifluorescence microscope equipped with a heated stage at 5s intervals. Panel A is a snapshot of a movie showing the motility of Gag-actin BiFC complexes. Panel B-F shows snapshots of an area of panel A. Arrowheads point to a migrating particle over the indicated time. Panel G is a frame linked to supplemental movie 2 demonstrating migration dynamics of Gag-Gag BiFC complexes. A series of snapshots of a small area in panel G are also presented (H-L). Arrowheads and arrows denote two individual BiFC complexes that migrated so rapidly resulting in comet tail-like streaks. Bars: 5 $\mu$ m.

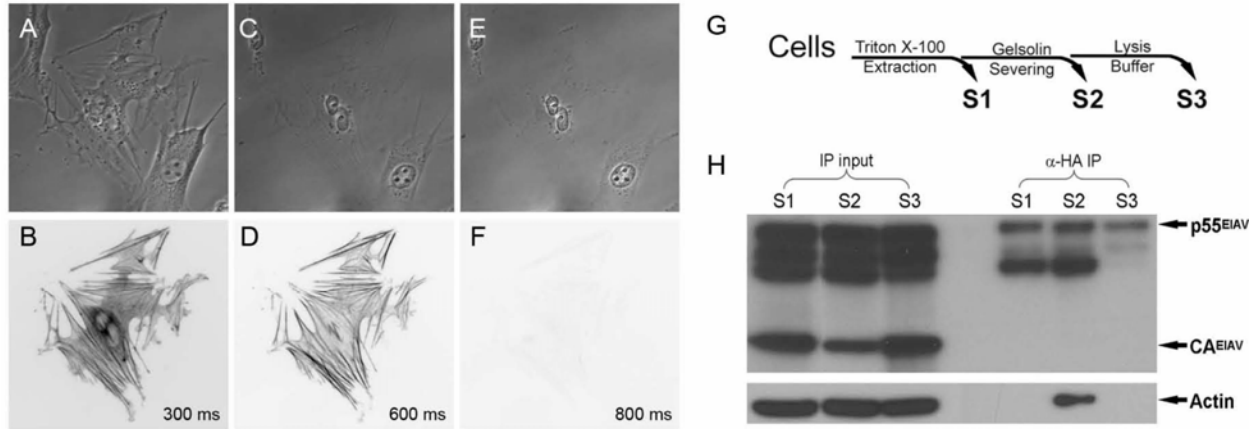


**Figure 3-5. Association of Gag with filamentous actin.**

**A-F:** Gelsolin-mediated F-actin severing in equine dermal cells expressing GFP-actin. Images were captured before (A&B) and after (C&D) cells were treated with 0.5% Triton X-100. Cells were then incubated with 1 $\mu$ M of gelsolin for 5 min (E&F). Phase (A, C, E) and inverted monochromatic fluorescence (B, D, F) images of the same field acquired after each experimental manipulation are shown here. The same imaging condition was used except for the exposure time as indicated.

With gelsolin-mediated F-actin severing, three fractions: Triton X-100 soluble (S1); gelsolin dissolved actin filaments and association proteins (S2); and residual insoluble components (S3) were prepared from fetal equine kidney (FEK) cells chronically infected with an EIAVuk virus that contains an HA epitope at the C-terminus of the MA of Gag (G). Each fraction normalized to about equal amount of Gag polyprotein was incubated with anti-HA antibody conjugated agarose beads to immunoprecipitate HA-tagged Gag and association proteins. Proteins bound to the beads were eluted and analyzed by SDS-PAGE and immunoblotting (right half). Rabbit anti-EIAV antibody was used to detect EIAV specific Gag proteins. The same blot was stripped and reprobed with anti- $\beta$ -actin antibody to detect cellular actin. The IP input lanes (left half) represent about 5% of each fraction used for IP experiments.

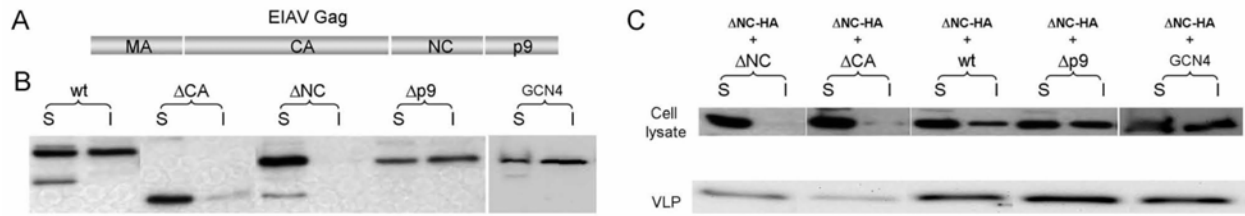


**Figure 3-6. Functions of Gag domains in F-actin association.**

**A:** Schematic diagram of Gag polyprotein protein structure. **B:** Cells expressing the indicated Gag constructs were fractionated into Triton X-100 soluble and insoluble fractions as described previously (23). EIAV Gag proteins in these fractions were detected by Western blotting using a reference serum from an EIAV-infected horse (23). **C:** The  $\Delta$ NC-HA was cotransfected into ED cells with the indicated (untagged) Gag constructs at an equal mass ratio. The  $\Delta$ NC-HA in Triton-soluble and -insoluble fractions (upper panel) and the amount of VLPs produced from each transfection (lower panel) were specifically detected with an anti-HA antibody. Data are representative of three independent experiments.

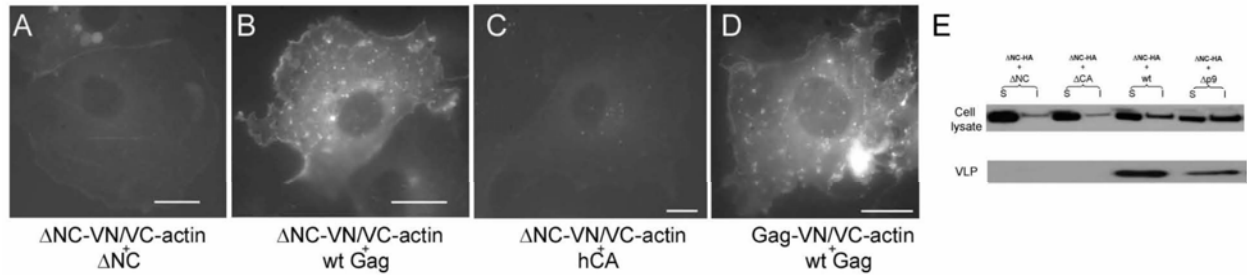


**Figure 3-7. Gag multimers interact with actin.**

Cos-7 cells grown on glass-bottom petri dishes were transfected with plasmid mixtures. A constant amount of 0.4  $\mu\text{g}$  total DNA was used for each dish with specified mass ratios (A: VN- $\Delta\text{NC}$ :VC-actin: $\Delta\text{NC}$ =2:5:33; B: VN- $\Delta\text{NC}$ :VC-actin:wtGag=2:5:33; C: VN- $\Delta\text{NC}$ :VC-actin:hCA=2:5:33; D: VN-Gag:VC-actin:wtGag=5:5:30). At 15 h post transfection, images were captured with a Nikon Diaphot inverted phase/epifluorescence microscope using the same conditions (Bars: 10  $\mu\text{m}$ ). Positive signals represent BiFC complexes resulting from association of VN- $\Delta\text{NC}$  with VC-actin under the indicated conditions (A-C). Cells transfected with the VN-Gag/VC-actin pair displayed characteristic punctuated staining (D). The hCA stands for a chimeric Gag with the EIAV CA replaced by HIV-1 CA. Complementation of the  $\Delta\text{NC}$  by the indicated Gag constructs using the same ratios as in panel A-D showed the similar result as in Figure 3-4 (E).

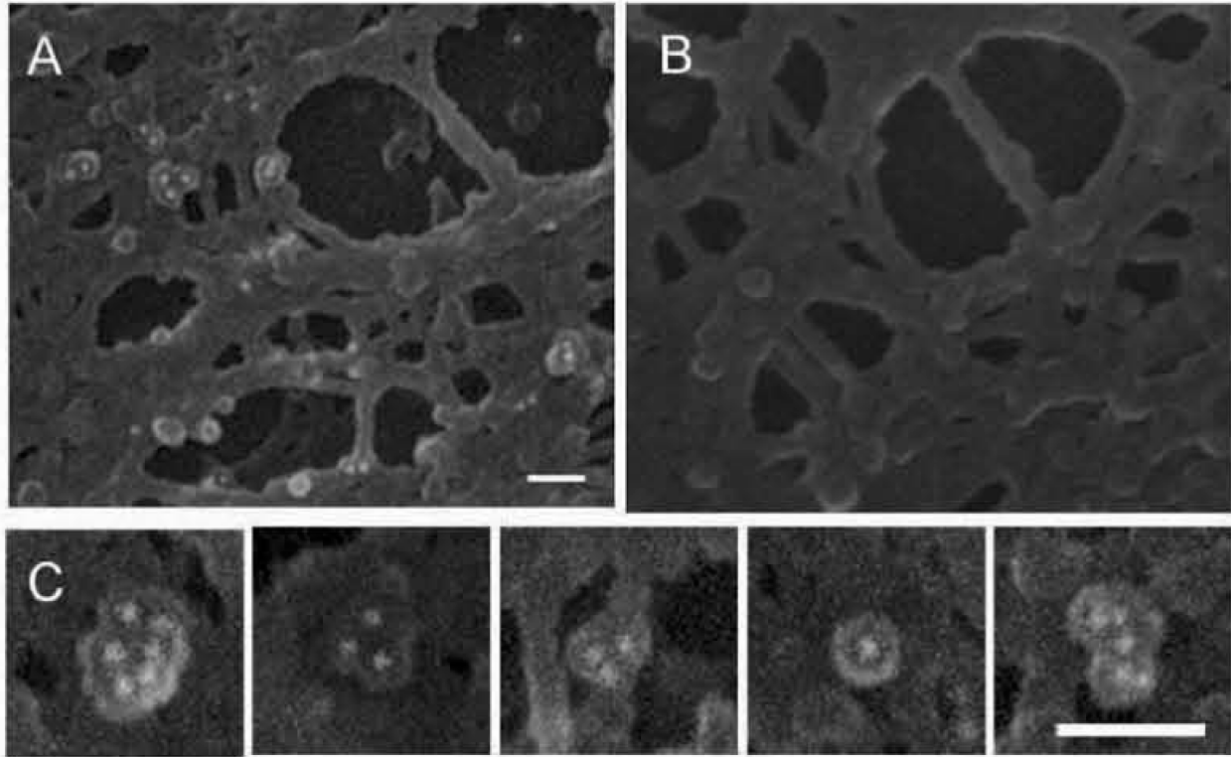


**Figure 3-8. Immuno-SEM images of Gag complexes associated with actin filaments.**

EIAV-infected and uninfected ED cells were Triton X-100 extracted before fixation and immuno-gold labeling. Rabbit anti-p26 antibody and 15nm gold conjugated secondary antibody were used to label Gag proteins. The actin cytoskeleton structure and gold signal from antibody labeling of the same fields were recorded separately and merged to reveal the association of Gag complexes with the actin cytoskeleton in infected (A) and uninfected (B) ED cells. Enlarged overlays showing individual examples of Gag complexes associated with actin filaments are shown in panel C. Bars: 0.1  $\mu\text{m}$ .

## **3.6 DISCUSSION**

There is a history of observations suggesting an involvement of the actin cytoskeleton in the assembly and budding of several retroviruses (Audoly et al., 2005;Chen et al., 2004;Edbauer and Naso, 1983;Fackler and Krausslich, 2006;Liu et al., 1999;Ott et al., 2000;Rey et al., 1996;Sasaki et al., 1995). However, a definitive mechanistic role for actin in these events has not been widely accepted due to concerns that co-purification of Gag and actin filaments in detergent fractionated cell lysates might represent insoluble Gag assembly complexes rather than specific Gag associations, and that actin-modulating reagents might potentially affect Gag assembly and virion budding in an indirect manner. Here we have used the recently developed BiFC technique to eliminate concerns of Gag insolubility or inhibitor specificity by analyzing actin-Gag interactions in living cells. The results presented here for the first time provide definitive evidence that Gag multimers interact with filamentous actin in transfected and infected cells and that specific Gag-actin interactions are positively correlated with the production of progeny virions.

### **3.6.1 Specificity of Gag-actin interactions**

Cellular actin is present in two forms, designated globular (G) and filamentous (F) actin. Whereas G-actin is soluble; F-actin is predominantly insoluble in detergents such as Triton X-100. In fact, co-purification of proteins with the insoluble F-actin has been used as evidence of F-actin interaction with EIAV Gag (Chen et al., 2004) and HIV-1 Gag (Liu et al., 1999;Rey et al.,

1996). However, this assay can not differentiate insoluble Gag aggregates from specific Gag-actin complexes. In the current studies we employed imaging and biochemical techniques that minimize the potential problem of insoluble actin aggregates to demonstrate the specific association of Gag and F-actin. First, the BiFC assay revealed highly specific and close Gag-actin interactions in live cells that were at a level similar to that observed for Gag-Gag and actin-actin interactions (**Fig. 3-2**). As BiFC depends on the two interacting proteins to bring the complementary fluorescence protein fragments close enough to fold into stable fluorescence complex, a positive BiFC signal implies a distance of less than 15 nm between the two interacting proteins (Hu et al., 2002; Kerppola, 2006). Consistent with our BiFC result, HIV-1 Gag-actin interactions were recently reported using fluorescence resonance energy transfer (FRET) assay, suggesting a distance less than 6 nm between the interacting Gag and actin (Poole et al., 2005) although these experiments did not distinguish between G-actin and F-actin. Importantly, the specificity of the interactions between Gag and actin detected by the BiFC assay was confirmed by the lack of BiFC activity between Gag and tubulin, another abundant cytoskeletal protein. Second, EIAV Gag protein was solubilized concomitantly with F-actin upon gelsolin treatment and co-immunoprecipitated with actin (**Fig. 3-5**), further suggesting a Gag association with F-actin. However, it should be noted that although both BiFC and co-immunoprecipitation assays demonstrated positive association of Gag polyprotein and F-actin it remains unclear whether the interaction is direct or indirect.

Gelsolin severing of the Triton X-100 insoluble fraction only released about 10% of total Gag proteins from the insoluble fraction, suggesting a small subset of Gag polyprotein is associated with F-actin. Similarly, about 10% of Gag-GFP and Gag-actin particles were detected as highly mobile particles in transfected cells. Transient association of Gag with F-actin during

intracellular transport might account for these phenomena. Further studies are under the way to examine whether other cellular factors are present in these Gag-actin complexes.

### **3.6.2 Gag multimerization before F-actin association**

Gag polyproteins play numerous roles in the production of viral particles (Zimmerman et al., 2002), and several assembly intermediates during this process have been described (Derdowski et al., 2004; Lee et al., 1999; Zimmerman et al., 2002). The current results identify a role for the association of Gag multimers with F-actin during virus assembly. The oligomerization function of the NC domain appears to be the primary determinant for the formation of this intermediate (**Fig. 3-6, panel B**); whereas the CA-mediated dimerization of homologous Gag polyproteins also contribute to the formation of Gag multimers (Bennett et al., 1993; Derdowski et al., 2004; Gamble et al., 1997). Our data support the hypothesis that Gag multimers utilize the dynamic actin network to transport themselves in the infected cell. Such a batch-transport mechanism could move Gag polyproteins more efficiently. Recent studies demonstrate that during early stages of retrovirus assembly, Gag polyproteins (presumably monomers) are distributed evenly throughout the cytoplasm (Gomez and Hope, 2006; Neil et al., 2006; Perlman and Resh, 2006). The  $\Delta$ NC mutant that fails to form multimers also showed a diffuse distribution pattern in transfected cells (data not shown). Association of Gag multimers with F-actin might reflect a stage during which Gag complexes are targeted to specific membrane compartments for virion assembly and budding. The specific association of F-actin with Gag-enriched complexes that we observed by immuno-SEM supports this idea. The actin interaction-competent intermediate identified in this study might be equivalent to the high-molecular-weight, detergent-resistant HIV-1 assembly intermediates previously described using a similar Triton X-100

extraction method (Dooher and Lingappa, 2004;Lee et al., 1999;Lee and Yu, 1998;Sandefur et al., 2000). Further characterization of these intermediates should shed light on the mechanism and regulation of Gag-actin interaction. In this regard, multimerization and heterologous complementation of HIV-1 and HIV-2 Gag has recently been reported, further emphasizing the critical role of Gag multimers in viral assembly (Boyko et al., 2006).

### **3.6.3 Roles of Gag-actin interaction**

An increasing number of microbes have been reported to exploit the actin cytoskeleton for intracellular transport (Dramsi and Cossart, 1998;Lakadamyali et al., 2003;Lehmann et al., 2005;Wolffe et al., 1997). The identified Gag-actin interactions in this report have led us to speculate that Gag multimers utilize the actin cytoskeleton for targeting to budding sites in the infected cell. There are two possible mechanisms by which F-actin can mediate the trafficking of Gag multimers. The processive movement of myosin and related motors along actin filaments can effectively transport associated components (Vale, 2003). Alternatively, nucleation and growth of actin filaments can also provide the mechanical force to propel components associated with the growing end of these structures, as utilized by *Listeria monocytogenes* to propel the pathogen in infected cells (Dabiri et al., 1990;Merz and Higgs, 2003). In either case, Gag-actin interaction is expected to be both transient and dynamic, consistent with our BiFC analysis of Gag-actin (**Fig. 3-4, panels A-F**) and Gag-Gag (**Fig. 3-4, panels G-L**) complexes, in which we observed about 10% of Gag-actin and Gag-Gag complexes in active migration. Further elucidation of the molecular and cellular mechanisms of Gag-actin interactions can provide new insights into the role of actin cytoskeleton in retrovirus assembly and budding.

The results of the current study are consistent with our previous hypothesis that the actin cytoskeleton is involved in intracellular transport of Gag polyproteins (Chen et al., 2004), similar to the trafficking of endocytic vesicles (Lee and De Camilli, 2002; Merrifield, 2004) and/or other microbes (Dramsı and Cossart, 1998; Lakadamyali et al., 2003; Wolffe et al., 1997). Further support for the involvement of the actin cytoskeleton in retroviral replication comes from a recent report that Moloney murine leukemia virus matrix protein interacts with IQGAP, an effector of Rho-family small GTPases (Rac1 and Cdc42) that modulates actin polymerization (Leung et al., 2006). Interestingly, proteomic analysis of highly purified HIV virion produced in monocyte-derived macrophages has identified many cellular factors that are known to modulate actin dynamics, such as Arp2/3, gelsolin, cofilin, profilin, cdc42 etc, implicating an involvement of the actin cytoskeleton in retroviral replication cycles (Chertova et al., 2006). It was also recently demonstrated that AIP1/Alix, a conserved endocytic protein recruited by retrovirus L domains, regulates actin cytoskeleton dynamics, providing further evidence for the functional involvement of actin in retrovirus assembly and budding (Pan et al., 2006). The identification of a role for the actin cytoskeleton in EIAV Gag transport has added one more player to the repertoire of viruses that have evolved to interact with cytoskeletal elements inside infected cells at different stages of viral replication cycle (Sodeik, 2000).

**4.0 CHAPTER TWO. DISTINCT INTRACELLULAR TRAFFICKING OF EIAV  
AND HIV-1 GAG DURING VIRAL ASSEMBLY AND BUDDING REVEALED BY  
BIMOLECULAR FLUORESCENCE COMPLEMENTATION ASSAYS**

**4.1 PREFACE**

This chapter is adapted from a published study (Jing Jin<sup>1,4</sup>, Timothy Sturgeon<sup>1</sup>, Chaoping Chen<sup>5</sup>, Simon C. Watkins<sup>3</sup>, Ora A. Weisz<sup>2,3</sup>, and Ronald C. Montelaro<sup>1</sup>. J Virol. 2007 Oct;81(20):11226-35.).

<sup>1</sup>Department of Molecular Genetics and Biochemistry, <sup>2</sup>Department of Medicine, Renal-Electrolyte Division, <sup>3</sup>Department of Cell Biology and Physiology, School of Medicine, University of Pittsburgh, Pittsburgh, Pennsylvania

<sup>4</sup>Department of Infectious Disease and Microbiology, Graduate School of Public Health, University of Pittsburgh, Pittsburgh, Pennsylvania

<sup>5</sup>Department of Biochemistry and Molecular Biology, Colorado State University, Fort Collins, Colorado

Work described in this chapter is in fulfillment of specific aim 2.

## 4.2 ABSTRACT

Retroviral Gag polyproteins are necessary and sufficient for virus budding. Numerous studies of HIV-1 Gag assembly and budding mechanisms have been reported, but relatively little is known about these fundamental pathways among animal lentiviruses. While there may be a general assumption that lentiviruses share common assembly mechanisms, studies of equine infectious anemia virus (EIAV) have indicated alternative cellular pathways and cofactors employed among lentiviruses for assembly and budding. In the current study we used bimolecular fluorescence complementation (BiFC) to characterize and compare assembly sites and budding efficiencies of EIAV and HIV-1 Gag in both human and rodent cells. The results of these studies demonstrated that replacing the natural RNA nuclear export element (Rev-response element (RRE)) used by HIV-1 and EIAV with the hepatitis B virus (HBV) posttranscriptional regulatory element (PRE) altered HIV-1, but not EIAV, Gag assembly sites and budding efficiency in human cells. Consistent with this novel observation, different assembly sites were revealed in human cells for Rev-dependent EIAV and HIV-1 Gag polyproteins. In rodent cells, Rev-dependent HIV-1 Gag assembly and budding were blocked, but changing RRE to PRE rescued HIV-1 Gag assembly and budding. In contrast, EIAV Gag polyproteins synthesized from mRNA exported via either Rev-dependent or PRE-dependent mechanisms were able to assemble and bud efficiently in rodent cells. Taken together, our results suggest that lentivirus assembly and budding are regulated by the RNA nuclear export pathway and that alternative cellular pathways can be adapted for lentiviral Gag assembly and budding.

### 4.3 INTRODUCTION

Retrovirus assembly and budding is a highly concerted process mediated by largely undefined spatially- and temporally-regulated interactions between viral proteins and cellular factors. During the viral assembly process, thousands of copies of viral structural polyproteins multimerize via noncovalent low affinity interactions to form virus particles. Expression of retroviral Gag polyprotein is generally sufficient for the assembly and release of non-infectious virus like particles (VLPs). The Gag polyprotein consists of matrix (MA), capsid (CA), nucleocapsid (NC), and late (L) domains and is cleaved into the distinct structural proteins upon virus maturation (Demirov and Freed, 2004;Morita and Sundquist, 2004). These Gag domains orchestrate the major steps in virus assembly and budding (reviews (Demirov and Freed, 2004;Morita and Sundquist, 2004)). Recent studies have revealed that retrovirus L domains recruit cellular factors that normally function in the invagination of late endosomes/multivesicular bodies (MVBs). However, where and how Gag assembly occurs is still controversial. Among the retroviruses, trafficking and assembly of HIV-1 Gag has been the most extensively studied. It is well established that HIV-1 Gag buds from the plasma membrane of T lymphocytes and of some epithelial cell lines such as HeLa and Cos cells (Demirov and Freed, 2004;Hermida-Matsumoto and Resh, 2000;Morita and Sundquist, 2004;Neil et al., 2006;Nguyen et al., 2003;Nydegger et al., 2003;Ono et al., 2004). In contrast, in macrophages and dendritic cells, the major histocompatibility complex (MHC) class II compartment or MVB is apparently the site of HIV-1 Gag accumulation and particle production (Blom J. et al., 1993;Morita and Sundquist, 2004;Neil et al., 2006;Nguyen et al., 2003;Pelchen-Matthews et al.,

2003;Rapooso et al., 2002). In addition, various studies also indicate that HIV-1 Gag may also target to MVBs in other cell types (Nydegger et al., 2003;Ono et al., 2004;Sherer et al., 2003). The critical cellular and viral determinants that mediate HIV-1 Gag targeting are not known, however, a recent report suggests that HIV-1 Gag assembly is regulated as early as nuclear export of its encoding mRNA (Swanson et al., 2004;Swanson and Malim, 2006).

Retroviral Gag polyproteins are synthesized from an unspliced full-length viral genomic mRNA that requires specific regulatory factors for nuclear export. Lentiviruses contain a *cis*-acting RNA element known as the Rev-response element (RRE) that binds to a viral *trans*-acting protein (Rev). Rev binds to the cellular Crm1 protein which in turn binds to Ran, a small GTPase that shuttles between the nucleus and the cytoplasm. At least some simple retroviruses, such as Mason-Pfizer monkey virus (M-PMV), contain *cis*-acting RNA export elements (constitutive transport elements or CTE) that do not require viral *trans*-acting factors and that function by interacting directly with cellular export factors NXF1/NXT (Swanson and Malim, 2006). Swanson *et al* (Swanson et al., 2004) recently demonstrated in murine cells, which are notable for their inability to support HIV-1 assembly and budding(Bieniasz and Cullen, 2000;Mariani et al., 2000;Swanson et al., 2004), that altering the RNA nuclear export element used by HIV-1 *gag-pol* mRNA from the RRE to the CTE resulted in efficient trafficking and assembly of Gag at cellular membranes. These results support the model that RNA export pathway selection during Gag expression and assembly can modulate the cytosolic fate or function of the viral core polyproteins. This model is also supported by earlier reports that the observed deficiency of assembly of avian leukosis virus (ALV) Gag proteins synthesized in mammalian cells could be overcome by replacement of the ALV CTE-mediated mRNA nuclear export pathway with the HIV-1 Rev-RRE-mediated mRNA nuclear export pathway (Nasioulas et al., 1995).

Equine infectious anemia virus (EIAV), an ungulate lentivirus, has been used to examine the mechanisms of animal lentivirus assembly and budding, and the results of these studies have provided novel insights into the molecular and cellular biology of these fundamental lentiviral processes. Unlike other retroviruses, EIAV Gag budding seems to be ubiquitin independent (Patnaik et al., 2002;Shehu-Xhilaga et al., 2004), and its unique YPDL L-domain recruits Alix/AIP1 as the budding partner (Chen et al., 2005;Martin-Serrano et al., 2003a;Strack et al., 2003;von Schwedler et al., 2003). Little is known about the trafficking pathway and assembly site(s) of EIAV Gag. Like other lentiviruses, EIAV Gag is expressed from full-length genomic mRNA that is exported from the nucleus with the aid of the viral accessory protein Rev. Whether or not EIAV Gag assembly and budding is regulated by nuclear export of its encoding mRNA is unknown. We previously generated an EIAV Gag expression vector by attaching the hepatitis B virus posttranscriptional regulatory element (PRE) to the *gag* gene (Patnaik et al., 2002). This PRE-based vector has been used successfully in various applications related to retrovirus assembly and budding (Chen et al., 2007;Patnaik et al., 2002;Shehu-Xhilaga et al., 2004), and similar results were obtained by using PRE-based EIAV Gag expression vector compared to Rev-dependent EIAV proviral constructs (Patnaik et al., 2002). Although the detailed mechanisms of PRE-mediated RNA nuclear export remain to be defined, the PRE appears to utilize an export pathway different from that of HIV-1 and EIAV Rev and of the M-PMV CTE (Otero et al., 1998;Zang and Benedict Yen, 1999), thus providing a novel system in which to examine the effects of nuclear export pathways on EIAV Gag assembly and budding in comparison to HIV-1.

In this study, we used the bimolecular fluorescence complementation (BiFC) assay to study both Rev-dependent and PRE-dependent (hereafter termed Rev-independent) EIAV and

HIV-1 Gag assembly and budding. The BiFC technique offers a powerful new tool to detect protein-protein interactions with high levels of specificity and sensitivity (Hu and Kerppola, 2003; Kerppola, 2006). The BiFC assay has been used to demonstrate co-assembly of HIV-1 and HIV-2 Gag (Boyko et al., 2006), and we recently used the BiFC assay to demonstrate close and specific interactions between EIAV Gag and actin (Chen et al., 2007). In this assay, a fluorescence protein gene is divided into N-terminal and C-terminal segments. Separately, the encoded fragments are unable to fluoresce; however, co-expression of interacting proteins individually fused to these fragments generates detectable fluorescence signal when the two fluorescent protein fragments are placed in close proximity (less than 15 nm). In the current studies, we utilized the BiFC assay to characterize and compare assembly of EIAV and HIV-1 Gag in human and rodent cell lines and to define the influence of variant mRNA nuclear export pathways on Gag assembly and budding by the two lentiviruses.

## **4.4 MATERIALS AND METHODS**

### **4.4.1 DNA mutagenesis**

Overlapping PCR was used to construct Gag mutations and fusion proteins (Chen et al., 2001b). For bimolecular fluorescence complementation (BiFC) assays, sequences encoding the amino (residues 1-173, VN)- or carboxyl (residues 155-238, VC)- fragments of Venus fluorescence protein (template generously provided by Dr. Atsushi Miyawaki, RIKEN Brain Science Institute, Saitama, JAPAN) were fused to the C-terminus of EIAV or HIV-1 Gag via a 6-alanine linker. To make HA-tagged Gag polyproteins, the YPYDVPDYA epitope from influenza virus HA protein was inserted into the C-terminus of p9 or p6 protein, respectively. All plasmids were isolated using the Qiagen Midiprep Kit (Qiagen, Valencia, CA), and the specific mutations were confirmed by DNA sequencing.

### **4.4.2 Cell culture and transfection**

HeLa SS6 and 293T cells were cultured in Dulbecco's Modified Essential Medium (DMEM) supplemented with 10% fetal bovine serum. NIH3T3 cells were maintained in DMEM supplemented with 10% newborn calf serum. ED cells were cultured in Minimum Essential Medium (MEM) supplemented with 10% fetal bovine serum. Cells were transfected using Lipofectamine 2000 (Invitrogen, Calsbad, CA) following the procedures outlined by the manufacturer.

#### **4.4.3 Gag protein expression assays**

At 48 h post transfection, cells were harvested and lysed in lysis buffer (25 mM Tris-HCl, pH 8.0, 150 mM NaCl, 1% deoxycholic acid, 1% Triton X-100, 1x protease inhibitor cocktail) and centrifuged at 20,800xg for 5 min to remove cell nuclei. Virus-like particles (VLPs) released into the culture medium were pelleted by centrifugation (20,800xg for 3 h at 4°C) and resuspended in PBS. HA-Gag contained in cell lysates and VLPs was analyzed by Western Blotting using rat anti-HA antibody epitope (Roche Applied Science, Indianapolis, IN) and HRP conjugated goat anti-rat IgG (Zymed, San Francisco, CA).

#### **4.4.4 Confocal microscopy**

Transfected cells grown on coverslips were fixed and permeabilized with 2% paraformaldehyde and 0.1% Triton X-100 in PBS. VLPs were adsorbed onto coverslips by overnight incubation at 4°C in the presence of 16 µg/ml polybrene, and then fixed with 2% paraformaldehyde. Images were captured using a Leica TCS-SL microscope and processed with Metamorph software.

#### **4.4.5 Flow cytometry analysis**

HeLa SS6 and NIH3T3 cells grown on 6-well plates were transfected with selected BiFC construct pairs. Cells were detached with PBS containing 2.5 mM EDTA and resuspended in PBS at 16 h post transfection for HeLa SS6 cells and at 48 h post transfection for NIH3T3 cells. For HA staining (**Fig. 4-3** and **Fig. 4-4**), cells were washed three times with PBS containing 5% FBS (wash buffer) and fixed in 1% paraformaldehyde for 1 h, followed by permeabilization with

PBS containing 5% fetal calf serum and 0.5% saponin. Mouse anti-HA epitope antibody (Santa Cruz Biotechnology, Santa Cruz, CA) and Cy5-conjugated goat anti-mouse IgG (Jackson ImmunoResearch Laboratory, West Grove, PA) were used to stain HeLa SS6 cells, while rat anti-HA epitope antibody and Cy5-conjugated goat anti-rat IgG (Zymed, San Francisco, CA) were used to stain NIH3T3 cells. A minimum of 30,000 gated live events were acquired on a FACSCalibur (Becton Dickinson, San Jose, CA) flow cytometer and analyzed with FlowJo batch analysis software (Treestar, San Carlos, CA) for both yellow fluorescence and HA staining (**Fig. 4-3** and **Fig. 4-4**).

## 4.5 RESULTS

### 4.5.1 Expression of Rev-dependent and Rev-independent EIAV and HIV-1 Gag-BiFC constructs

Using the optimized amino (VN) and carboxy (VC) terminal fragments of Venus fluorescence protein (Shyu et al., 2006), we first generated a panel of Gag-BiFC constructs (**Fig. 4-1, panel A**) for EIAV and HIV-1 Gag. The EIAV *gag* gene in pPRE-Gag (Patnaik et al., 2002) was replaced with VN- or VC-tagged EIAV or HIV-1 Gag genes to generate Rev-independent expression vectors. Rev-dependent EIAV and HIV-1 Gag-BiFC constructs were generated based on EIAV and HIV-1 proviral constructs pCMVuk (Patnaik et al., 2002) and pNL4-3/KFS (Freed and Martin, 1995), respectively. The U3 regions of both EIAV and HIV-1 proviral constructs were replaced by a CMV promoter to obtain similar transcriptional levels from both Rev-dependent and Rev-independent vectors. Envelope glycoprotein expression was eliminated by introduction of premature stop codon or frame shift, and *pol* genes were deleted to facilitate cloning. The inserted HA epitope provides a common tag to directly compare the expression of the various fusion constructs. We first examined the relative efficiency of protein expression and VLP budding by the panel of Gag constructs (**Fig. 4-1, panel B**) in 293T cells transfected with the individual vectors. At 48 h post transfection, cell lysates and supernatant VLPs were subjected to SDS-PAGE and Western Blot analysis with HA antibody. The immunoblot data indicated that all of the Gag-BiFC fusion proteins for EIAV and HIV-1 were expressed and released in VLPs. However, differences in the influence of mRNA nuclear export pathways on

Gag budding efficiency was observed between EIAV and HIV-1. Expression and budding of EIAV Gag-BiFC constructs were similar when expressed in 293T cells from plasmids encoding either Rev-independent (**Fig. 4-1, lanes 1 and 2**) or Rev-dependent (**Fig. 4-1, lanes 3 and 4**) Gag constructs. In contrast, the budding efficiency of HIV-1 Gag-BiFC fusion proteins expressed from Rev-independent vectors was roughly 10-fold lower than that of Rev-dependent Gag fusion proteins (compare VLPs in lanes 5 and 6 with lanes 7 and 8 and their 10 fold dilution showed in lanes 9 and 10 of **Fig. 4-1**), although the amount of proteins produced in the transfected cells was highly comparable under both conditions (compare lysates in lanes 5 and 6 with lanes 7 and 8 of **Fig. 4-1**).

#### **4.5.2 Demonstration of EIAV Gag assembly by BiFC assay**

We next used the BiFC assay to examine EIAV Gag assembly by confocal microscopy in EIAV permissive equine dermal (ED) cells (**Fig. 4-2, panels a-c**) and in HeLa cells (**Fig. 4-2, panels d-f**). Both ED (**Fig. 4-2, panel b**) and HeLa (**Fig. 4-2, panel e**) cells expressing Rev-independent EIAV-Gag-YFP displayed intracellular punctate YFP signals. In ED (**Fig. 4-2, panel a**) and HeLa cells (**Fig. 4-2, panel d**) transfected with the Rev-independent EIAV Gag-VN/Gag-VC pair, intracellular YFP fluorescence was observed indicating the interaction of Gag monomers with one another during VLP assembly. This EIAV Gag-Gag-BiFC distribution pattern resembled the Rev-independent EIAV-Gag-YFP intracellular distribution pattern, suggesting Gag-Gag-BiFC signals correctly represent intracellular Gag assembly. We previously used the BiFC assay and demonstrated a lack of detectable interaction between EIAV Gag and tubulin in transfected cells (Chen et al., 2007), so the EIAV Gag-VN/VC-tubulin pair was employed in the current study as a negative control for the current BiFC assays. No positive BiFC signal was

observed in ED (**Fig. 4-2, panel c**) or HeLa cells (**Fig. 4-2, panel f**) transfected with the Gag-VN/VC-tubulin control pair, confirming the specificity of the observed Gag-Gag interactions.

### **4.5.3 Comparison of Rev-dependent and Rev-independent EIAV and HIV-1 Gag assembly**

We next used the BiFC assay to characterize and compare EIAV and HIV-1 Gag assembly in human (**Fig. 4-3**) and rodent (**Fig. 4-4**) cells by confocal microscopic and flow cytometric analysis of cells transfected with the indicated Gag-VN/Gag-VC pairs. Due to the lower expression level of HIV-Gag-VN compared to HIV-Gag-VC (**Fig. 4-1, panel B**), a 5:2 mass ratio of HIV-1 Gag-VN expression vector to HIV-1 Gag-VC expression vector was used for HIV-1 Gag-VN/Gag-VC co-transfection to optimize the BiFC signal. Four  $\mu\text{g}$  of total DNA was used to transfect one well of cells grown in 6-well-plate for both confocal microscopy and flow cytometry analyses.

Both Rev-dependent and Rev-independent EIAV Gag polyproteins assembled efficiently in HeLa and 293T cells (**Fig. 4-3, panels A-a, -b, -e and -f**), and expression of EIAV Gag-VN/Gag-VC pairs resulted in a bright punctate fluorescent signal distributed throughout the cytoplasm and along the cell surface, with some concentration in the juxtannuclear region. In contrast, we observed a dramatic difference between the BiFC patterns in cells expressing Rev-independent compared to Rev-dependent HIV-1 Gag constructs. Co-transfection of Rev-independent HIV-1 Gag-VN/Gag-VC constructs into human cells resulted in a weak BiFC signal overall, consisting of a few intracellular puncta over a diffuse cytoplasmic background (**Fig. 4-3, panels A-c and -g**). In marked contrast, human cells expressing Rev-dependent HIV-1 Gag-VN/Gag-VC constructs displayed bright cell surface BiFC signal (**Fig. 4-3, panels A-d and -h**).

Examining cells transfected with 4  $\mu$ g or 0.4  $\mu$ g of DNA after overnight transfection or as early as 9 h post transfection yielded similar results (data not shown). These results indicate that the mRNA nuclear export pathways can alter HIV-1 Gag assembly sites, as reported previously (Swanson et al., 2004), and that alternative assembly/budding sites are apparently utilized by EIAV and HIV-1 Gag.

To quantify the assembly efficiency of Rev-dependent and Rev-independent EIAV and HIV-1 Gag, HeLa cells expressing the indicated BiFC pairs were analyzed by flow cytometry (**Fig. 4-3, panel B**). To normalize differences in transfection efficiency and Gag expression levels, fixed and permeabilized cells were stained with mouse HA antibody followed by Cy5 conjugated secondary antibody. The ratio of HA and BiFC double-positive population to the total HA-positive population was used to calculate assembly efficiency. Cells transfected with an HA-tagged VN-actin/VC-actin pair were used as a positive control, as described previously (Chen et al., 2007). In VN-actin/VC-actin co-transfected human cells, almost 44% of HA-positive cells exhibited positive BiFC signal (**Fig. 4-3, panel B-e**), while none of HA-positive cells displayed yellow fluorescence in mock-transfected control (**Fig. 4-3, panel B-f**). A similar assembly efficiency was observed for Rev-independent (**Fig. 4-3, panel B-a**) or Rev-dependent (**Fig. 4-3, panel B-b**) EIAV Gag (13.3% and 14.6%, respectively). In contrast, lower assembly efficiency (0.5%) was observed for Rev-independent HIV-1 Gag (**Fig. 4-3, panel B-c**) compared with the assembly efficiency (2.4%) for Rev-dependent HIV-1 Gag (**Fig. 4-3, panel B-d**).

As observed in human cells, expression of both Rev-independent (**Fig. 4-4, panel A-a**) and Rev-dependent (**Fig. 4-4, panel A-b**) EIAV Gag-VN/Gag-VC pairs in mouse-derived NIH3T3 cells resulted in an intracellular punctate BiFC pattern. In contrast, a weak but distinct BiFC signal was observed when Rev-independent HIV-1 Gag-VN/Gag-VC constructs were

expressed in NIH3T3 cells (**Fig. 4-4, panel A-c**), while only background signal could be detected in NIH3T3 cells expressing the Rev-dependent HIV-1 Gag-VN/Gag-VC pair (**Fig. 4-4, panel A-d**). These qualitative microscopy results were further supported by quantitative flow cytometry data (**Fig. 4-4, panel B**). In NIH3T3 cells co-transfected with either Rev-independent (**Fig. 4-4, panel B-a**) or Rev-dependent (**Fig. 4-4, panel B-b**) EIAV Gag-VN/Gag-VC pairs, about 62% and 48% of HA-positive cells displayed positive BiFC signals, respectively. However, roughly five fold higher assembly efficiency (49% vs 10%) of Rev-independent (**Fig. 4-4, panel B-c**) HIV-1 Gag was observed in NIH3T3 cells compared to Rev-dependent HIV-1 Gag (**Fig. 4-4, panel B-d**). Approximately 60% of HA positive cells were BiFC positive in VN-actin/VC-actin co-transfected NIH3T3 cells (**Fig. 4-4, panel B-e**), and no BiFC signal was detected in negative control rodent cells (**Fig. 4-4, panel B-f**). These results indicate that the block of HIV-1 Gag assembly in NIH3T3 cells with Rev-dependent Gag expression could be overcome by PRE-mediated RNA nuclear export. In marked contrast, both Rev-independent and Rev-dependent EIAV Gag could assemble efficiently in NIH3T3 cells, indicating critical differences in EIAV and HIV-1 Gag assembly processes in rodent cells.

To confirm that the Gag-Gag-BiFC signals observed in cells transfected with various Gag-BiFC pairs represented functional Gag assembly, VLPs released from 293T (**Fig. 4-5**) or NIH3T3 (data not shown) cells were visualized by confocal microscopy. Positive BiFC labeled particles could be detected in supernatant pellets produced from 293T cells transfected with various Gag-VN/Gag-VC pairs, indicating that the Gag-Gag-BiFC complexes could be successfully incorporated into VLPs and that BiFC signals observed in cells represented functional assembly of Gag polyproteins.

#### 4.5.4 Comparison of Rev-dependent and Rev-independent EIAV and HIV-1 Gag budding

Rev-dependent and Rev-independent EIAV and HIV-1 Gag budding efficiencies were also examined by Western Blot analysis (**Fig. 4-6**). Four  $\mu\text{g}$  of total DNA was used to transfect one well of cells grown in 6-well-plate as described above for confocal microscopic and flow cytometric analysis. Cell lysates and pelleted VLPs produced from transfected 293T (**Fig. 4-6, panel A**) or NIH3T3 (**Fig. 4-6, panels A, B and C**) cells were analyzed by Western Blot at 48 h post transfection. In human cells, the HIV-1 VLP budding efficiency from Rev-independent HIV-1 Gag-VN/Gag-VC pair was roughly 10-fold lower than that of the Rev-dependent HIV-1 Gag-VN/Gag-VC pair (compare lane 3 with lane 4 and 5 in **Fig. 6-6, panel A**), consistent with the budding efficiency of singly-transfected HIV-1 Gag-BiFC constructs shown in Fig 1B. Both Rev-independent (**Fig. 6-6, panel A, lane 1**) and Rev-dependent (**Fig. 6-6, panel A, lane 2**) EIAV Gag budded with comparable efficiency to Rev-dependent (**Fig. 6-6, panel A, lane 4**) HIV-1 Gag in 293T cells.

In NIH3T3 cells, both Rev-independent EIAV (**Fig. 6-6, panel A, lane 6**) and HIV-1 (**Fig. 6-6, panel A, lane 8**) Gag-BiFC constructs expressed Gag proteins and released VLPs at similar levels. However, the expression level of Rev-dependent EIAV (**Fig. 6-6, panel A, lane 7**) and HIV-1 (**Fig. 6-6, panel A, lane 9**) Gag-BiFC constructs were relatively low in NIH3T3 cells. These reduced Gag-BiFC construct expression levels correlated with greatly reduced VLP production by Rev-dependent EIAV Gag-BiFC (**Fig. 6-6, panel A, lane 7**) and undetectable VLP production by Rev-dependent HIV-1 Gag-BiFC (**Fig. 6-6, panel A, lane 9**).

To determine if the reduced VLP production by Rev-dependent EIAV or HIV-1 Gag in NIH3T3 cells was the result of low Gag protein expression, cells were transfected with reduced amounts of Rev-independent EIAV (**Fig. 6-6, panel B**) and HIV-1 (**Fig. 6-6, panel C**) Gag-BiFC

plasmids and serial dilution of VLP and cell lysates from Rev-independent Gag-BiFC plasmids transfected cells were used to compare Rev-dependent and Rev-independent Gag budding at equally low protein expression levels. Similar levels of VLPs were released from NIH3T3 cells expressing comparable amounts of Rev-dependent (**Fig. 6-6, panel B, lane 8**) and Rev-independent (**Fig. 6-6, panel B, lanes 5 and 7**) EIAV Gag-BiFC constructs. However, in NIH3T3 cells expressing comparable levels of Rev-independent (**Fig. 6-6, panel C, lanes 5 and 7**) and Rev-dependent (**Fig. 6-6, panel C, lane 8**) HIV-1 Gag-BiFC constructs, Gag-VN and Gag-VC were released only in cells expressing the Rev-independent constructs.



(B) correspond directly to constructs 1-8 in (A). Lanes 9 and 10 were loaded with 1:10 diluted samples loaded in lanes 7 and 8, respectively. At 48 h post transfection, cell lysates (upper panel) and VLPs (lower panel) were analyzed by immunoblotting using HA antibody.

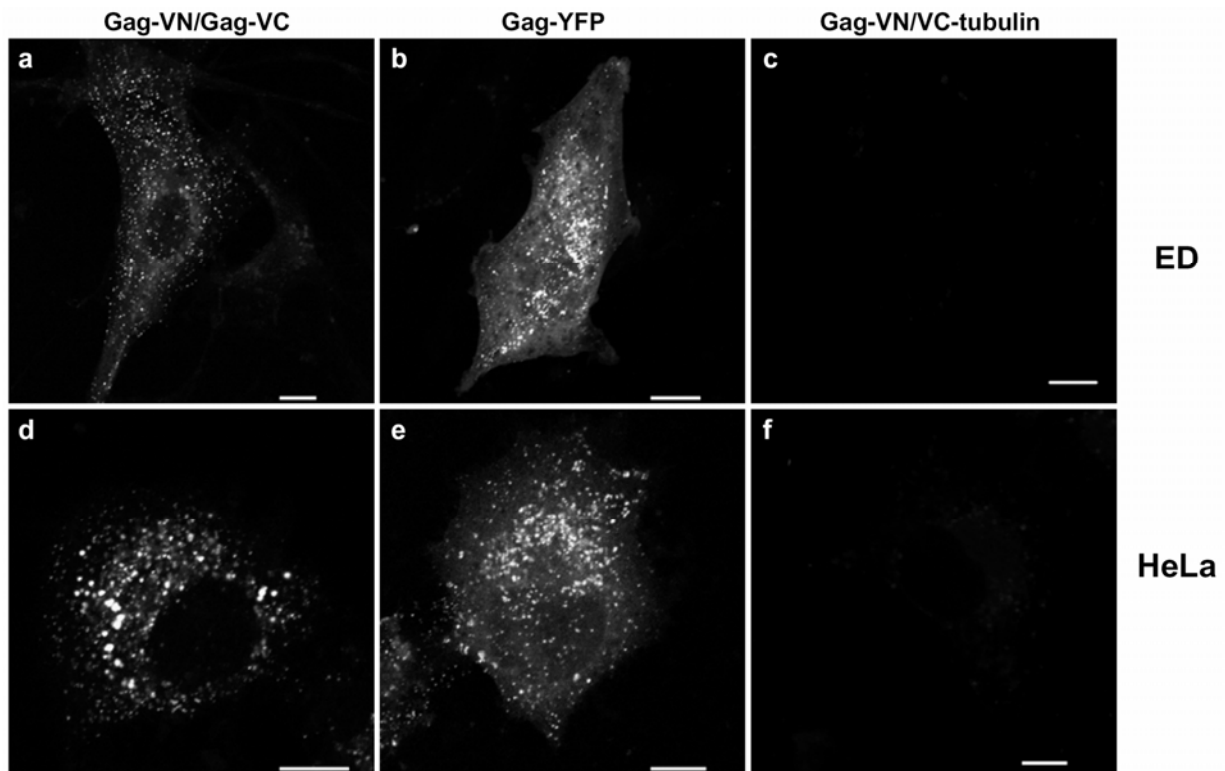


**Figure 4-2. Demonstration of EIAV Gag assembly by the BiFC assay.**

ED (panels a-c) and HeLa (panels d-f) cells grown on glass coverslips were transfected with pPRE-EIAV-Gag-VN and pPRE-EIAV-Gag-VC (panels a and d), pPRE-EIAV-Gag-YFP (panels b and e), pPRE-EIAV-Gag-VN and pCMV-VC-tubulin (panels c and f) plasmid using Lipofectamine 2000. At 24 h post transfection, cells were fixed and imaged with a Leica TCS-SL confocal microscope. Bar: 10  $\mu$ m.

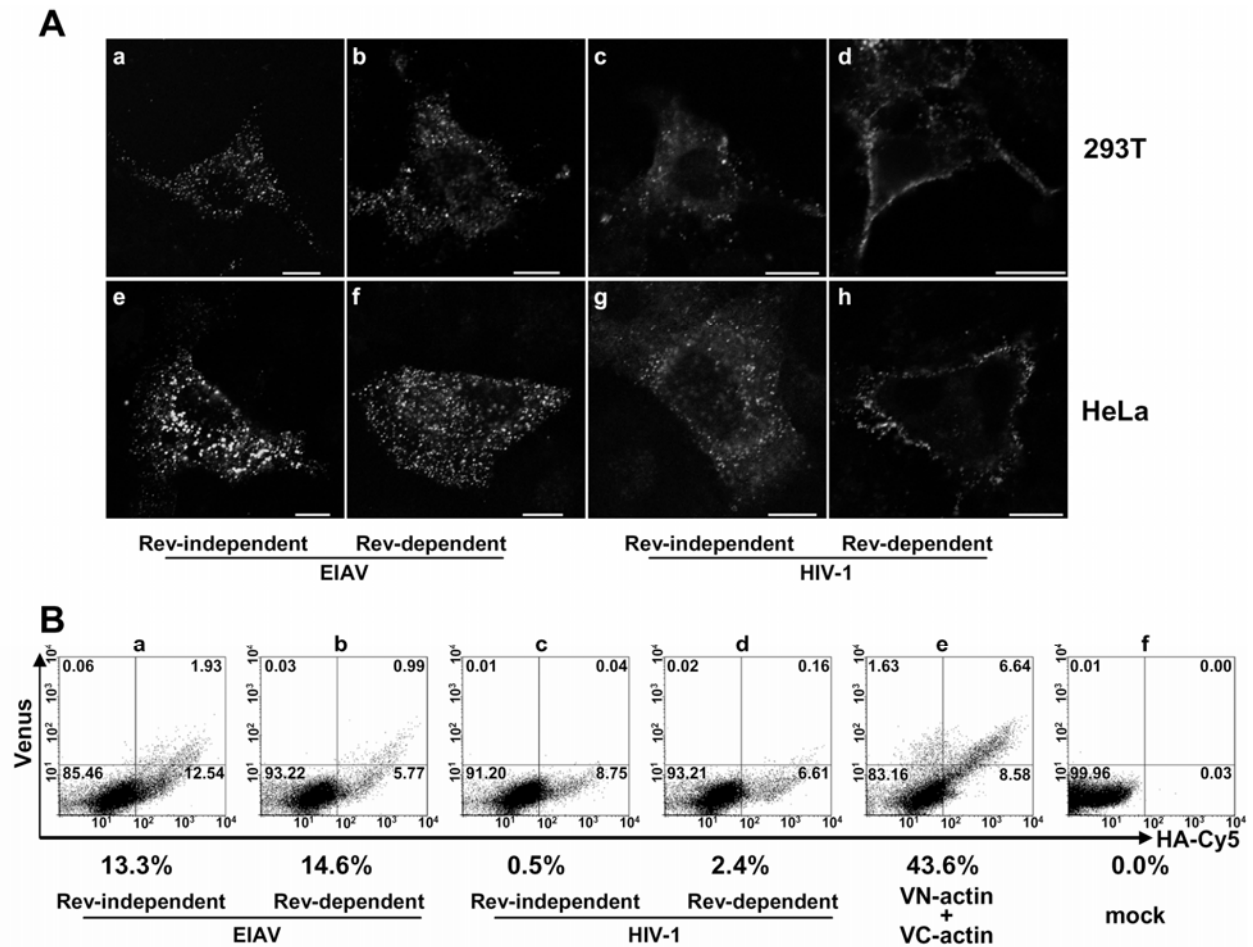


**Figure 4-3. BiFC analysis of EIAV and HIV-1 Gag assembly in human cells.**

(A) Visualization of Gag assembly by BiFC assay. 293T (panels a-d) and HeLa (panels e-h) cells grown on glass coverslips were transfected with Rev-independent EIAV-Gag-VN/Gag-VC (panels a and e), Rev-dependent EIAV-Gag-VN/Gag-VC (panels b and f), Rev-independent HIV-Gag-VN/Gag-VC (panels c and g), Rev-dependent HIV-Gag-VN/Gag-VC (panels d and h) plasmid pairs using Lipofectamine 2000. At 16 h post transfection, cells were fixed and imaged with a Leica TCS-SL confocal microscope. Bar: 10  $\mu$ m. (B) Quantitative analysis by flow cytometry of BiFC signals in transiently transfected HeLa cells described in (A). At 16 h post transfection, permeabilized cells were stained with mouse HA antibody and Cy5 conjugated goat anti-mouse IgG. A minimum of 30,000 gated live events were acquired and analyzed both yellow

and HA-Cy5 fluorescence. Percentage of HA and BiFC double positive cells in total HA positive cells was calculated and labeled below each quadrant plot.

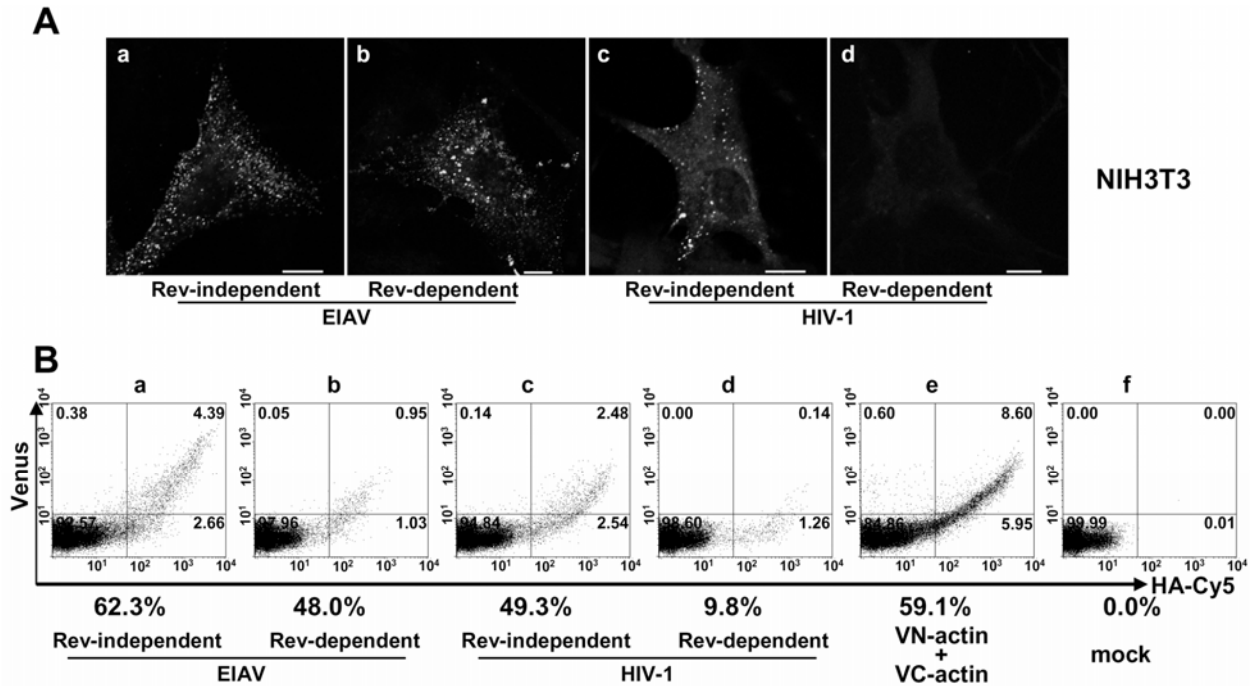


**Figure 4-4. BiFC analysis of EIAV and HIV-1 Gag assembly in NIH3T3 cells.**

(A) Visualization of Gag assembly by BiFC assay. NIH3T3 cells grown on glass coverslips were transfected with Rev-independent EIAV-Gag-VN/Gag-VC (panel a), Rev-dependent EIAV-Gag-VN/Gag-VC (panel b), Rev-independent HIV-Gag-VN/Gag-VC (panel c), Rev-dependent HIV-Gag-VN/Gag-VC (panel d) plasmid pairs using Lipofectamine 2000. At 16 h post transfection, cells were fixed and imaged with a Leica TCS-SL confocal microscope. Bar: 10  $\mu$ m. (B) Quantitative analysis by flow cytometry of BiFC signals in transiently transfected NIH3T3 cells described in (A). At 48 h post transfection, cells were analyzed by flow cytometry as described in Fig. 4-3 except that rat HA antibody and Cy5 conjugated goat anti-rat IgG were used.

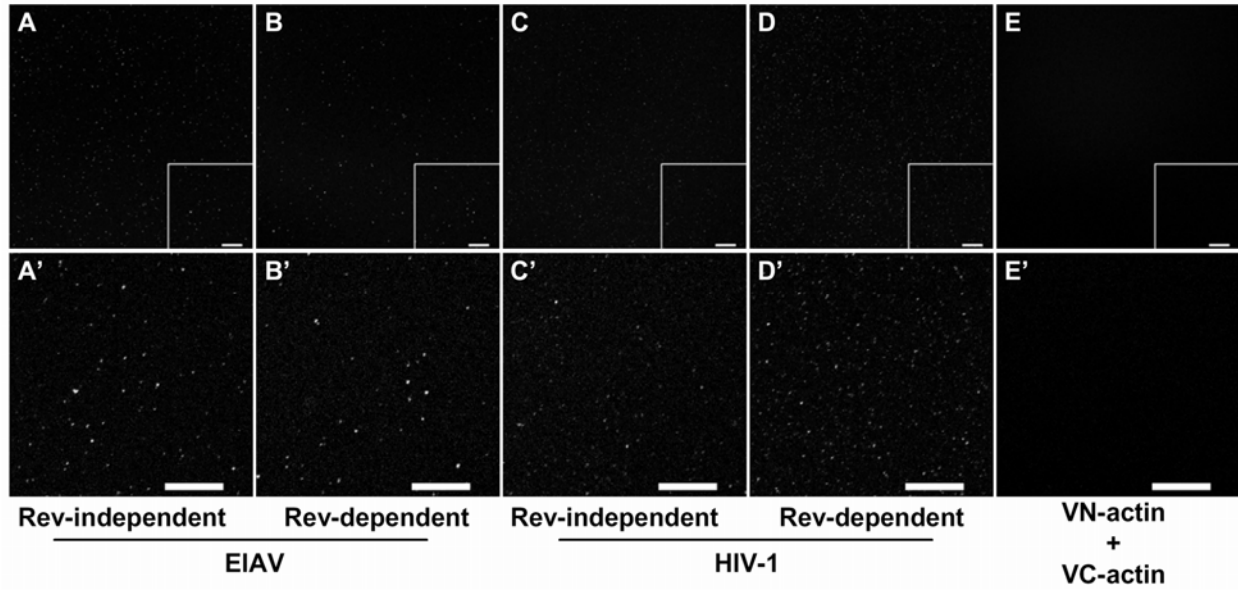


**Figure 4-5. Demonstration of BiFC Gag complexes in assembled VLPs.**

VLPs produced from 293T cells transfected with Rev-independent EIAV-Gag-VN/Gag-VC (A), Rev-dependent EIAV-Gag-VN/Gag-VC (B), Rev-independent HIV-Gag-VN/Gag-VC(C), Rev-dependent HIV-Gag-VN/Gag-VC (D), VN-actin/VC-actin (E) plasmid pairs were immobilized on coverslips and fixed. Images were acquired on a Leica TCS-SL confocal microscope. Enlarged images of boxed areas in A-E were presented as A'-E'. Bar: 10  $\mu$ m.

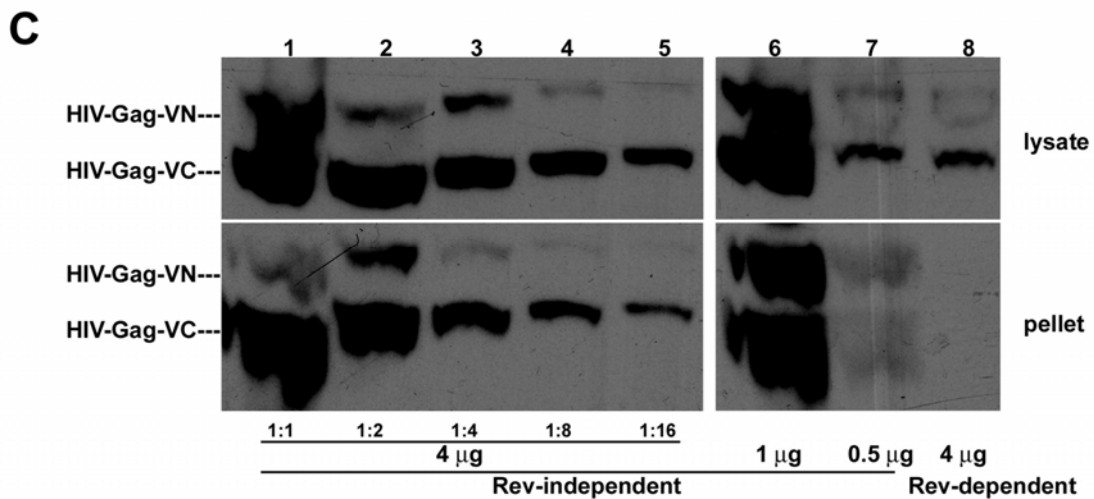
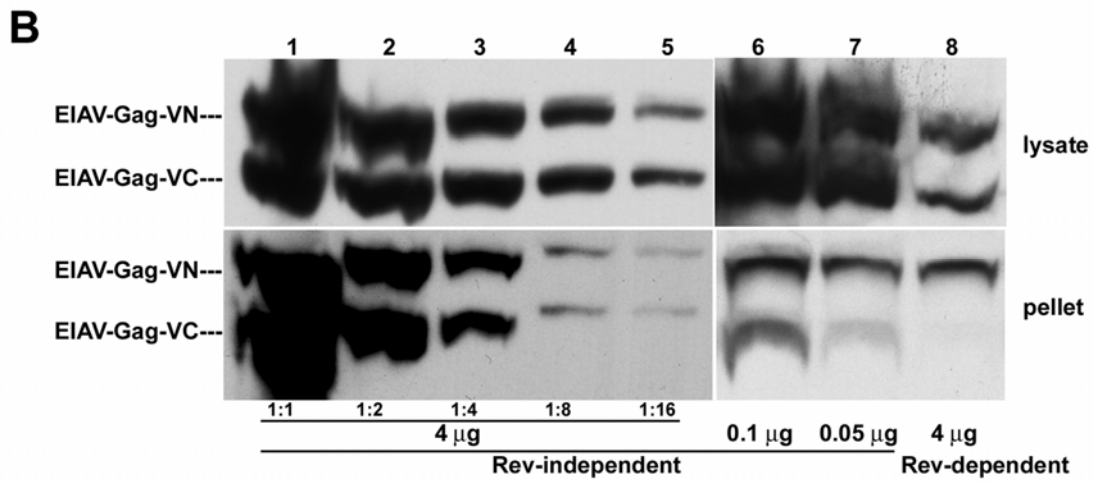
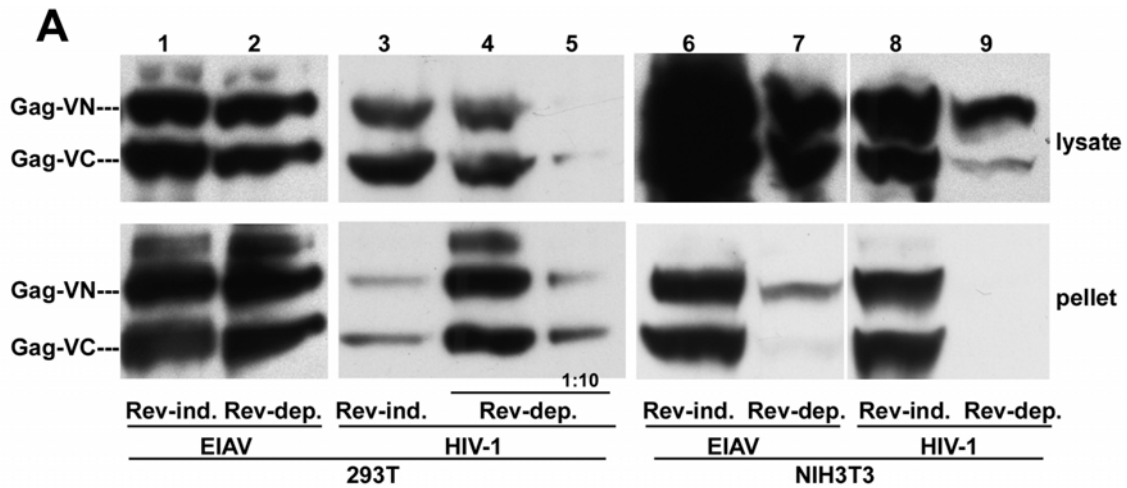


Figure 4-6. Comparison budding efficiency of Rev-dependent and Rev-independent EIAV and HIV-1 Gag in human and rodent cells.

#### Figure 4-6. continue

**(A)** Expression and budding of co-transfected Gag-BiFC constructs. 293T (lanes 1-5) and NIH3T3 (lanes 6-9) cells were co-transfected with Rev-independent EIAV-Gag-VN/Gag-VC (lanes 1 and 6), Rev-dependent EIAV-Gag-VN/Gag-VC (lanes 2 and 7), Rev-independent HIV-Gag-VN/Gag-VC (lanes 3 and 8), Rev-dependent HIV-Gag-VN/Gag-VC (lanes 4, 5 and 9) plasmid pairs using Lipofectamine 2000. At 48 h post transfection, cell lysates (upper panel) and VLPs (lower panel) were analyzed by immunoblotting using HA antibody. 10 fold diluted sample loaded on lane 4 was loaded on lane 5. **(B)** Comparison of budding efficiencies of Rev-independent and Rev-dependent EIAV in NIH3T3 cells. The indicated amount of Rev-independent and Rev-dependent EIAV and Gag-BiFC plasmid pairs were used for transfection in NIH3T3 cells. At 48 h post transfection, cell lysates (upper panel) and VLPs (lower panel) were analyzed by immunoblotting using HA antibody. Serial dilutions of Rev-independent samples were analyzed in parallel. **(C)** Compare budding efficiencies of Rev-independent and Rev-dependent HIV-1 in NIH3T3 cells as described in (B) except that HIV-1 Gag-BiFC plasmid pairs were used for transfection.

## 4.6 DISCUSSION

In the current study, we utilized the newly developed BiFC assay to study EIAV and HIV-1 Gag assembly and budding in human and mouse cell types, both qualitatively and quantitatively. Using the BiFC method, which enables highly specific and sensitive detection of *in vivo* protein-protein interactions (Hu et al., 2002; Kerppola, 2006; Nyfeler et al., 2005), we were able to correlate Gag assembly efficiency with VLP budding efficiency, as well as to confirm the incorporation of Gag-Gag BiFC complexes into VLPs, further validating this technique as a tool to study functional viral assembly. The BiFC studies described here for the first time compare in one study the Gag assembly sites of an animal lentivirus with HIV-1, directly testing the assumption that all lentiviruses assemble via identical pathways in the same target cell. Thus, the results of these comparative studies reveal novel insights into fundamental properties of lentivirus assembly mechanisms and identify new systems in which to elucidate specific virus-cell interactions that can facilitate or inhibit assembly in human or rodent cells.

### 4.6.1 EIAV and HIV-1 Gag use distinct trafficking routes during viral assembly/budding

Currently, the sites of retrovirus assembly and budding are vigorously debated topics. It has been generally assumed that lentiviral assembly and budding pathways follow the assembly pathway defined for type-C oncoviruses, such as murine or avian leukemia viruses, in which Gag polyproteins assemble and bud at specific plasma membrane sites to form viral particles. Although a large number of studies have been performed to characterize HIV-1 assembly and

budding in various cell types using diverse techniques, assembly and budding mechanisms of other lentiviruses have not been well characterized. Data from our lab and others have previously indicated that EIAV and HIV-1 may use related but distinct assembly pathways, and that these differences could be exploited to define critical virus-cell interactions that mediate Gag trafficking and assembly (Chen et al., 2005; Patnaik et al., 2002; Puffer et al., 1998; Shehu-Xhilaga et al., 2004). For example, EIAV is unique from other retroviruses in that its assembly and budding is insensitive to proteasome inhibitor treatments that deplete intracellular free ubiquitin, whereas budding of HIV-1 and other retroviruses were inhibited by the same proteasome inhibitor treatments (Patnaik et al., 2000; Patnaik et al., 2002). Like other retroviruses, EIAV assembly and budding is suppressed by dominant negative VPS4A (Martin-Serrano et al., 2003b; Shehu-Xhilaga et al., 2004; Tanzi et al., 2003), but is insensitive to the expression of carboxy-terminal fragments of TSG101 that inhibit PTAP and PPPY L domain-mediated Gag assembly and budding (Shehu-Xhilaga et al., 2004). EIAV Gag utilizes a unique L domain, YPDL motif, that recruits host VPS protein Alix/AIP1 (Martin-Serrano et al., 2003a; Strack et al., 2003; von Schwedler et al., 2003) and adaptor protein complex AP-2 (Puffer et al., 1998), both of which are required for efficient EIAV budding (Chen et al., 2005). Therefore, although EIAV Gag assembly and budding pathways converge with other retroviral assembly and budding pathways at the final step by entry into ESCRTs endosomal sorting network, these differences suggest that EIAV Gag may use a unique portal of entry to endosomal sorting network and upstream trafficking pathway.

In the current study we characterized EIAV Gag assembly in various cell lines and compared EIAV Gag and HIV-1 Gag assembly and budding by the BiFC assay. Distinct assembly sites for EIAV Gag (intracellular) and HIV-1 Gag (cell surface) were revealed in

human cells where both Gag species budded efficiently. In rodent cells, compared to the efficient assembly and budding of EIAV Gag, HIV-1 Gag neither assembled nor budded. It is important to note that there was a close correlation between the levels of Gag multimerization detected by BiFC in various cell types and the levels of VLP production from the respective cell types. Taken together, these data indicate distinct intracellular trafficking of EIAV and HIV-1 Gag in the same target human or rodent cells. Interestingly, while the intracellular assembly pattern of EIAV Gag in fibroblastic cells is distinct from that of HIV-1 in these cells (Demirov and Freed, 2004; Morita and Sundquist, 2004; Neil et al., 2006; Ono and Freed, 2004), it is reminiscent of HIV-1 Gag intracellular assembly observed in human macrophages (Pelchen-Matthews et al., 2003; Raposo et al., 2002). Recent studies have suggested that HIV-1 in human macrophages may assemble and bud from invaginated membrane domains that resemble endosomal structures but are contiguous with the plasma membrane (Deneka et al., 2007; Welsch et al., 2007). Earlier reports demonstrated a failure to release HIV-1 Gag that was targeted to endosomes either by inducing phosphatidylinositol 4,5-bisphosphate synthesis on endosome membranes (Ono et al., 2004) or by replacing the HIV-1 Gag membrane targeting signal with phosphatidylinositol 3-phosphate binding domains (Jouvenet et al., 2006), supporting the model that plasma membrane is the productive budding site for HIV-1 in human cells. In contrast to HIV-1 Gag, intracellularly assembled EIAV Gag budded efficiently from both human and rodent cells, the latter being unable to support HIV-1 Gag assembly and budding. Identification of the intracellular sites where EIAV Gag assembles and the cellular factors that mediate EIAV release in various cell types will enable us to determine both common and distinct paradigms of retrovirus assembly and budding.

The intracellular assembly pattern of EIAV Gag was also observed in equine fibroblasts. It remains to be determined if these patterns are also observed in equine macrophages, the natural target cell for primary isolates of EIAV. However, it is important to note that the EIAVuk proviral strain used in this study is cell-adapted via changes in its LTR sequences (Cook et al., 1998) such that it can productively infect cultured equine fibroblastic cells and is able to produce fully infectious virus particles from various transfected human cell lines. In this regard, equine and human fibroblastic cell lines have been used extensively to study EIAV assembly and budding (Chen et al., 2005; Chen et al., 2007; Li et al., 2002; Patnaik et al., 2002; Shehu-Xhilaga et al., 2004). With the development of the BiFC assay to study EIAV Gag assembly, it should now be possible to extend these types of studies to define EIAV assembly in its natural target cells.

#### **4.6.2 mRNA nuclear export pathways influence Gag assembly and budding sites**

Although no obvious changes in EIAV Gag assembly and budding were observed after altering Rev-mediated mRNA nuclear export to HBV PRE-mediated mRNA nuclear export, marked changes in HIV-1 Gag assembly location and assembly/budding efficiency were observed. These differences included relocation of HIV-1 Gag assembly sites from the plasma membrane to intracellular sites in human cells and rescue of HIV-1 Gag assembly and budding in NIH3T3 cells. Rev-dependent HIV-1 Gag was reported to form condensed, electron-dense structures (Mariani et al., 2000), presumably aggregates of Gag polyproteins, and to display a diffuse distribution pattern in NIH3T3 cells, indicating an assembly deficiency (Chen et al., 2001a; Swanson et al., 2004). The current results showed that Rev-dependent HIV-1 Gag did not form BiFC complexes in mouse cells, indicating either that the reported abnormal aggregation of HIV-1 Gag in NIH3T3 cells is extremely inefficient or that Gag polyproteins in the aggregates

are not associated in an arrangement that favors BiFC complex formation. Alternative HIV-1 Gag assembly and budding pathways were previously reported in different cells types (Nydegger et al., 2003; Ono and Freed, 2004), as well as in nonlymphoid cell lines expressing HLA-DR epigenetically (Finzi et al., 2006). However, the mechanisms that drive the selection of alternative assembly and budding pathways are largely unknown. Consistent with a recent study (Swanson et al., 2004), the current data indicate that distinct mRNA export pathways regulate HIV-1 Gag assembly and budding pathways.

RNA export pathways could modulate the cytosolic fate or function of Gag polyproteins at three levels. (1) Retroviral genomic RNA (gRNA) is associated with proteins to form ribonucleoprotein particles (RNP), and RNP components might regulate gRNA trafficking and subsequent Gag assembly (Cochrane et al., 2006). Indeed, one such component (hnRNP A2) has previously been reported to regulate HIV-1 gRNA trafficking and virus production (Levesque et al., 2006). (2) Retrovirus Gag assembly is a stepwise, energy-dependent process that requires chaperone proteins (Dooher and Lingappa, 2004; Gurer et al., 2002; Hong et al., 2001; Zimmerman et al., 2002). Therefore differences in Gag synthesis sites as a consequence of different RNA nuclear export pathways might lead to exposure of Gag to different cellular factors. The failure to recruit necessary chaperones could result in defective assembly and explain the inefficient assembly of Rev-dependent HIV-1 Gag in NIH3T3 cells. (3) Retroviral Gag trafficking to budding sites also depends on other cellular factors including motor proteins and membrane trafficking regulators (Chen et al., 2005; Chen et al., 2007; Demirov and Freed, 2004; Dong et al., 2005; Leung et al., 2006; Morita and Sundquist, 2004; Sasaki et al., 1995; Tang et al., 1999). Mislocalization of Gag polyproteins might prevent recruitment of partners required

for Gag transport, even if Gag assembly *per se* is competent. The latter might explain the low budding efficiency of intracellularly assembled HIV-1 Gag in human cells.

Elucidating the mechanisms by which Rev-dependent HIV-1 Gag assembly is blocked in rodent cells and by which Rev-independent Gag overcomes this block could help to develop small animal models of HIV-1 replication and pathogenesis. Further studies are needed to examine how RNA export regulates HIV-1 Gag trafficking and assembly, to define what factors regulate the release of intracellular versus plasma membrane assembled HIV-1 in human cells, and to identify the machinery that enables efficient intracellular assembly/budding of EIAV Gag. Based on the current studies of EIAV and HIV-1 Gag assembly, we propose that additional comparisons of animal and human lentivirus assembly pathways can accelerate these mechanistic studies of lentivirus Gag assembly and budding processes and increase the potential to develop novel antiviral therapies targeting Gag assembly and budding.

**5.0 CHAPTER THREE. LIPID RAFT ASSOCIATION OF HIV-1 GAG IS  
REGULATED BY THE TRAFFICKING OF GAG-ENCODING MRNA**

**5.1 PREFACE**

This chapter is adapted from a manuscript submitted for publication. (Jing Jin<sup>1,4</sup>, Timothy Sturgeon<sup>1</sup>, Simon C. Watkins<sup>3</sup>, Ora A. Weisz<sup>2,3</sup>, and Ronald C. Montelaro<sup>1</sup>).

<sup>1</sup>Department of Molecular Genetics and Biochemistry, <sup>2</sup>Department of Medicine, Renal-Electrolyte Division, <sup>3</sup>Department of Cell Biology and Physiology, School of Medicine, University of Pittsburgh, Pittsburgh, Pennsylvania

<sup>4</sup>Department of Infectious Disease and Microbiology, Graduate School of Public Health, University of Pittsburgh, Pittsburgh, Pennsylvania

Work described in this chapter is in fulfillment of specific aim 3.

## 5.2 ABSTRACT

Retroviral Gag polyproteins are necessary and sufficient for virus budding. Productive HIV-1 Gag assembly takes place at the plasma membrane, however, little is known about the mechanisms by which thousands of Gag proteins are transported to the plasma membrane. Using a bimolecular fluorescence complementation (BiFC) assay, we recently reported that the cellular sites and efficiency of HIV-1 Gag assembly depend on the precise pathway of Gag mRNA export from the nucleus, known to be mediated by Rev. In the current study, we further explore the defect of Rev-independent HIV-1 Gag. It assembles with slower kinetics, accumulates intracellularly and does not reach a lipid raft compartment at the surface where the wild-type Rev-dependent HIV-1 Gag efficiently assembles. Importantly, the defect of Rev-independent Gag can be rescued by co-expression of Rev-dependent Gag. Rescue *in trans* depends on the ability of Gag to interact with other Gag molecules and the ability to interact with cellular membrane. All other known functions of the rescuing Gag molecule such as matrix-dependent trafficking or the engagement of Tsg101 are not required. In addition, Rev-independent HIV-1 Gag assembly and budding could be rescued by plasma membrane targeting signals provided *in cis* and correlated with the restored lipid raft association. Taken together, our results suggest that lipid rafts are critical for HIV-1 Gag assembly and budding and that raft targeting of HIV-1 Gag is regulated as early as nuclear export of Gag-encoding mRNA.

### 5.3 INTRODUCTION

Retrovirus assembly and budding is a highly concerted process mediated by largely undefined spatially- and temporally-regulated interactions between viral proteins and cellular factors. During the viral assembly process, thousands of copies of viral structural polyproteins multimerize to form virus particles *via* an energy-dependent, multi-step process. Expression of retroviral Gag polyprotein is generally sufficient for the assembly and release of non-infectious virus like particles (VLPs). The Gag polyprotein consists of matrix (MA), capsid (CA), nucleocapsid (NC), late domain and spacer proteins and is cleaved into the distinct structural proteins upon virus maturation (Demirov and Freed, 2004;Morita and Sundquist, 2004). These Gag domains orchestrate the major steps in virus assembly and budding (reviews (Demirov and Freed, 2004;Morita and Sundquist, 2004)). It is well established that HIV-1 Gag buds from the plasma membrane of T lymphocytes and some epithelial cell lines (Demirov and Freed, 2004;Hermida-Matsumoto and Resh, 2000;Morita and Sundquist, 2004;Neil et al., 2006;Nguyen et al., 2003;Nydegger et al., 2003;Ono et al., 2004). In contrast, the major histocompatibility complex (MHC) class II compartments or multivesicular bodies (MVBs) are apparently the sites of HIV-1 Gag accumulation and particle production in macrophages and dendritic cells (Blom J. et al., 1993;Morita and Sundquist, 2004;Neil et al., 2006;Nguyen et al., 2003;Pelchen-Matthews et al., 2003;Rapooso et al., 2002). Based various studies showing that HIV-1 Gag may also target to MVBs in other cell types (Nydegger et al., 2003;Ono et al., 2004;Sherer et al., 2003), MVBs are thought to be the common budding sites for HIV-1. However, recent studies appeared to contradict this model by indicating the plasma membrane as the productive sites for HIV-1 Gag assembly and budding in various cells (Deneka et al., 2007;Finzi et al., 2007;Jouvenet et al., 2006;Welsch et al., 2007), including macrophages where HIV-1 virions bud from invaginated

plasma membranes (Deneka et al., 2007;Welsch et al., 2007). Little is known about the precise mechanisms by which thousands of copies of Gag molecules synthesized from ribosomes in the cytoplasm are transported to specific locations on the plasma membrane for assembly and budding. Consistent with results published by Malim and colleagues (Swanson et al., 2004;Swanson and Malim, 2006), our recent work suggests that HIV-1 Gag assembly is regulated at a step as early as nuclear export of its encoding mRNA (Jin et al., 2007).

Retroviral Gag polyproteins are synthesized from an unspliced full-length viral genomic mRNA that requires specific regulatory factors for nuclear export. The HIV-1 genome contains a *cis*-acting RNA element known as the Rev-response element (RRE) that binds to a viral *trans*-acting protein. Rev binds to the cellular Crm1 protein which in turn binds to Ran, a small GTPase that shuttles between the nucleus and the cytoplasm. Some simple retroviruses, such as Mason-Pfizer monkey virus (M-PMV), contain *cis*-acting RNA export elements (constitutive transport elements or CTE) that do not require viral *trans*-acting factors and that function by interacting directly with cellular export factors NXF1/NXT (Swanson and Malim, 2006). Swanson *et al* (Swanson et al., 2004) recently demonstrated that altering the RNA nuclear export element used by HIV-1 *gag-pol* mRNA from the RRE to the CTE resulted in efficient trafficking and assembly of Gag at cellular membranes in murine cells, which are notable for their inability to support HIV-1 assembly and budding (Bieniasz and Cullen, 2000;Mariani et al., 2000;Swanson et al., 2004). Our recent study also demonstrated that HIV-1 Gag assembly and budding in mouse cells could be rescued by substitution of the Rev-dependent RNA nuclear export signal with the hepatitis B virus posttranscriptional regulatory element (PRE) (Jin et al., 2007). Interestingly, in human cells the PRE-dependent, Rev-independent HIV-1 Gag showed lower assembly efficiency and different assembly sites compared with Rev-dependent HIV-1

Gag (Jin et al., 2007). These results support the model that RNA export pathway selection during Gag expression and assembly can affect the cytosolic fate or function of the HIV-1 Gag polyproteins.

In the current study, we sought to define the determinants for this RNA export dependence of efficient HIV-1 Gag assembly in human cells and to test whether Rev-independent HIV-1 Gag assembly and budding can be rescued by altering these determinants.

## **5.4 MATERIALS AND METHODS**

### **5.4.1 DNA mutagenesis**

Overlapping PCR was used to construct Gag mutations and fusion proteins. Rev-dependent and Rev-independent HIV-1 [pNL4-3 proviral clone(Adachi et al., 1986)] and EIAV [pEIAVuk proviral clone (Cook et al., 1998)] Gag expression vectors were described previously (Jin et al., 2007). For BiFC assays, gene sequences encoding the amino (residues 1-173, VN)- or carboxyl (residues 155-238, VC)- fragments of Venus fluorescence protein were fused to the C-terminus of EIAV or HIV-1 Gag via a 6-alanine linker as described previously (Jin et al., 2007). To make the VC-Tsg101 construct, VC was fused to the N-terminus of human Tsg101 (template generously provided by Dr. Walther Mothes, Yale University, CT) via a 6-alanine linker. To make hemagglutinin (HA) epitope-tagged Gag polyproteins, the YPYDVPDYA epitope from influenza virus HA protein was inserted into the C-terminus of p9 or p6 protein, respectively. All plasmids were isolated using the Qiagen Midiprep Kit (Qiagen, Valencia, CA), and the specific mutations were confirmed by DNA sequencing.

### **5.4.2 Cell culture and transfection**

HeLa SS6 and 293T cells were cultured in Dulbecco's Modified Essential Medium (DMEM) supplemented with 10% fetal bovine serum. Cells were transfected using Lipofectamine 2000 (Invitrogen, Carlsbad, CA) following the procedures outlined by the manufacturer.

### 5.4.3 Gag budding assays

At 24 h post transfection, cells were harvested and lysed in lysis buffer (25 mM Tris-HCl, pH 8.0, 150 mM NaCl, 1% deoxycholic acid, 1% Triton X-100, 1x protease inhibitor cocktail) and centrifuged at 20,800xg for 5 min to remove cell nuclei. Virus-like particles (VLPs) released into the culture medium were pelleted by centrifugation (20,800xg for 3 h at 4°C) and resuspended in PBS. HA-Gag contained in cell lysates and VLPs was analyzed by Western Blotting using rat anti-HA antibody (Roche Applied Science, Indianapolis, IN) and HRP conjugated goat anti-rat IgG (Invitrogen, Carlsbad, CA), as described previously (Jin et al., 2007).

### 5.4.4 Confocal microscopy

Transfected cells grown on coverslips were fixed and permeabilized with 2% paraformaldehyde and 0.1% Triton X-100 in PBS. Images were captured using a Leica TCS-SL microscope and processed with Metamorph software.

### 5.4.5 Flow cytometry analysis

HeLa SS6 cells grown on 6-well plates were transfected with selected BiFC construct pairs. Cells were detached with PBS containing 2.5 mM EDTA and resuspended in PBS at 16 h post-transfection. For HA staining (**Figs. 5-3 and 5-4**), cells were washed three times with PBS containing 5% FBS (wash buffer) and fixed in 1% paraformaldehyde for 1 h, followed by permeabilization with PBS containing 5% fetal calf serum and 0.5% saponin. Cells were incubated with mouse anti-HA epitope antibody (Santa Cruz Biotechnology, Santa Cruz, CA),

washed, and then incubated with Cy5-conjugated goat anti-mouse IgG (Jackson ImmunoResearch Laboratory, West Grove, PA). A minimum of 30,000 gated live events were acquired on a FACSCalibur (Becton Dickinson, San Jose, CA) flow cytometer and analyzed with FlowJo batch analysis software (Treestar, San Carlos, CA) for both yellow fluorescence and HA staining.

#### **5.4.6 Membrane flotation analysis**

Membrane flotation procedures were performed as described (Chatel-Chaix et al., 2007; Ono and Freed, 1999). At 24 h post-transfection, 293T cells were washed twice with phosphate-buffered saline, collected, and homogenized in 300  $\mu$ l of TE buffer (10mM Tris [pH 7.4], 1mM EDTA [pH 8]) containing 10% sucrose and protease inhibitor cocktail by passaging 24 times through a 23G11/4 needle. Nuclei were removed by centrifugation at 1,000xg. A 250  $\mu$ l sample of post nuclear supernatants (PNSs) were mixed with 1.25 ml of TE 85.5% sucrose (adjusting the concentration of sucrose to 73%) and deposited at the bottom of a 5-ml centrifugation tube. TE 65% sucrose (2.5ml) and then 1ml of TE 10% sucrose were layered above the lysate. The samples were subjected to ultracentrifugation at 100,000xg for at least 14 h at 4°C in a SW55Ti rotor (Beckman Coulter). For lipid raft association, PNSs were treated with Trion X-100 (final concentration 0.5%) for 30 min on ice prior to flotation centrifugation. Nine fractions of 550  $\mu$ l were collected from the top and analyzed by Western Blotting using the rat monoclonal anti-HA antibody (Roche Applied Science, Indianapolis, IN), mouse monoclonal anti-human transferrin receptor antibody (Invitrogen, Carlsbad, CA) and mouse monoclonal anti- $\beta$  actin antibody (Sigma-Aldrich, Saint Louis, MO).

#### **5.4.7 Immunoprecipitation**

At 24 h post-transfection, 293T cells were washed twice with phosphate-buffered saline, collected, and lysed in RIPA buffer. Clarified cell lysates were immunoprecipitated with monoclonal anti-HA agarose conjugate (Sigma-Aldrich, Saint Louis, MO) overnight at 4°C prior to SDS-PAGE and Western Blot analysis with mouse anti-GFP (Roche Applied Science, Indianapolis, IN) and rat anti-HA antibody (Roche Applied Science, Indianapolis, IN).

## 5.5 RESULTS

### 5.5.1 Distinct Intracellular Distribution of Rev-dependent and Rev-independent HIV-1

#### Gag

We recently demonstrated different assembly efficiencies and assembly sites between Rev-dependent and Rev-independent HIV-1 Gag in both human and mouse cell lines (Jin et al., 2007). We proposed that distinct intracellular traffic of Gag after synthesis from mRNA exported from the nucleus via different pathways accounted for this distinct Gag assembly pattern. Since the BiFC assays used in our previous study only revealed *assembled* Gag multimers inside cells, in the current study we first compared the steady-state distribution of the total population of Rev-dependent or Rev-independent HIV-1 Gag-GFP in HeLa cells. The results of these studies revealed that Rev-dependent HIV-1 Gag-GFP was primarily localized to cell surface puncta in most cells (**Fig. 5-1, panel A-a**). In contrast, Rev-independent HIV-1 Gag-GFP was present largely in intracellular puncta (**Fig. 5-1, panel A-c**). These observations are consistent with the different Gag trafficking patterns between Rev-dependent and Rev-independent HIV-1 Gag that we demonstrated previously using the BiFC assay (Jin et al., 2007). We also observed a diffuse distribution pattern in some cells expressing either Rev-dependent or Rev-independent HIV-1 Gag (**Fig. 5-1, panels A-b and -d**), consistent with the reported distribution of Rev-independent HIV-1 Gag distribution at early times after expression (Gomez and Hope, 2006; Jouvenet et al., 2006; Perez-Caballero et al., 2004; Perlman and Resh, 2006). The distribution patterns of Rev-dependent and Rev-independent HIV-1 Gag-GFP were quantified at 8 h and 16 h post-

transfection (**Fig. 5-1, panel A-e**). At least 100 GFP positive cells were randomly chosen for each condition, and their distribution patterns scored as punctate or diffuse. The distribution of Rev-dependent HIV-1 Gag-GFP was punctate in a majority (>80%) of cells at both time points. In contrast, the distribution of Rev-independent HIV-1 Gag-GFP changed with expression time. Gag distribution was diffuse in >90% of cells at 8 h post transfection, and the diffuse population decreased to 40% by 16 h post transfection. This trend is reminiscent of the time-dependent distribution pattern of codon-optimized HIV-1 Gag (another Rev-independent HIV-1 Gag) in 293T cells (Jouvenet et al., 2006). If the punctate Gag-GFP signal represents assembled Gag multimers as previously suggested (Gomez and Hope, 2006), our results indicate faster assembly kinetics of Rev-dependent HIV-1 Gag compared with Rev-independent HIV-1 Gag, consistent with our recent report that Rev-dependent HIV-1 Gag assembles more efficiently in human cells compared with Rev-independent HIV-1 Gag.

We next took advantage of the BiFC assay that enables us to selectively observe interacting protein complexes (as opposed to the total pool of expressed proteins) to compare the interactions of Rev-dependent or Rev-independent HIV-1 Gag with Tsg101, the budding partner for HIV-1 late domain PTAP. The amino (VN) terminal fragment of Venus fluorescence protein was appended to the C-terminus of HIV-1 Gag to make Rev-dependent and Rev-independent HIV-1 Gag-VN constructs (Jin et al., 2007), and the carboxy (VC) terminal fragment was added to the N-terminus of human Tsg101 to make VC-Tsg101. HeLa cells were transfected with VC-Tsg101 paired with either Rev-dependent or Rev-independent HIV-1 Gag-VN. The results showed that at 8 h post-transfection, both Rev-dependent and Rev-independent HIV-1 Gag interacted with Tsg101, resulting in bright BiFC signals in Gag-VN and VC-Tsg101 co-transfected HeLa cells (**Fig. 5-1, panel B**). However Rev-dependent HIV-1 Gag and Rev-

independent HIV-1 Gag appeared to recruit Tsg101 to different sites. The Rev-dependent HIV-1 Gag-Tsg101 BiFC signal was located at the cell surface and at intracellular sites that colocalized with late endosome/MVB marker CD63 (**Fig. 5-1, panels B-a to -d**). In contrast, Rev-independent HIV-1 Gag interacted with Tsg101 exclusively at intracellular sites that did not colocalize with CD63 (**Fig. 5-1, panels B-e to -h**). These results further confirm the distinct trafficking of Rev-dependent and Rev-independent HIV-1 Gag in human cells.

### **5.5.2 Co-assembly of Rev-dependent and Rev-independent HIV-1 Gag Rescues Budding of Rev-independent HIV-1 Gag**

We next sought to test whether Rev-dependent and Rev-independent HIV-1 Gag can interact with each other even though they take different trafficking pathways. Co-expression of Rev-dependent Gag-VC with Rev-independent Gag-VN (**Fig. 5-2, panel A-c**) or of Rev-dependent Gag-VN with Rev-independent Gag-VC (**Fig. 5-2, panel A-d**) both resulted in bright punctate BiFC signals on the plasma membrane. This pattern was similar to the BiFC pattern obtained upon coexpression of Rev-dependent HIV-1 Gag VN and VC pairs (**Fig. 5-2, panel A-a**). In marked contrast, expression of Rev-independent HIV-1 Gag VN and VC pairs resulted in a weaker intracellular punctate signal above a diffuse background (**Fig. 5-2, panel A-b**) as we reported previously (Jin et al., 2007).

Recently, several groups reported that the plasma membrane is the productive assembly and budding sites for HIV-1 (Deneka et al., 2007; Finzi et al., 2007; Jouvenet et al., 2006; Welsch et al., 2007), even in primary macrophages (Nguyen et al., 2003; Nydegger et al., 2003; Pelchen-Matthews et al., 2003; Raposo et al., 2002). Our previous observation that Rev-dependent HIV-1 Gag assembled at plasma membrane budded far more efficiently than Rev-independent HIV-1

Gag, which failed to assemble at the plasma membrane also supports this model (Jin et al., 2007). Since Rev-dependent HIV-1 Gag could co-assemble with Rev-independent Gag at the plasma membrane, we next tested whether this co-assembly at productive sites can rescue Rev-independent HIV-1 Gag budding in human cells. Rev-independent HIV-1 Gag-GFP was co-transfected with HA-tagged Rev-independent or Rev-dependent HIV-1 Gag in 293T cells. At 24 h post transfection, cell lysates and supernatant pellets (VLPs) were subjected to SDS-PAGE and Western Blotting to determine budding efficiencies. Co-expression with Rev-dependent HIV-1 Gag-HA enhanced Rev-independent HIV-1 Gag-GFP budding by about 10 fold (**Fig. 5-2, panel D**, compare lanes 1 and 3). In contrast, co-expression of Rev-independent HIV-1 Gag-HA only enhanced budding of Rev-independent HIV-1 Gag-GFP by less than 2 fold (**Fig. 5-2, panel D**, compare lanes 1 and 2). This modest enhancement is likely due to the increase in intracellular Gag concentration when the two Rev-independent constructs are co-expressed.

To gain further insight into the key determinants in Rev-dependent Gag required to restore budding of co-expressed Rev-independent Gag, we generated a panel of Rev-dependent HIV-1 Gag mutants (**Fig. 5-2, panel B**) and tested their ability to rescue Rev-independent HIV-1 Gag-GFP budding (**Fig. 5-2, panel D**). All of these constructs expressed well in 293T cells, and as expected, the deletion of CA ( $\Delta$ CA) or mutation of two critical amino acids at the Gag dimerization interface W<sub>184</sub>M<sub>185</sub> (WM<sub>184,185</sub>AA) abrogated Gag budding, presumably due to their deficiency in Gag multimerization (**Fig. 5-2, panel C, lanes 6 and 7**). The myristoylation deficient G2A mutant, which cannot insert into membranes, was also deficient in VLP release (**Fig. 5-2, panel C, lane 3**). In addition, budding of PTAP L domain deletion mutant ( $\Delta$ PTAP) was lower than wild type Gag (**Fig. 5-2, panel C, lane 2**), as expected due to the lack of interaction with endocytic co-factors. Replacing MA with the myristoylation signal of v-Src

(Src $\Delta$ MA) or deletion of the MA globular head (residues 8-126;  $\Delta$ 8-126) to produce Gag polyproteins with constitutively exposed myristoyl residues (Reil H et al., 1998; Saad et al., 2006; Spearman et al., 1997; Tang et al., 2004) yielded Gag constructs that both were budding competent (**Fig. 5-2, panel C, lanes 4 and 5**). This panel of mutants was then co-expressed with Rev-independent HIV-1 Gag-GFP, and budding of the latter was monitored (**Fig. 5-2, panel D**). The L-domain mutant (**Fig. 5-2, panel D, lane 4**) and two MA mutants with constitutively exposed myristoyl residues (**Fig. 5-2, panel D, lanes 5 and 6**) could rescue budding of co-expressed Rev-independent HIV-1 Gag-GFP as efficiently as wild type Rev-dependent HIV-1 Gag. However, the G2A mutant (**Fig. 5-2, panel D, lane 7**) and the two dimerization mutants (**Fig. 5-2, panel D, lanes 8 and 9**) were unable to enhance budding of co-expressed Rev-independent HIV-1 Gag-GFP compared to co-expression of Rev-independent wild type HIV-1 Gag (**Fig. 5-2, panel D, lane 2**).

To test if the inability to rescue Rev-independent HIV-1 Gag assembly and budding by G<sub>2</sub>A mutant was due to its inability to bind membrane and to interact with Rev-independent HIV-1 Gag, we next performed a co-immunoprecipitation assay to assess the ability of these Rev-dependent HIV-1 Gag constructs to interact with co-expressed Rev-independent Gag in 293T cells (**Fig. 5-2, panel E**). Rev-independent HIV-1 Gag-GFP was co-expressed with wild type or mutant Rev-dependent HIV-1 Gag-HA or with Rev-independent HIV-1 Gag-HA, as described above. HA-tagged Gag and associated proteins were then immunoprecipitated by adding agarose-bound anti-HA antibodies to the cell lysates, and the immunoprecipitated proteins were examined by immunoblotting using HA- and GFP-specific antibodies. The results of these assays revealed that Rev-independent HIV-1 Gag-GFP co-precipitated with wild type and with  $\Delta$ PTAP Rev-dependent HIV-1 Gag (**Fig. 5-2, panel E, lanes 3 and 4**), but not with

Rev-independent HIV-1 Gag(**Fig. 5-2, panel E, lane 2**), indicating higher Gag assembly efficiency in a system containing Rev-dependent Gag relative to one containing only Rev-independent Gag. The co-precipitation specificity was confirmed by the lack of detectable Gag-GFP precipitated by anti-HA antibody (**Fig. 5-2, panel E, lane 1**). As expected, Rev-independent HIV-1 Gag-GFP could not be precipitated with  $\Delta$ CA and WM<sub>184,185</sub>AA mutants that lost Gag-Gag interaction ability (**Fig. 5-2, panel E, lanes 6 and 7**). In contrast, the G<sub>2</sub>A mutant was able to bind with Rev-independent HIV-1 Gag-GFP (**Fig. 5-2, panel E, lane 5**). Together, these data demonstrate that proper membrane association of Rev-dependent HIV-1 Gag construct and co-assembly of Rev-dependent Gag with Rev-independent Gag are required to rescue the budding of Rev-independent HIV-1 Gag in human cells.

### **5.5.3 Substitution of the Membrane Binding Domain Rescues Rev-independent HIV-1 Gag Assembly and Budding**

Because our results suggested that membrane targeting of Rev-dependent HIV-1 Gag is required to rescue budding of co-expressed Rev-independent HIV-1 Gag, we next asked whether Rev-independent HIV-1 Gag assembly and budding in human cells can be rescued by substitution of the HIV-1 membrane binding motif with other membrane targeting motifs. As we previously reported that unlike HIV-1 Gag, both Rev-dependent and Rev-independent EIAV Gag could efficiently assemble and bud from human cells (Jin et al., 2007), we also tested whether switching MA domains of EIAV and HIV-1 Gag altered their assembly and budding phenotypes.

We first constructed a panel of Rev-independent HIV-1 Gag and EIAV Gag MA mutants (**Fig. 5-3, panel A**). For each, we made three constructs: a C-terminally HA-tagged construct for the budding assay (**Fig. 5-3, panel B**), and C-terminal HA-VN and HA-VC tagged pairs for the

BiFC-based assembly assays (**Fig. 5-3, panel C**). 293T cells were transfected with this panel of HA tagged Rev-independent HIV-1 Gag and EIAV Gag constructs, followed by Western Blotting of cell lysates and pelleted VLPs at 24 h post transfection. The results of these assays revealed that the budding efficiency of Rev-independent HIV-1 Gag in human cells was as low as that of the myristoylation-deficient G<sub>2</sub>A mutant (**Fig. 5-3, panel B**, compare lanes 1 and 5). Replacing the HIV MA with the v-Src myristoylation signal or adding the v-Src myristoylation signal directly to the N-terminus of HIV-1 Gag both rescued Rev-independent HIV-1 Gag budding (**Fig. 5-3, panel B, lane 2 and lane 3**). Consistent with what we reported previously (Jin et al., 2007), and in contrast to Rev-independent HIV-1 Gag, Rev-independent EIAV Gag could bud efficiently from human cells (**Fig. 5-3, panel B**, compare lane 1 and lane 6). Interestingly, MA swapping reversed this phenotype. Rev-independent chimeric HIV-1 Gag containing EIAV MA budded efficiently (**Fig. 5-3, panel B, lane 4**), whereas Rev-independent chimeric EIAV Gag containing HIV MA did not (**Fig. 5-3, panel B, lane 8**). This Rev-independent EIAV Gag budding deficiency seemed to be specific for the HIV MA, because replacing EIAV MA with the v-Src myristoylation signal did not interfere with chimeric EIAV Gag budding (**Fig. 5-3, panel B, lane 7**).

We next used the BiFC assay to characterize and compare Rev-independent HIV-1 Gag and EIAV Gag assembly in HeLa cells (**Fig. 5-3, panel C**). Cells were transfected with Gag-BiFC pairs, and then analyzed by confocal microscopy at 8 h post transfection to reveal the intracellular Gag assembly pattern. At 16 h post transfection, cells were analyzed by flow cytometry to quantify Gag assembly efficiency, as described previously (Jin et al., 2007). Briefly, cells were fixed and permeabilized, stained with mouse HA antibody followed by Cy5 conjugated secondary antibody, and then both BiFC and Cy5 signals were analyzed by flow

cytometry. To normalize differences in transfection efficiency and Gag expression levels, the ratio of the HA and BiFC double-positive population to the total HA-positive population was used to calculate assembly efficiency. Cells transfected with an HA-tagged VN-actin/VC-actin pair were used as a positive control (Chen et al., 2007; Jin et al., 2007). In VN-actin/VC-actin co-transfected HeLa cells, 92% of HA-positive cells exhibited positive BiFC signal (**Fig. 5-3, panel C-i**), while none of the HA-positive cells displayed yellow fluorescence in a mock-transfected control (**Fig. 5-3, panel C-j**). As we reported previously, Rev-independent HIV-1 Gag assembled inefficiently in HeLa cells with an efficiency (13%) as low as the myristoylation deficient Gag mutant (**Fig. 5-3, panel C**, compare panels C-a and C-e). Replacing HIV matrix with the v-Src myristoylation signal (**Fig. 5-3, panel C-b**) or adding it directly to the N-terminus of HIV-1 Gag (**Fig. 5-3, panel C-c**) rescued Rev-independent HIV-1 Gag assembly, resulting in bright intracellular and cell surface BiFC signals with assembly efficiencies of 40% and 37%, respectively. Interestingly, replacing HIV MA with EIAV MA also increased Rev-independent HIV-1 Gag assembly from 13% to 39% (**Fig. 5-3, panel C**, compare panel C-a and C-d). However, substitution of EIAV MA with HIV MA reduced Rev-independent EIAV Gag assembly efficiency from 41% to 24% (**Fig. 5-3, panel C**, compare panel C-f and C-h). Moreover, the block of chimeric EIAV Gag assembly seemed to be specific for HIV-1 MA, because the chimeric EIAV Gag with EIAV MA substituted by the v-Src myristoylation signal still yielded bright BiFC signals with high efficiency (53%) (**Fig. 5-3, panel C-g**). Thus, the efficiency of Gag assembly as determined using BiFC assays (**Fig. 5-3, panel C**) correlated well with VLP release as demonstrated by immunoblotting analysis (**Fig. 5-3, panel B**).

#### 5.5.4 mRNA Nuclear Export Pathway Regulates HIV-1 Gag Targeting to Lipid Raft

Our results showed that budding of Rev-independent HIV-1 Gag in human cells could be rescued by providing correct membrane targeting signals either *in trans* [by co-expressing dimerization and membrane targeting competent Rev-dependent HIV-1 Gag (**Fig. 5-2**)] or *in cis* [by replacing HIV-1 matrix with other functional membrane binding motifs (**Fig. 5-3**)]. This observation suggests that membrane targeting of Rev-independent HIV-1 Gag is deficient in human cells. Therefore, we tested whether membrane association of HIV-1 is regulated by mRNA nuclear export pathways (**Fig. 5-4, panel A**). Postnuclear supernatants derived from 293T cells expressing either Rev-dependent HIV-1 Gag or Rev-independent HIV-1 Gag were analyzed using membrane flotation to segregate membrane-associated and soluble Gag (Chatel-Chaix et al., 2007;Ono and Freed, 1999). After centrifugation, gradient fractions were collected and analyzed for Gag content by Western blotting. Transferrin receptor and actin were used as markers for membrane (fraction 1 to 3) and soluble (fraction 7 to 9) fractions, respectively. Roughly equal amounts of Rev-dependent and Rev-independent HIV-1 Gag were found in membrane fractions, and these populations represented a significant proportion of the total Gag expressed in each case. Under the same condition, myristoylation deficient G2A mutants were not present in membrane fractions regardless of whether they were expressed in a Rev-dependent or Rev-independent context, consistent with previous reports (Ding et al., 2003;Jager et al., 2007;Ono and Freed, 1999). These data indicate that Rev-independent HIV-1 Gag can target cell membranes and is unlikely to be myristoylation deficient in human cells, consistent with other studies showing efficient membrane association of Rev-independent HIV-1 Gag in human cells (Hatzioannou et al., 2005;Jager et al., 2007;Spearman et al., 1997).

It has been reported that plasma membrane lipid rafts play a critical role in HIV-1 Gag assembly and budding (Brugger et al., 2006; Ono et al., 2007; Ono and Freed, 2001), so we next tested whether Rev-dependent and Rev-independent HIV-1 Gag were differentially targeted to lipid rafts (**Fig. 5-4, panel B**). Postnuclear supernatants derived from 293T cells expressing either Rev-dependent HIV-1 Gag or Rev-independent HIV-1 Gag were analyzed as described above except that they were treated with 0.5% Triton X-100 on ice for 30 min before being subjected to membrane flotation. Under these conditions, transferrin receptor, a membrane protein known to not partition into detergent-insoluble microdomains, was not detected in membrane fractions. As reported previously, Rev-dependent HIV-1 Gag could still be detected in membrane fractions after cold Triton X-100 treatment, demonstrating its association with lipid rafts or detergent-resistant membranes. In contrast, Rev-independent HIV-1 Gag was present exclusively in non-membrane fractions after detergent extraction, suggesting it is localized to non-raft membrane fractions in human cells.

Since our previous results showed that substitution of HIV MA with either v-Src membrane targeting signal or EIAV MA rescued Rev-independent HIV-1 Gag assembly and budding in human cells (**Fig. 5-3**), we next tested if these mutants associate with lipid rafts (**Fig. 5-4, panel C**). Postnuclear supernatants derived from 293T cells expressing wild type and mutant Rev-independent HIV-1 Gag were subjected to membrane flotation assay with or without prior treatment with 0.5% Triton X-100 on ice for 30 min. Membrane fractions (fraction 1 to 3) and soluble fractions (fraction 7 to 9) were pooled together before Western blotting analysis for Gag content. As shown in Fig. 4B, most of the membrane-bound Rev-independent HIV-1 Gag shifted to the soluble fractions upon cold Triton X-100 treatment. In contrast, Src $\Delta$ MA, Src<sup>+</sup> and eMA $\Delta$ MA mutants, all of which are assembly and budding competent (**Fig. 5-3**), were still

present in membrane fractions after Triton X-100 extraction, demonstrating their association with lipid rafts. Taken together, these results demonstrate a positive correlation between lipid raft association of HIV-1 Gag and Gag assembly and budding.

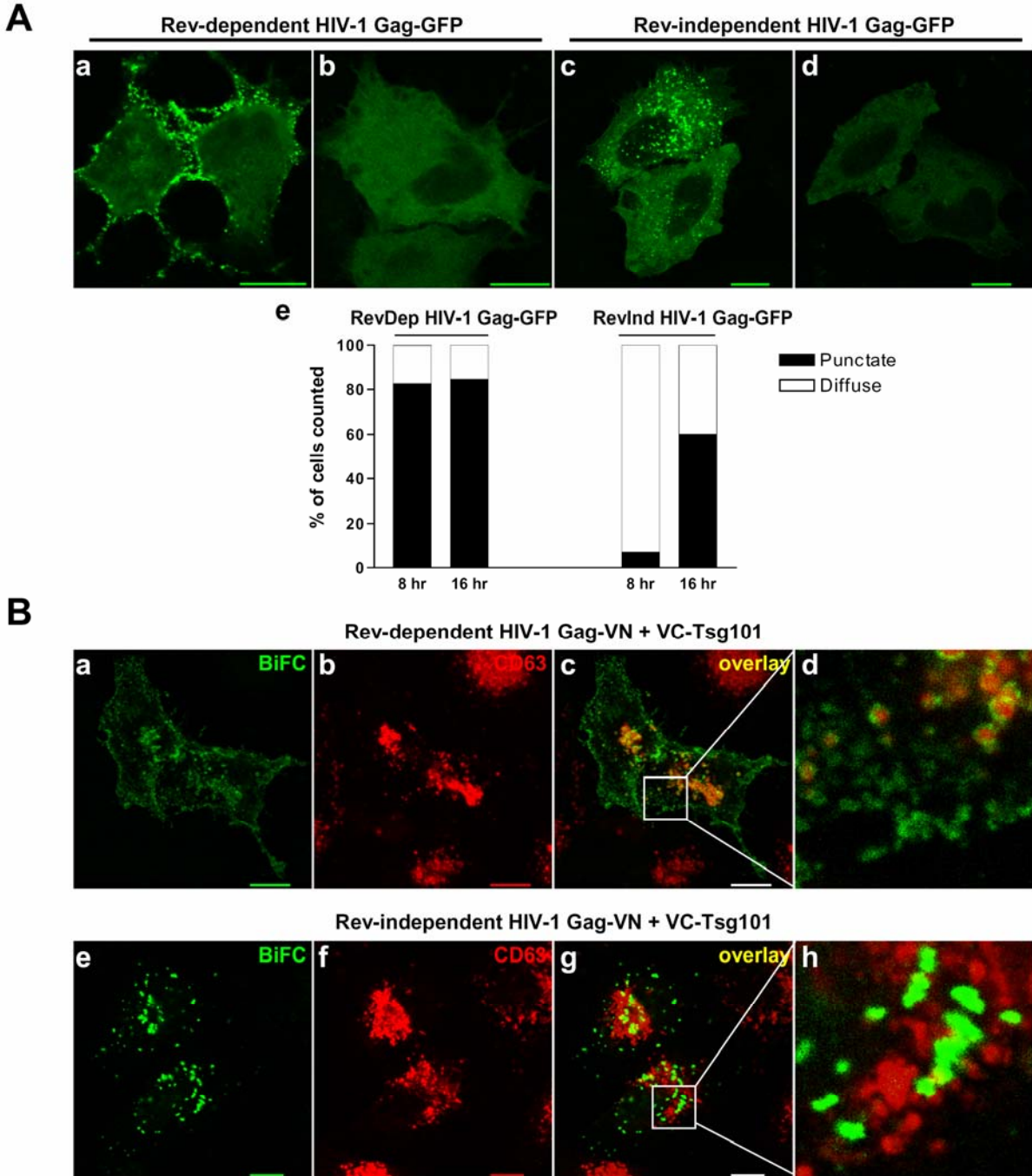


**Figure 5-1. Distinct intracellular distribution of Rev-dependent and Rev-independent HIV-1 Gag.**

(A) Distribution of Rev-dependent and Rev-independent HIV-1 Gag-GFP in HeLa cells. HeLa cells grown on glass coverslips were transfected with Rev-dependent HIV-1 Gag-GFP (panels a and b) or Rev-independent HIV-1 Gag-GFP (panels c and d) expression vectors. At 8 h and 16 h post transfection, cells were fixed and imaged. Bar: 10  $\mu$ m. The number of cells in which Gag-

GFP accumulation was observed as punctate or as diffuse signals was counted (panel e). At least 100 randomly picked GFP positive cells were evaluated at each time point. **(B)** BiFC analysis of Rev-dependent and Rev-independent HIV-1 Gag interaction with Tsg101. HeLa cells grown on glass coverslips were transfected with plasmid pairs expressing Rev-dependent HIV-1 Gag-VN and VC-Tsg101 (panels a to d) or Rev-independent HIV-1 Gag-VN and VC-Tsg101 (panels e to h). At 8 h post transfection, cells were fixed, permeabilized, and stained with mouse anti-CD63 and Alexa 647 conjugated secondary antibody. Cells were imaged by confocal microscopy. Enlarged images of boxed areas in panels c and g are presented in panels d and h. Bar: 10  $\mu$ m.

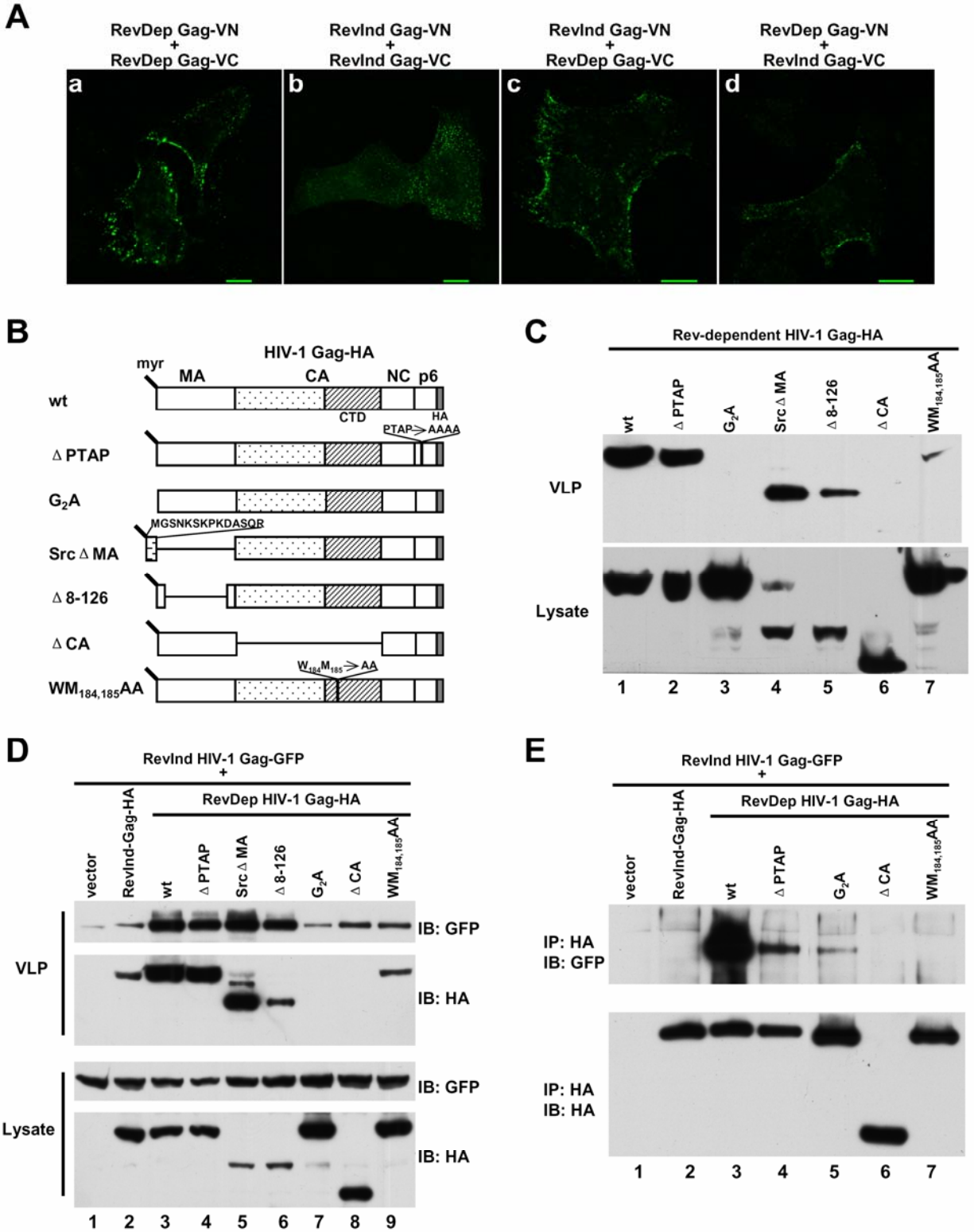


Figure 5-2. Co-assembly with Rev-dependent HIV-1 Gag rescued Rev-independent HIV-1 Gag budding.

### Figure 5-2. continue

(A) Demonstration of co-assembly of Rev-dependent and Rev-independent HIV-1 Gag by BiFC. HeLa cells grown on glass coverslips were transfected with plasmids expressing the indicated HIV-1 Gag-BiFC pair. At 8 h post transfection, cells were fixed and imaged. Bar: 10  $\mu$ m. (B) Schematic diagram of plasmids expressing HA tagged Rev-dependent HIV-1 Gag mutants. (C) Expression and budding of the constructs depicted in (A) in transfected 293T cells. At 24 h post transfection, VLPs (upper panel) and cell lysates (lower panel) were analyzed by immunoblotting using anti-HA antibody. (D) Budding of Rev-independent HIV-1 Gag-GFP upon co-expression with Rev-independent or Rev-dependent HIV-1 Gag-HA. Rev-independent HIV-1 Gag-GFP was co-transfected at an equal molar ratio into 293T cells with empty vector, Rev-independent HIV-1 Gag-HA, or the indicated Rev-dependent HIV-1 Gag-HA constructs described in A and B. At 24 h post transfection, VLPs (upper panel) and cell lysates (lower panel) were analyzed by immunoblotting using GFP and HA antibody. (E) Interaction of Rev-independent HIV-1 Gag-GFP with co-expressed Gag-HA. Rev-independent HIV-1 Gag-GFP was transfected into 293T cells with empty vector, Rev-independent HIV-1 Gag-HA, or indicated Rev-dependent HIV-1 Gag-HA at an equal molar ratio. At 24 h post transfection, cell lysates were subjected to immuno-precipitation with HA antibody followed by immunoblotting analysis of precipitated proteins using GFP and HA antibody.

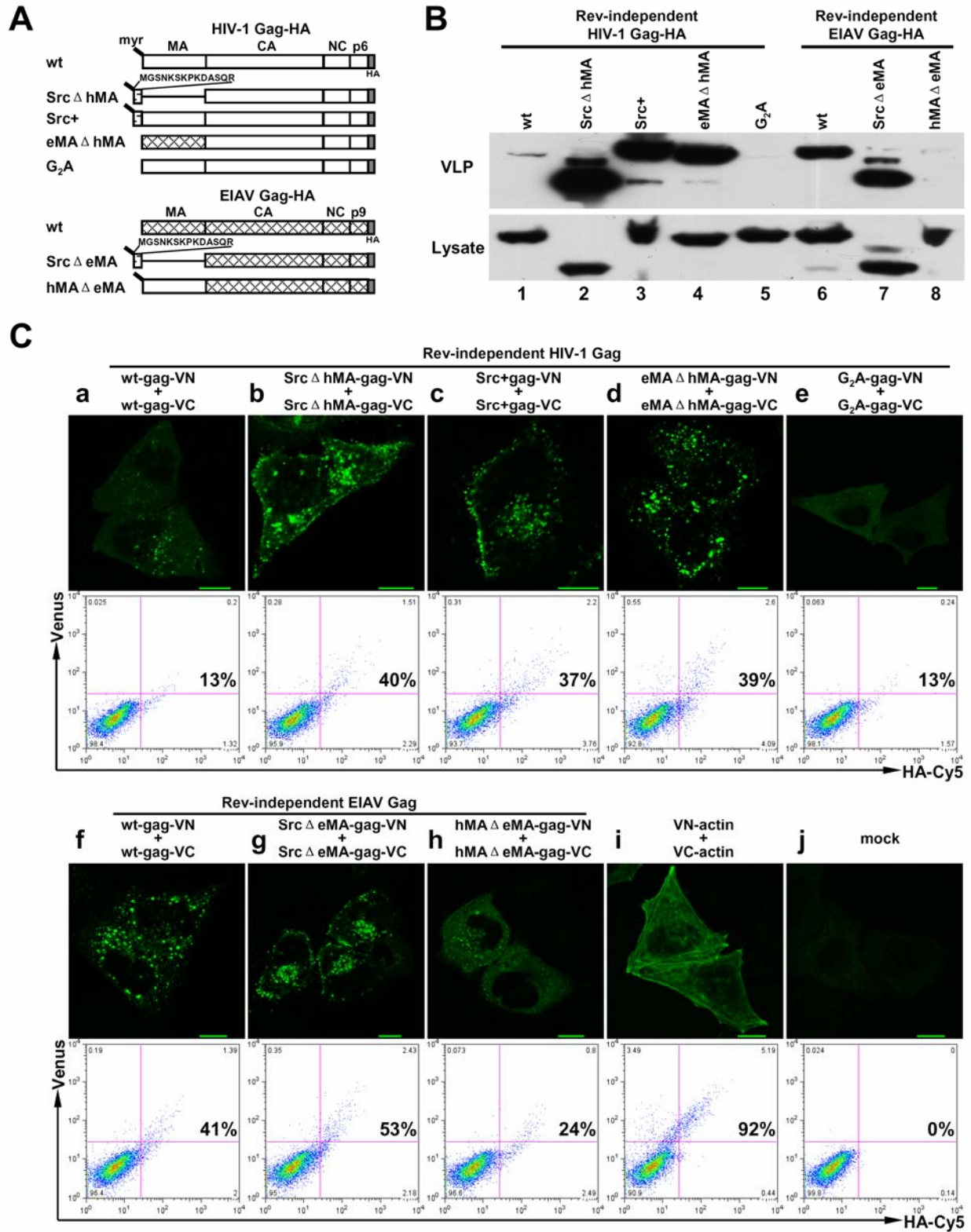


Figure 5-3. Substitution of HIV-1 matrix with other membrane targeting domains rescued Rev-independent HIV-1 Gag assembly and budding in human cells.

**Figure 5-3. continue**

**(A)** Schematic diagram of plasmids expressing HA tagged Rev-independent HIV-1 Gag mutants (upper panel) and EIAV Gag mutants (lower panel). **(B)** Budding of Rev-independent HIV-1 and EIAV Gag mutants. 293T cells were transfected with the indicated Rev-independent HIV-1 and EIAV Gag mutants described in (A). At 24 h post transfection, VLPs (upper panel) and cell lysates (lower panel) were analyzed by immunoblotting using HA antibody. **(C)** Demonstration of Rev-independent HIV-1 (panels a to e) and EIAV Gag mutant (panels f to h) association by BiFC assays. HeLa cells were transfected with the indicated BiFC pairs and imaged at 8 h post transfection. At 16 h post transfection cells were fixed and analyzed using flow cytometry to quantify BiFC signals as described in Materials and Methods. The percentage of HA and BiFC double-positive cells relative to total HA positive cells was calculated and labeled in each quadrant plot. Bar: 10  $\mu$ m.

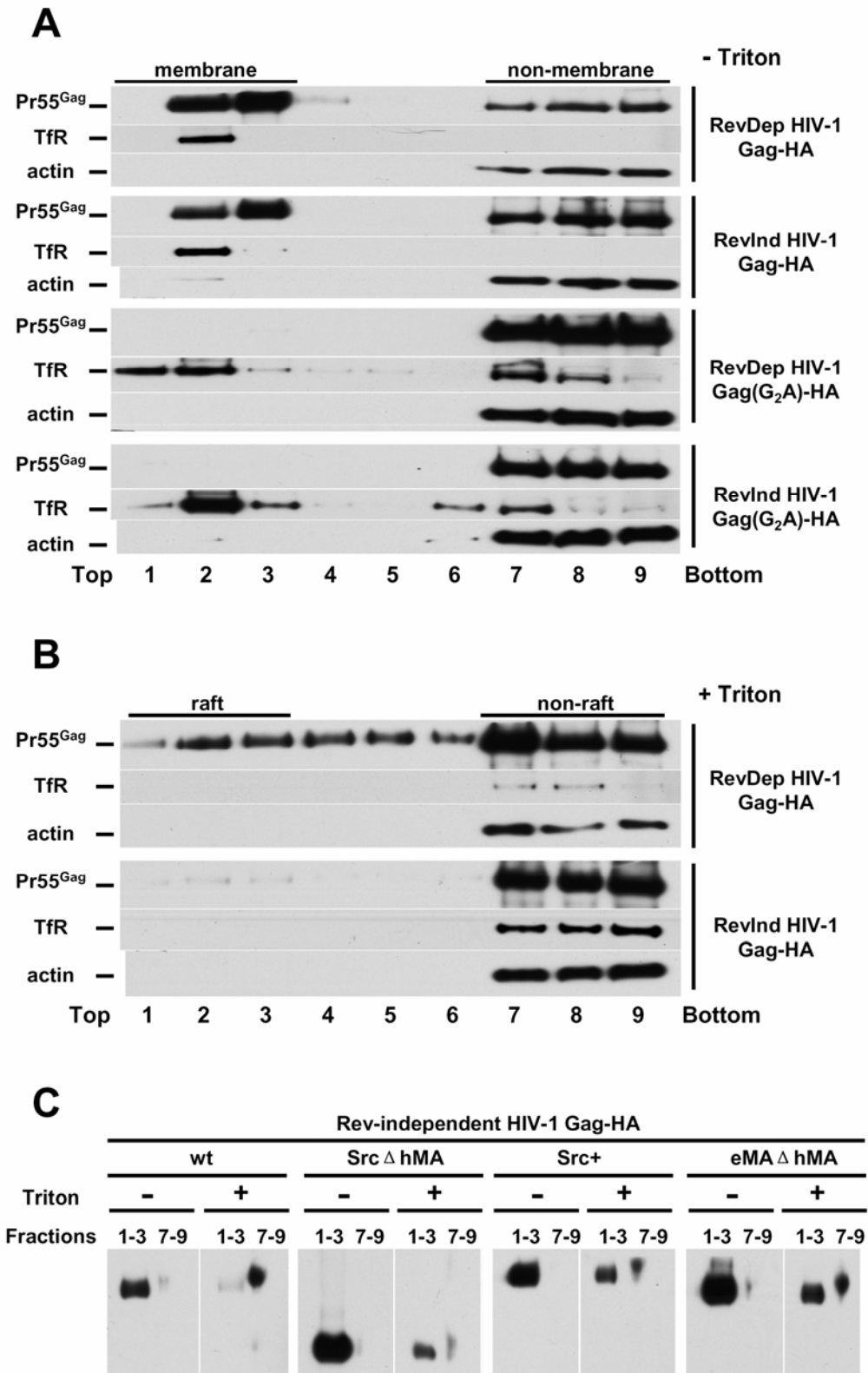


Figure 5-4. Rev-independent HIV-1 Gag failed to associate with lipid raft in human cells.

### Figure 5-5. continue

(A) Both Rev-dependent and Rev-independent HIV-1 Gag are membrane-associated in human cells. Postnuclear supernatants derived from 293T cells expressing Rev-dependent or Rev-independent HIV-1 Gag, Rev-dependent or Rev-independent G2A mutant were subjected to equilibrium flotation centrifugation. Pr55<sup>Gag</sup>, TfR and actin were detected by Western Blotting. Membrane- and non-membrane-associated fractions were shown. (B) Rev-dependent HIV-1 Gag but not Rev-independent HIV-1 Gag is associated with Triton X-100 insoluble lipid rafts in human cells. Postnuclear supernatants derived from 293T cells expressing Rev-dependent or Rev-independent HIV-1 Gag were treated with 0.5% Triton X-100 on ice for 30 min prior to membrane flotation analysis. Pr55<sup>Gag</sup>, TfR and actin were detected by Western Blotting. Raft and non-raft fractions are indicated. (C) Assembly and budding competent Rev-independent HIV-1 Gag mutants are associated with Triton X-100 insoluble lipid rafts in human cells. Postnuclear supernatants derived from 293T cells expressing wild type or mutant Rev-independent HIV-1 Gag were treated with or without 0.5% Triton X-100 on ice for 30 min prior to membrane flotation analysis. Pooled membrane fractions (fraction 1-3) and soluble fractions (fraction 7-9) were analyzed for Gag content by Western Blotting.

## 5.6 DISCUSSION

Recently, we reported that HIV-1 Gag assembly and budding are regulated by the nuclear export pathway of Gag-encoding mRNA and proposed that altered Gag trafficking is responsible for these differences in Gag assembly and budding. In the current study, we have confirmed differential trafficking of Rev-dependent and Rev-independent HIV-1 Gag in human cells and performed a mechanistic analysis of the regulation of HIV-1 Gag traffic by mRNA nuclear export pathways. The current studies for the first time clearly demonstrate that HIV-1 Gag targeting to lipid rafts is regulated as early as nuclear export of the Gag encoding mRNA.

HIV-1 assembly and budding have been proposed to occur at plasma membrane microdomains that are highly enriched in sphingolipids and cholesterol, termed lipid rafts (Ono and Freed, 2001; Simons and Toomre, 2000; Simons and Vaz, 2004). Clustering of separate rafts exposes raft associated proteins to a new membrane environment and facilitates raft protein interactions. This dynamic feature enables rafts to serve as concentrating platforms for signal transduction and protein trafficking (Kusumi et al., 2004; Simons and Toomre, 2000). Lipid rafts have been implicated in the assembly and release of several families of enveloped viruses including orthomyxoviruses, paramyxoviruses, filoviruses, and retroviruses (Briggs et al., 2003a; Ono and Freed, 2005; Schmitt and Lamb, 2005; Suomalainen, 2002). Multiple lines of evidence suggest that lipid rafts play a critical role in HIV-1 assembly and budding: (1) The HIV-1 lipid bilayer has long been known to be enriched (relative to the host cell plasma membrane) in sphingolipids and cholesterol (Aloia et al., 1993; Brugger et al., 2006); (2) HIV-1 Gag was found to associate with rafts in detergent-resistant membrane (DRM) binding assays

that isolate lipid rafts biochemically based on their insolubility in a number of nonionic detergents (e.g., Triton X-100) at low temperature (Ding et al., 2003; Lindwasser and Resh, 2001; Nguyen and Hildreth, 2000; Ono and Freed, 2001); (3) Gag proteins colocalize or “co-patch” with raft markers (Nguyen and Hildreth, 2000; Ono and Freed, 2001); and (4) Higher-order Gag assembly and particle production of HIV-1 is inhibited by cholesterol depletion (Brugger et al., 2006; Ono et al., 2007; Ono and Freed, 2001). Together, these studies suggest that HIV-1 Gag assembly and budding depend on Gag targeting to lipid rafts, however the mechanism of targeting is unknown. In the current study we demonstrated that HIV-1 Gag targeting to lipid rafts in human cells is regulated as early as Gag mRNA nuclear export. Although both Rev-dependent and Rev-independent HIV-1 Gag could associate with membrane, only Rev-dependent HIV-1 Gag associated with lipid rafts (**Fig. 5-4**). In human cells, the non-raft associated, Rev-independent HIV-1 Gag showed slower assembly kinetics (**Fig. 5-1, panel A**) and lower assembly and budding efficiency (Jin et al., 2007) relative to raft-associated Rev-dependent HIV-1 Gag. Replacing HIV-1 Gag membrane targeting signal with v-Src or EIAV Gag membrane targeting signals restored lipid raft association of Rev-independent HIV-1 Gag (**Fig. 5-4, panel C**) as well as Gag assembly and budding (**Fig. 5-3**). Association with lipid rafts may enhance Gag multimerization and virion assembly and budding, possibly *via* the coalescence of lipid raft microdomains to form an assembly and budding platform. Lipid rafts are most abundant at the plasma membrane, but they can also be found in the biosynthetic and endocytic pathways. Our results clearly demonstrate that Rev-independent HIV-1 Gag associates with membranes, however, the specificity of these membrane fractions remains to be defined, because the membrane flotation assays used in this study could not distinguish plasma membrane and other cellular membrane fractions. Based on our BiFC studies, it is likely that Rev-independent

HIV-1 Gag fails to target plasma membrane. A membrane fractionation assay that is able to separate plasma membrane from other cellular membrane will be needed to define the membrane fractions where Rev-independent HIV-1 Gag is preferentially targeted.

HIV-1 encodes the accessory protein Vpu that regulates virus assembly and budding efficiency (Harila et al., 2006;Neil et al., 2006;Varthakavi et al., 2003). The Rev-independent HIV-1 Gag expression vectors used in this study do not encode Vpu, in contrast to the Rev-dependent Gag expression vectors that also encode Vpu. Thus, the difference in Vpu expression might explain the differences we reported in this and a previous study between Rev-dependent and Rev-independent HIV-1 Gag assembly and budding (Jin et al., 2007). However we think that Vpu expression is unlikely to explain the different Gag trafficking patterns, because not all co-expressed Rev-dependent HIV-1 Gag constructs could rescue Rev-independent HIV-1 Gag assembly and budding (**Fig. 5-2**). It is known that retroviral genomic RNA (gRNA) is associated with proteins to form ribonucleoprotein particles (RNP), and RNP components might regulate gRNA trafficking and subsequent Gag assembly (Cochrane et al., 2006). For example, RNP component hnRNP A2 and Staufen1 have been reported to regulate HIV-1 virus production (Chatel-Chaix et al., 2007;Levesque et al., 2006). Because the panel of Rev-dependent HIV-1 Gag constructs showed differences in their ability to rescue assembly and budding of co-expressed Rev-independent HIV-1 Gag, it is unlikely that the missing gRNA region in Rev-independent HIV-1 Gag expression vectors can cause deficient assembly and budding of Rev-independent HIV-1 Gag.

Our results suggest that HIV MA is the determinant for Rev-independent HIV-1 Gag assembly/budding deficiency in human cells, because replacing HIV MA with EIAV MA rescued Rev-independent HIV-1 Gag assembly and budding; however substitution of EIAV MA

with HIV MA blocked Rev-independent EIAV assembly and budding (**Fig. 5-3**). The primary function of the MA domain in retrovirus assembly is thought to be membrane association. The three-dimensional structure of HIV-1 MA reveals a globular head formed by four  $\alpha$ -helices and a C-terminal  $\alpha$ -helix that projects away from the core domain (Hill et al., 1996; Massiah et al., 1994). The myristic acid that is covalently attached to the N-terminal glycine residue and the highly basic patch formed by conserved positive charged residues clustered on the surface of the MA globular head both contribute to HIV-1 MA dependent membrane binding of Gag precursors (Scarlata and Carter, 2003). The membrane association of the myristoylated Gag is regulated by a so-called “myristoyl switch” mechanism whereby the myristate can adopt either an exposed or a sequestered conformation. Recent structural studies demonstrate specific interactions between myristoylated HIV-1 MA and phosphatidylinositol-(4,5)-bisphosphate [PI(4,5)P2] trigger a change in protein conformation that flips myristate from the sequestered to the exposed conformation, therefore promoting the stable association of MA with the membrane (Saad et al., 2006). Previous *in vivo* functional studies also demonstrate that PI(4,5)P2 plays a key role in Gag targeting to the plasma membrane (Ono et al., 2004). The PI(4,5)P2 induced myristoyl switch might regulate lateral targeting of PI(4,5)P2:Gag complexes to lipid rafts, since PI(4,5)P2 may preferentially associate with lipid rafts (Caroni Pico, 2001; Golub and Caroni, 2005) although this is controversial (McLaughlin and Murray, 2005; van Rheene et al., 2005). Therefore, it is possible that Rev-independent HIV-1 Gag may lack PI(4,5)P2 binding ability, resulting in a loss of membrane selection and/or PI(4,5)P2-mediated myristoyl switching. It is likely that the myristic acid moiety of Rev-independent HIV-1 Gag is exposed rather than in the sequestered conformation, because of its demonstrated ability to associate with membranes, in distinct contrast to myristoylation deficient mutants (**Fig. 5-4, panel A**). However it is possible that

myristic acid exposure is not regulated, resulting in a relatively nonspecific association of the Rev-independent HIV-1 Gag with various cellular membranes. Two Rev-independent HIV-1 Gag mutants containing constitutively exposed myristate (Src $\Delta$ MA and Src<sup>+</sup>) both assembled and budded efficiently in human cells (**Fig. 5-3**).

At this time, we can only speculate as to how RNA export pathways affect the cytosolic fate or function of Gag polyproteins. One possibility is that these pathways expose newly synthesized Gag to distinct cellular factors that mediate the differential membrane targeting observed in the current studies. HIV-1 MA has been shown to recruit cellular factors to regulate Gag trafficking. For example, clathrin adaptor complex AP-3 was found to associate with the N-terminal helix of HIV-1 MA and to direct the intracellular trafficking of HIV-1 Gag (Dong et al., 2005). Recently, AP-1 was reported to facilitate HIV-1 budding through direct binding to HIV-1 MA (Camus et al., 2007). However, it is unlikely that failure to recruit AP-3 or AP-1 accounts for Rev-independent HIV-1 Gag trafficking deficiency, as co-expression with Rev-dependent HIV-1 Gag mutants with a deletion of the MA globular head or with MA replaced by the v-Src myristoylation signal rescued Rev-independent HIV-1 Gag assembly and budding to the same level as wild type Gag, although these two mutants lack the ability to recruit AP-3 and AP-1. It is possible that Rev-independent HIV-1 Gag fails to recruit chaperone proteins like HP68 and HP70 (Dooher and Lingappa, 2004;Gurer et al., 2002;Hong et al., 2001;Zimmerman et al., 2002) or motor proteins, such as kinesin superfamily member 4 (KIF4) (Tang et al., 1999), and therefore fails to target to correct membrane microdomains that support efficient Gag assembly and budding. Further comparative studies will be needed to define the differences in cellular factor recruitment between HIV-1 Gag polyproteins expressed from mRNAs that utilize distinct nuclear export pathways. Results from these studies will help us to better understand how HIV-1

Gag trafficking is regulated at early stages in viral assembly and offer the potential of suggesting novel antiviral therapies targeting this pathway.

## **6.0 OVERALL DISCUSSION AND FUTURE DIRECTIONS**

### **6.1 SUMMARY OF FINDINGS**

Retrovirus assembly and budding is the last step of the viral life cycle. Temporally and spatially regulated interactions between host factors and viral proteins direct this energy dependent multi-step process. The major retroviral structural protein, Gag polyprotein, is synthesized from unspliced viral genomic RNA (gRNA) in the cytoplasm. Thousands copies of Gag polyproteins assemble at specific virus budding sites. Recent advances in retrovirus assembly and budding study suggest that different retroviruses usurp host Vps machinery to stimulate their final release from host cells (Morita and Sundquist, 2004). Studies from our lab and other groups suggest that the integrity and dynamics of host cytoskeleton is critical for retrovirus assembly and budding and that different retroviruses might take alternative trafficking pathways before they converge at the final step by entering the Vps network. Most recent studies also indicate that different gRNA nuclear export pathways lead to differences in Gag assembly and budding. Based on these studies, I hypothesized that retroviruses utilize the host cell cytoskeleton for Gag trafficking, that alternative Gag trafficking pathways might be adapted for assembly and budding of different retroviruses, and that these pathways might be regulated as early as nuclear export of the viral genomic RNA.

To test this hypothesis, I developed the following specific aims: (1) To characterize the Gag-actin interaction sites and the determinants for this interaction; (2) To characterize and compare assembly sites and budding efficiencies of EIAV and HIV-1 Gag; (3) To explore the mechanism by which HIV-1 Gag assembly and budding is regulated by nuclear export pathway taken by viral genomic RNA.

The study in Chapter I demonstrated close and specific interaction between EIAV Gag and cellular actin by newly developed BiFC assays. This interaction was further characterized to be an interaction between Gag multimers and actin filaments by biochemical and imaging approaches. This study for the first time provides definitive evidence that Gag multimers interact with filamentous actin in transfected and infected cells and that specific Gag-actin interactions are positively correlated with the production of progeny virions, suggesting that actin cytoskeleton is utilized for retrovirus assembly and budding.

The study in Chapter I revealed an intracellular assembly pattern for EIAV that is different from that reported for the closely related lentivirus, HIV-1, suggesting that different retroviruses can utilize different assembly and budding pathways. In Chapter II, using BiFC assays developed for these studies, I characterized and compared assembly sites and budding efficiencies of EIAV and HIV-1 Gag in both human and rodent cells. The results demonstrated that replacing the natural RNA nuclear export element (Rev-response element (RRE)) used by HIV-1 and EIAV with the hepatitis B virus (HBV) posttranscriptional regulatory element (PRE) altered HIV-1, but not EIAV, Gag assembly sites and budding efficiency in human cells. In addition, different assembly sites were revealed in human cells for Rev-dependent EIAV and HIV-1 Gag polyproteins. In contrast to the inability of Rev-dependent HIV-1 Gag to assemble and bud in rodent cells, both Rev-dependent and Rev-independent EIAV Gag were able to

assemble and bud efficiently in rodent cells. Taken together, our results suggest that alternative cellular pathways can in fact be adapted for lentiviral Gag assembly and budding.

The study in Chapter II suggests that HIV-1 assembly and budding are regulated by the RNA nuclear export pathway by an unknown mechanism. In Chapter III, mechanistic studies were performed to examine how mRNA export regulates HIV-1 Gag assembly. The results demonstrated slower assembly kinetics of Rev-independent HIV-1 Gag in human cells compared to Rev-dependent HIV-1 Gag and also revealed differences in the respective Gag-Tsg101 recruitment sites. Co-assembly with membrane targeting and multimerization competent Rev-dependent HIV-1 Gag could rescue the release of the Rev-independent Gag. In addition, Rev-independent HIV-1 Gag assembly and budding could also be rescued by plasma membrane targeting signals provided *in cis*. Finally, using a membrane flotation assay, we demonstrated deficient lipid raft association of Rev-independent HIV-1 Gag in human cells and an ability of exogenous membrane targeting signals provided *in cis* to restore lipid raft association of Rev-independent HIV-1 Gag. Taken together, these studies suggest that lipid rafts are critical for HIV-1 Gag assembly and budding and for the first time clearly demonstrate that HIV-1 Gag targeting to lipid rafts is regulated as early as nuclear export of the Gag encoding mRNA.

## 6.2 PUBLIC HEALTH SIGNIFICANCE

Acquired immunodeficiency syndrome (AIDS) is the name given to the end-stage disease caused by infection with HIV. By killing or damaging cells of the body's immune system, HIV progressively destroys the body's ability to fight infections and certain cancers. People diagnosed with AIDS may get life-threatening diseases called opportunistic infections, which are caused by microbes such as viruses or bacteria that usually do not make healthy people sick.

**Table 6-1. Global AIDS epidemic**

	<b>People living with HIV</b>	<b>New infections 2006</b>	<b>AIDS deaths 2006</b>	<b>Adult prevalence %</b>
<b>Sub-Saharan Africa</b>	24.7 million	2.8 million	2.1 million	5.9%
<b>South and South East Asia</b>	7.8 million	860,000	590,000	0.6%
<b>East Asia</b>	750 000	100,000	43,000	0.1%
<b>Latin America</b>	1.7 million	140,000	65,000	0.5%
<b>North America</b>	1.4 million	43,000	18,000	0.8%
<b>Western &amp; Central Europe</b>	740 000	22,000	12,000	0.3%
<b>Eastern Europe &amp; Central Asia</b>	1.7 million	270,000	84,000	0.9%
<b>Middle-East &amp; North Africa</b>	460,000	68,000	36,000	0.2%
<b>Caribbean</b>	250,000	27,000	19,000	1.2%
<b>Oceania</b>	81,000	7,100	4,000	0.4%
<b>Total</b>	<b>39.5 million</b>	<b>4.3 million</b>	<b>2.9 million</b>	<b>1%</b>

AIDS was first reported in the United States in 1981 and has since become a major worldwide epidemic. HIV continues to spread faster than any known persistent infectious agent in the last half century. According to the latest UNAIDS/WHO AIDS Epidemic Update (**Table 6-1**), an estimated 39.5 million people were living with HIV in 2006. There were 4.3 million new infections in 2006 (400 000 more than in 2004) with 2.8 million (65%) of these occurring in sub-Saharan Africa and important increases in Eastern Europe and Central Asia, where there are some indications that infection rates have risen by more than 50% since 2004. In 2006, 2.9 million people died of AIDS-related illnesses. In many regions of the world, new HIV infections are heavily concentrated among young people (15–24 years of age). Among adults 15 years and older, young people accounted for 40% of new HIV infections in 2006. By almost any criteria, HIV qualifies as one of the world's deadliest scourges.

The high rate of viral replication, low fidelity of reverse transcription, and the ability to recombine are the viral characteristics that lead to the diversity of HIV-1 species (quasi-species) in chronically infected individuals. Therefore drug and vaccine developers have to face an ever-changing target. The ability of HIV to mutate and reproduce itself in the presence of antiretroviral drugs is called HIV drug resistance. The consequences of drug resistance include treatment failure, increased direct and indirect health costs associated with the need to start more costly second-line treatment for patients, the spread of resistant strains of HIV and the need to develop new anti-HIV drugs (Simon et al., 2006).

The high genetic variability of HIV provided the rationale for highly active antiretroviral treatments (HAART) – a combination of three antiretrovirals (ARVs) from at least two drug classes. There are three classes of ARVs are currently prescribed. They are nucleoside reverse transcriptase inhibitors (NRTIs), non-nucleoside reverse transcriptase inhibitors (NNRTIs) and

protease inhibitors (PIs). The first two classes are designed to target virus reverse transcriptase, and the third class targets viral protease. Since the advent in 1995 of HAART (Gulick et al., 1997; Hammer et al., 1997; Ho, 1995), a dramatic improvement has been seen in the number of patients attaining undetectable viral loads, improved CD4 counts, and improved survival. However, viral resistance has been described to every antiretroviral drug and therefore poses a serious clinical as well as public-health problem (Simon et al., 2006). Other problems with these agents, such as persistence of viral reservoirs, poor patient compliance due to complicated regimens, and toxic side effects, have emphasized the need for development of new drugs with novel mechanisms of action. Multiple steps in HIV life cycle, including virus entry (Este and Telenti, 2007), integration of proviral DNA (Zeinalipour-Loizidou et al., 2007), virus assembly and budding (Li and Wild, 2005), and the final maturation step (Li et al., 2003) provide novel targets for new ARVs development.

Retrovirus assembly and budding is a multistep process that provides a number of potentially attractive targets for the development of new therapeutic agents. Compounds targeting CA assembly, NC zinc fingers, Tsg101 interaction with p6 are being developed and evaluated (Li and Wild, 2005). The studies described here help to better understand the complicated retrovirus assembly and budding process by elucidating the mechanism by which the virus regulates this last step in its life cycle. This information can be used to develop novel targets for ARIs. For example, the dramatic difference in virus budding efficiency between Rev-dependent and Rev-independent HIV-1 Gag in human cell lines suggests that disturbing viral gRNA trafficking has the potential to inhibit HIV-1 release.

One challenge to the development of an HIV vaccine and anti-HIV drugs is the lack of small animal models due to various defects in HIV replication in rodent cells. Our results

showing that altering HIV-1 Gag encoding mRNA nuclear export pathway from Rev-dependent to Rev-independent pathway overcame a cellular block in virus assembly and budding in rodent cells. In addition, the closely related lentivirus, EIAV, can release from rodent cells no matter which RNA nuclear export pathway is used. Using these viral systems, it is now possible to examine the mechanisms by which different Gag trafficking pathways are regulated in rodent cells, with the goal of developing small animal model for HIV-1 research.

## **6.3 FUTURE DIRECTION**

### **6.3.1 Characterize and compare retroviruses assembly and budding in live cells**

The study in chapter II clearly demonstrated different assembly sites between two lentiviruses, HIV-1 and EIAV. We propose this is due to the different Gag trafficking pathways that should be able to be revealed by live cell imaging.

Most recent studies of HIV-1 assembly and budding indicate that the plasma membrane is the productive site for HIV-1 assembly and budding (Deneka et al., 2007; Finzi et al., 2007; Jouvenet et al., 2006; Welsch et al., 2007). However, different locations have been reported previously for intracellular HIV-1 Gag (Ono and Freed, 2004; Sherer et al., 2003). With the identification of the apparently intracellular membranes from which HIV-1 buds in macrophage as plasma membrane (Deneka et al., 2007; Welsch et al., 2007), it will be interesting to characterize the intracellular membranes where HIV-1 buds in other cell types. One possibility resulting in different HIV-1 Gag distribution patterns in different cell types is the different endocytic properties between different cell types. The difference in the balance between virus budding and endocytosis rates may lead to the difference in viral Gag location at steady state. To study this delicate balance between dynamic processes, state-of-the-art live-cell imaging techniques are needed.

Because EIAV (Jin et al., 2007) and MLV (Sherer et al., 2003) Gag displayed an intracellular distribution pattern in cells whereas HIV-1 Gag showed an exclusively plasma membrane location, it is interesting to compare their trafficking pathways with HIV-1 Gag in

live cells. Results from these live cell imaging studies will better illustrate the complicated retroviruses assembly and budding process, therefore increasing the potential to identify novel targets for antiviral therapeutics.

### **6.3.2 Explore the mechanism by which mRNA nuclear export pathway regulates HIV-1**

#### **Gag lipid rafts targeting**

The study in chapter III clearly demonstrates that Rev-independent HIV-1 Gag is deficient in lipid raft targeting. Results in chapter II demonstrate that Rev-independent HIV-1 Gag is able to bud efficiently from rodent cells where Rev-dependent HIV-1 Gag fails to assemble and bud. It should be interesting to perform similar raft association studies in rodent cells to see if raft targeting is blocked for Rev-dependent HIV-1 Gag in rodent cells. Comparison studies between EIAV and HIV-1 will help to address whether lipid raft targeting is critical for other lentiviruses or only critical for HIV-1 and whether the difference in dependence on lipid rafts association results in the difference in ability to release between HIV-1 and EIAV in rodent cells.

Our studies, for the first time, link viral gRNA trafficking to HIV-1 Gag association with lipid rafts, two previous recognized elements critical for HIV-1 assembly and budding (Ono and Freed, 2001; Swanson et al., 2004). However, there is a big gap that needs to be filled between these two steps. It is possible that different mRNA nuclear export pathways lead to different Gag synthesis sites that result in recruitment of different host factors either by Gag itself or by viral RNA. The different host factors might direct Gag trafficking via different pathways, therefore targeting Gag to different cellular membranes and resulting in different assembly and budding efficiencies. It is worth performing similar comparison studies between Rev-dependent and Rev-independent HIV-1 Gag in HIV-1 natural target cells (T lymphocytes and macrophages) to

confirm the phenotype we reported. Once confirmed, comparison proteomic studies of Rev-dependent and Rev-independent HIV-1 Gag polyproteins and their interacting proteins will help to address what dictates their different fates. In addition, tracking different Gag encoding mRNA trafficking in the same cell by tagging them with MS2 (Haim et al., 2007) and lambdaN22 (Daigle and Ellenberg, 2007) will help to address whether different RNA trafficking results in different Gag synthesis sites.

### **6.3.3 Develop BiFC based antiviral compound screening system**

Viral assembly is the final stage of viral replication, requiring multimerization of viral structural proteins to form mature, infectious virions. Viral structural proteins, normally Gag for retroviruses, and Matrix (M) or Capsid (CA) protein for other enveloped RNA viruses, are the driving force for viral assembly. Viral structure proteins (Gag, M, or CA) mediate formation of a multimeric budding structure through a complex combination of interactions between themselves, between them and other viral components, and between them and cellular proteins. Numerous protein-protein interactions take place during assembly and should provide several targets for novel therapeutics. A relatively subtle perturbation in the efficiency and timing of multimerization can disrupt proper viral assembly and block virus infectivity (Li et al., 2003; Sticht et al., 2005; Stray et al., 2005; Stray et al., 2006; Tang et al., 2003). This is the foundation for two recently described novel inhibitors that disrupt HIV-1 Gag assembly (Sticht et al., 2005; Tang et al., 2003). Unfortunately, few viral assembly inhibitors have been identified to date in any viral system including HIV, in part because a lack in suitable screening methods.

Our results and studies from other lab clearly demonstrated that BiFC assay is a powerful tool to study functional retroviral assembly (Boyko et al., 2006; Jin et al., 2007; Lee et al., 2007b).

This technique was also used to demonstrate assembly of herpes simplex virus glycoprotein gB, gD, gH, and interaction between gD and receptor recently (Avitabile et al., 2007). Together with our results showing interaction between EIAV Gag and cellular actin by BiFC (Chen et al., 2007), we propose that this technique can be used to monitor interactions between viral structural proteins and between viral protein and critical host factors. With its quantitative features, the BiFC based assay provides the potential to screen antiviral compounds targeting viral assembly as well as critical virus-host interfaces, not only for retroviruses but also for other important human viruses.

## BIBLIOGRAPHY

- Accola, M.A., Strack, B., and Gottlinger, H.G. (2000). Efficient Particle Production by Minimal Gag Constructs Which Retain the Carboxy-Terminal Domain of Human Immunodeficiency Virus Type 1 Capsid-p2 and a Late Assembly Domain. *J. Virol.* *74*, 5395-5402.
- Adachi, A., Gendelman, H.E., Koenig, S., Folks, T., Willey, R., Rabson, A., and Martin, M.A. (1986). Production of acquired immunodeficiency syndrome-associated retrovirus in human and nonhuman cells transfected with an infectious molecular clone. *J. Virol.* *59*, 284-291.
- Alfadhli, A., Dhenub, T.C., Still, A., and Barklis, E. (2005). Analysis of Human Immunodeficiency Virus Type 1 Gag Dimerization-Induced Assembly. *J. Virol.* *79*, 14498-14506.
- Aloia, R.C., Tian, H., and Jensen, F.C. (1993). Lipid Composition and Fluidity of the Human Immunodeficiency Virus Envelope and Host Cell Plasma Membranes. *PNAS* *90*, 5181-5185.
- Alroy, I., Tuvia, S., Greener, T., Gordon, D., Barr, H.M., Taglicht, D., Mandil-Levin, R., Ben Avraham, D., Konforty, D., Nir, A., Levius, O., Bicoviski, V., Dori, M., Cohen, S., Yaar, L., Erez, O., Propheta-Meirani, O., Koskas, M., Caspi-Bachar, E., Alchanati, I., Sela-Brown, A., Moskowicz, H., Tessmer, U., Schubert, U., and Reiss, Y. (2005). The trans-Golgi network-associated human ubiquitin-protein ligase POSH is essential for HIV type 1 production. *PNAS* *102*, 1478-1483.
- Amarasinghe, G.K., Zhou, J., Miskimon, M., Chancellor, K.J., McDonald, J.A., Matthews, A.G., Miller, R.R., Rouse, M.D., and Summers, M.F. (2001). Stem-loop SL4 of the HIV-1 [Psi] RNA packaging signal exhibits weak affinity for the nucleocapsid protein. structural studies and implications for genome recognition. *Journal of Molecular Biology* *314*, 961-970.
- Anderie, I. and Schmid, A. (2007). In vivo visualization of actin dynamics and actin interactions by BiFC. *Cell Biology International* *31*, 1131-1135.
- Audoly, G., Popoff, M., and Gluschkof, P. (2005). Involvement of a small GTP binding protein in HIV-1 release. *Retrovirology* *2*, 48.

- Avitabile,E., Forghieri,C., and Campadelli-Fiume,G. (2007). Complexes between herpes simplex virus glycoproteins gD, gB, gH detected in cells by complementation of split enhanced green fluorescence protein. *J. Virol.* [Epub ahead of print]
- Basyuk,E., Galli,T., Mougel,M., Blanchard,J.M., Sitbon,M., and Bertrand,E. (2003). Retroviral genomic RNAs are transported to the plasma membrane by endosomal vesicles. *Dev Cell* 5, 161-174.
- Batonick,M., Favre,M., Boge,M., Spearman,P., Honing,S., and Thali,M. (2005). Interaction of HIV-1 Gag with the clathrin-associated adaptor AP-2. *Virology* 342, 190-200.
- Bennett,R.P., Nelle,T.D., and Wills,J.W. (1993). Functional chimeras of the Rous sarcoma virus and human immunodeficiency virus gag proteins. *J. Virol.* 67, 6487-6498.
- Berthet-Colominas,C., Monaco,S., Novelli,A., Sibai,G., Mallet,F., and Cusack,S. (1999). Head-to-tail dimers and interdomain flexibility revealed by the crystal structure of HIV-1 capsid protein (p24) complexed with a monoclonal antibody Fab. *EMBO J.* 18, 1124-1136.
- Bieniasz,P.D. and Cullen,B.R. (2000). Multiple Blocks to Human Immunodeficiency Virus Type 1 Replication in Rodent Cells. *J. Virol.* 74, 9868-9877.
- Blom J., Nielsen C., and Rhodes J.M. (1993). An ultrastructural study of HIV-infected human dendritic cells and monocytes/macrophages. *APMIS* 101, 672-680.
- Bouamr,F., Melillo,J.A., Wang,M.Q., Nagashima,K., Los Santos,M., Rein,A., and Goff,S.P. (2003). PPPYEPTAP Motif Is the Late Domain of Human T-Cell Leukemia Virus Type 1 Gag and Mediates Its Functional Interaction with Cellular Proteins Nedd4 and Tsg101. *J. Virol.* 77, 11882-11895.
- Boyko,V., Leavitt,M., Gorelick,R., Fu,W., Nikolaitchik,O., Pathak,V.K., Nagashima,K., and Hu,W.S. (2006). Coassembly and Complementation of Gag Proteins from HIV-1 and HIV-2, Two Distinct Human Pathogens. *Molecular Cell* 23, 281-287.
- Briggs,J.A.G., Simon,M.N., Gross,I., Krausslich,H.G., Fuller,S.D., Vogt,V.M., and Johnson,M.C. (2004). The stoichiometry of Gag protein in HIV-1. *Nat Struct Mol Biol* 11, 672-675.
- Briggs,J.A.G., Wilk,T., and Fuller,S.D. (2003a). Do lipid rafts mediate virus assembly and pseudotyping? *Journal of General Virology* 84, 757-768.
- Briggs,J.A.G., Wilk,T., Welker,R., Krausslich,H.G., and Fuller,S.D. (2003b). Structural organization of authentic, mature HIV-1 virions and cores. *EMBO J.* 22, 1707-1715.
- Brugger,B., Glass,B., Haberkant,P., Leibrecht,I., Wieland,F.T., and Krausslich,H.G. (2006). The HIV lipidome: A raft with an unusual composition. *PNAS* 103, 2641-2646.

- Bryant, M. and Ratner, L. (1990). Myristoylation-Dependent Replication and Assembly of Human Immunodeficiency Virus 1. *PNAS* 87, 523-527.
- Bryant, M.L., Heuckeroth, R.O., Kimata, J.T., Ratner, L., and Gordon, J.I. (1989). Replication of Human Immunodeficiency Virus 1 and Moloney Murine Leukemia Virus is Inhibited by Different Heteroatom-Containing Analogs of Myristic Acid. *PNAS* 86, 8655-8659.
- Buckman, J.S., Bosche, W.J., and Gorelick, R.J. (2003). Human Immunodeficiency Virus Type 1 Nucleocapsid Zn<sup>2+</sup> Fingers Are Required for Efficient Reverse Transcription, Initial Integration Processes, and Protection of Newly Synthesized Viral DNA. *J. Virol.* 77, 1469-1480.
- Burniston, M.T., Cimarelli, A., Colgan, J., Curtis, S.P., and Luban, J. (1999). Human Immunodeficiency Virus Type 1 Gag Polyprotein Multimerization Requires the Nucleocapsid Domain and RNA and Is Promoted by the Capsid-Dimer Interface and the Basic Region of Matrix Protein. *J. Virol.* 73, 8527-8540.
- Camus, G., Segura-Morales, C., Molle, D., Lopez-Verges, S., Begon-Pescia, C., Cazevielle, C., Schu, P., Bertrand, E., Berlioz-Torrent, C., and Basyuk, E. (2007). The Clathrin Adaptor Complex AP-1 Binds HIV-1 and MLV Gag and Facilitates Their Budding. *Mol. Biol. Cell* 18, 3193-3203.
- Caroni Pico (2001). New EMBO members' review: actin cytoskeleton regulation through modulation of PI(4,5)P(2) rafts. *EMBO J.* 20, 4332-4336.
- Chatel-Chaix, L., Abrahamyan, L., Frechina, C., Mouland, A.J., and DesGroseillers, L. (2007). The Host Protein Stauf1 Participates in Human Immunodeficiency Virus Type 1 Assembly in Live Cells by Influencing pr55Gag Multimerization. *J. Virol.* 81, 6216-6230.
- Chen, B.K., Rousso, I., Shim, S., and Kim, P.S. (2001a). Efficient assembly of an HIV-1/MLV Gag-chimeric virus in murine cells. *PNAS* 98, 15239-15244.
- Chen, C., Jin, J., Rubin, M., Huang, L., Sturgeon, T., Weixel, K.M., Stolz, D.B., Watkins, S.C., Bamburg, J.R., Weisz, O.A., and Montelaro, R.C. (2007). Association of Gag Multimers with Filamentous Actin during Equine Infectious Anemia Virus Assembly. *Current HIV Research* 5, 315-323.
- Chen, C., Li, F., and Montelaro, R.C. (2001b). Functional Roles of Equine Infectious Anemia Virus Gag p9 in Viral Budding and Infection. *J. Virol.* 75, 9762-9770.
- Chen, C., Vincent, O., Jin, J., Weisz, O.A., and Montelaro, R.C. (2005). Functions of Early (AP-2) and Late (AIP1/ALIX) Endocytic Proteins in Equine Infectious Anemia Virus Budding. *J. Biol. Chem.* 280, 40474-40480.
- Chen, C., Weisz, O.A., Stolz, D.B., Watkins, S.C., and Montelaro, R.C. (2004). Differential Effects of Actin Cytoskeleton Dynamics on Equine Infectious Anemia Virus Particle Production. *J. Virol.* 78, 882-891.

- Chertova,E., Chertov,O., Coren,L.V., Roser,J.D., Trubey,C.M., Bess,J.W., Jr., Sowder,R.C., II, Barsov,E., Hood,B.L., Fisher,R.J., Nagashima,K., Conrads,T.P., Veenstra,T.D., Lifson,J.D., and Ott,D.E. (2006). Proteomic and Biochemical Analysis of Purified Human Immunodeficiency Virus Type 1 Produced from Infected Monocyte-Derived Macrophages. *J. Virol.* *80*, 9039-9052.
- Cochrane,A., McNally,M., and Mouland,A. (2006). The retrovirus RNA trafficking granule: from birth to maturity. *Retrovirology* *3*, 18.
- Coffin,J.M., Hughes,S.H., and Varmus,H.E. (1997). *Retroviruses*. Cold Spring Harbor Laboratory Press.
- Cook,R.F., Leroux,C., Cook,S.J., Berger,S.L., Lichtenstein,D.L., Ghabrial,N.N., Montelaro,R.C., and Issel,C.J. (1998). Development and Characterization of an In Vivo Pathogenic Molecular Clone of Equine Infectious Anemia Virus. *J. Virol.* *72*, 1383-1393.
- Cullen,B.R. (2005). Human immunodeficiency virus: Nuclear RNA export unwound. *Nature* *433*, 26-27.
- Dabiri,G.A., Sanger,J.M., Portnoy,D.A., and Southwick,F.S. (1990). *Listeria Monocytogenes* Moves Rapidly Through the Host-Cell Cytoplasm by Inducing Directional Actin Assembly. *PNAS* *87*, 6068-6072.
- Daigle,N. and Ellenberg,J. (2007). [lambda]N-GFP: an RNA reporter system for live-cell imaging. *Nat Meth* *4*, 633-636.
- Dalton,A.K., Ako-Adjei,D., Murray,P.S., Murray,D., and Vogt,V.M. (2007). Electrostatic Interactions Drive Membrane Association of the Human Immunodeficiency Virus Type 1 Gag MA Domain. *J. Virol.* *81*, 6434-6445.
- Datta,S.A.K., Curtis,J.E., Ratcliff,W., Clark,P.K., Crist,R.M., Lebowitz,J., Krueger,S., and Rein,A. (2007a). Conformation of the HIV-1 Gag Protein in Solution. *Journal of Molecular Biology* *365*, 812-824.
- Datta,S.A.K., Zhao,Z., Clark,P.K., Tarasov,S., Alexandratos,J.N., Campbell,S.J., Kvaratskhelia,M., Lebowitz,J., and Rein,A. (2007b). Interactions between HIV-1 Gag Molecules in Solution: An Inositol Phosphate-mediated Switch. *Journal of Molecular Biology* *365*, 799-811.
- de Virgilio,M., Kiosses,W.B., and Shattil,S.J. (2004). Proximal, selective, and dynamic interactions between integrin  $\alpha$ IIb $\beta$ 3 and protein tyrosine kinases in living cells. *J. Cell Biol.* *165*, 305-311.
- Demidov,V.V., Dokholyan,N.V., Witte-Hoffmann,C., Chalasani,P., Yiu,H.W., Ding,F., Yu,Y., Cantor,C.R., and Broude,N.E. (2006). Fast complementation of split fluorescent protein triggered by DNA hybridization. *PNAS* *103*, 2052-2056.
- Demirov,D.G. and Freed,E.O. (2004). Retrovirus budding. *Virus Research* *106*, 87-102.

- Demirov,D.G., Ono,A., Orenstein,J.M., and Freed,E.O. (2002). Overexpression of the N-terminal domain of TSG101 inhibits HIV-1 budding by blocking late domain function. *PNAS* *99*, 955-960.
- Deneka,M., Pelchen-Matthews,A., Byland,R., Ruiz-Mateos,E., and Marsh,M. (2007). In macrophages, HIV-1 assembles into an intracellular plasma membrane domain containing the tetraspanins CD81, CD9, and CD53. *J. Cell Biol.* *177*, 329-341.
- der Lehr,N., Johansson,S., Wu,S., Bahram,F., Castell,A., Cetinkaya,C., Hydbring,P., Weidung,I., Nakayama,K., Nakayama,K.I., Soderberg,O., Kerppola,T.K., and Larsson,L.G. (2003). The F-Box Protein Skp2 Participates in c-Myc Proteosomal Degradation and Acts as a Cofactor for c-Myc-Regulated Transcription. *Molecular Cell* *11*, 1189-1200.
- Derdowski,A., Ding,L., and Spearman,P. (2004). A Novel Fluorescence Resonance Energy Transfer Assay Demonstrates that the Human Immunodeficiency Virus Type 1 Pr55Gag I Domain Mediates Gag-Gag Interactions. *J. Virol.* *78*, 1230-1242.
- Ding,L., Derdowski,A., Wang,J.J., and Spearman,P. (2003). Independent Segregation of Human Immunodeficiency Virus Type 1 Gag Protein Complexes and Lipid Rafts. *J. Virol.* *77*, 1916-1926.
- Ding,Z., Liang,J., Lu,Y., Yu,Q., Songyang,Z., Lin,S.Y., and Mills,G.B. (2006). A retrovirus-based protein complementation assay screen reveals functional AKT1-binding partners. *PNAS* *103*, 15014-15019.
- Dong,X., Li,H., Derdowski,A., Ding,L., Burnett,A., Chen,X., Peters,T.R., Dermody,T.S., Woodruff,E., Wang,J.J., and Spearman,P. (2005). AP-3 Directs the Intracellular Trafficking of HIV-1 Gag and Plays a Key Role in Particle Assembly. *Cell* *120*, 663-674.
- Doohar,J.E. and Lingappa,J.R. (2004). Conservation of a Stepwise, Energy-Sensitive Pathway Involving HP68 for Assembly of Primate Lentivirus Capsids in Cells. *J. Virol.* *78*, 1645-1656.
- Doohar,J.E., Schneider,B.L., Reed,J.C., and Lingappa,J.R. (2007). Host ABCE1 is at Plasma Membrane HIV Assembly Sites and Its Dissociation from Gag is Linked to Subsequent Events of Virus Production. *Traffic* *8*, 195-211.
- Dramsi,S. and Cossart,P. (1998). INTRACELLULAR PATHOGENS AND THE ACTIN CYTOSKELETON. *Annual Review of Cell and Developmental Biology* *14*, 137-166.
- Edbauer,C. and Naso,R. (1983). Cytoskeleton-associated Pr65gag and retrovirus assembly. *Virology* *130*, 415-426.
- Ehrlich,L.S., Agresta,B.E., and Carter,C.A. (1992). Assembly of recombinant human immunodeficiency virus type 1 capsid protein in vitro. *J. Virol.* *66*, 4874-4883.

- Emans,N., Gorvel,J.P., Walter,C., Gerke,V., Kellner,R., Griffiths,G., and Gruenberg,J. (1993). Annexin II is a major component of fusogenic endosomal vesicles. *J. Cell Biol.* *120*, 1357-1369.
- Este,J.A. and Telenti,A. HIV entry inhibitors. (2007). *The Lancet* *370*, 81-88.
- Fackler,O.T. and Krausslich,H.G. (2006). Interactions of human retroviruses with the host cell cytoskeleton. *Current Opinion in Microbiology* *9*, 409-415.
- Fang,D. and Kerppola,T.K. (2004). Ubiquitin-mediated fluorescence complementation reveals that Jun ubiquitinated by Itch/AIP4 is localized to lysosomes. *PNAS* *101*, 14782-14787.
- Feng,Y.X., Copeland,T.D., Henderson,L.E., Gorelick,R.J., Bosche,W.J., Levin,J.G., and Rein,A. (1996). HIV-1 nucleocapsid protein induces "maturation" of dimeric retroviral RNA in vitro. *PNAS* *93*, 7577-7581.
- Finzi,A., Brunet,A., Xiao,Y., Thibodeau,J., and Cohen,E.A. (2006). Major Histocompatibility Complex Class II Molecules Promote Human Immunodeficiency Virus Type 1 Assembly and Budding to Late Endosomal/Multivesicular Body Compartments. *J. Virol.* *80*, 9789-9797.
- Finzi,A., Orthwein,A., Mercier,J., and Cohen,E.A. (2007). Productive Human Immunodeficiency Virus Type 1 Assembly Takes Place at the Plasma Membrane. *J. Virol.* *81*, 7476-7490.
- Fisher,R.D., Chung,H.Y., Zhai,Q., Robinson,H., Sundquist,W.I., and Hill,C.P. (2007). Structural and Biochemical Studies of ALIX/AIP1 and Its Role in Retrovirus Budding. *Cell* *128*, 841-852.
- Futter,C.E. and White,I.J. (2007). Annexins and Endocytosis. *Traffic* *8*, 951-958.
- Freed,E.O. and Martin,M.A. (1995). Virion incorporation of envelope glycoproteins with long but not short cytoplasmic tails is blocked by specific, single amino acid substitutions in the human immunodeficiency virus type 1 matrix. *J. Virol.* *69*, 1984-1989.
- Freed,E.O. (1998). HIV-1 Gag Proteins: Diverse Functions in the Virus Life Cycle. *Virology* *251*, 1-15.
- Gamble,T.R., Yoo,S., Vajdos,F.F., von Schwedler,U.K., Worthylake,D.K., Wang,H., McCutcheon,J.P., Sundquist,W.I., and Hill,C.P. (1997). Structure of the Carboxyl-Terminal Dimerization Domain of the HIV-1 Capsid Protein. *Science* *278*, 849-853.
- Gamier,L., Wills,J.W., Verderame,M.F., and Sudol,M. (1996). WW domains and retrovirus budding. *Nature* *381*, 744-745.
- Garrus,J.E., von Schwedler,U.K., Pornillos,O.W., Morham,S.G., Zavitz,K.H., Wang,H.E., Wettstein,D.A., Stray,K.M., Cote,M., Rich,R.L., Myszka,D.G., and Sundquist,W.I. (2001). Tsg101 and the Vacuolar Protein Sorting Pathway Are Essential for HIV-1 Budding. *Cell* *107*, 55-65.

- Gitti,R., Lee,B., Walker,J., Summers,M.F., Yoo,S., and Sundquist,W.I. (1996). Structure of the amino-terminal core domain of the HIV-1 capsid protein. *Science* 273, 231-235.
- Golub,T. and Caroni,P. (2005). PI(4,5)P2-dependent microdomain assemblies capture microtubules to promote and control leading edge motility. *J. Cell Biol.* 169, 151-165.
- Gomez,C.Y. and Hope,T.J. (2006). Mobility of Human Immunodeficiency Virus Type 1 Pr55Gag in Living Cells. *J. Virol.* 80, 8796-8806.
- Gottlinger,H.G., Dorfman,T., Cohen,E.A., and Haseltine,W.A. (1993). Vpu Protein of Human Immunodeficiency Virus Type 1 Enhances the Release of Capsids Produced by Gag Gene Constructs of Widely Divergent Retroviruses. *PNAS* 90, 7381-7385.
- Gottlinger,H.G., Sodroski,J.G., and Haseltine,W.A. (1989). Role of Capsid Precursor Processing and Myristoylation in Morphogenesis and Infectivity of Human Immunodeficiency Virus Type 1. *PNAS* 86, 5781-5785.
- Gottwein,E., Bodem,J., Muller,B., Schmechel,A., Zentgraf,H., and Krausslich,H.G. (2003). The Mason-Pfizer Monkey Virus PPPY and PSAP Motifs Both Contribute to Virus Release. *J. Virol.* 77, 9474-9485.
- Grinberg,A.V., Hu,C.D., and Kerppola,T.K. (2004). Visualization of Myc/Max/Mad Family Dimers and the Competition for Dimerization in Living Cells. *Mol. Cell. Biol.* 24, 4294-4308.
- Gross,I., Hohenberg,H., Wilk,T., Grattinger M, Muller,B., Fuller,S.D., and Krausslich,H.G. (2000). A conformational switch controlling HIV-1 morphogenesis. *EMBO J.* 19, 103-113.
- Gulick,R.M., Mellors,J.W., Havlir,D., Eron,J.J., Gonzalez,C., McMahon,D., Richman,D.D., Valentine,F.T., Jonas,L., Meibohm,A., Emini,E.A., Chodakewitz,J.A., Deutsch,P., Holder,D., Schleif,W.A., and Condra,J.H. (1997). Treatment with Indinavir, Zidovudine, and Lamivudine in Adults with Human Immunodeficiency Virus Infection and Prior Antiretroviral Therapy. *N Engl J Med* 337, 734-739.
- Gurer,C., Cimorelli,A., and Luban,J. (2002). Specific Incorporation of Heat Shock Protein 70 Family Members into Primate Lentiviral Virions. *J. Virol.* 76, 4666-4670.
- Haim,L., Zipor,G., Aronov,S., and Gerst,J.E. (2007). A genomic integration method to visualize localization of endogenous mRNAs in living yeast. *Nat Meth* 4, 409-412.
- Hammer,S.M., Squires,K.E., Hughes,M.D., Grimes,J.M., Demeter,L.M., Currier,J.S., Eron,J.J., Feinberg,J.E., Balfour,H.H., Deyton,L.R., Chodakewitz,J.A., Fischl,M.A., Phair,J.P., Pedneault,L., Nguyen,B.Y., Cook,J.C., and The AIDS Clinical Trials Group (1997). A Controlled Trial of Two Nucleoside Analogues plus Indinavir in Persons with Human Immunodeficiency Virus Infection and CD4 Cell Counts of 200 per Cubic Millimeter or Less. *N Engl J Med* 337, 725-733.

- Harila,K., Prior,I., Sjoberg,M., Salminen,A., Hinkula,J., and Suomalainen,M. (2006). Vpu and Tsg101 Regulate Intracellular Targeting of the Human Immunodeficiency Virus Type 1 Core Protein Precursor Pr55gag. *J. Virol.* 80, 3765-3772.
- Harvey,K.F. and Kumar,S. (1999). Nedd4-like proteins: an emerging family of ubiquitin-protein ligases implicated in diverse cellular functions. *Trends in Cell Biology* 9, 166-169.
- Hatanaka,H., Iourin,O., Rao,Z., Fry,E., Kingsman,A., and Stuart,D.I. (2002). Structure of Equine Infectious Anemia Virus Matrix Protein. *J. Virol.* 76, 1876-1883.
- Hatzioannou,T., Martin-Serrano,J., Zang,T., and Bieniasz,P.D. (2005). Matrix-Induced Inhibition of Membrane Binding Contributes to Human Immunodeficiency Virus Type 1 Particle Assembly Defects in Murine Cells. *J. Virol.* 79, 15586-15589.
- Heidecker,G., Lloyd,P.A., Fox,K., Nagashima,K., and Derse,D. (2004). Late Assembly Motifs of Human T-Cell Leukemia Virus Type 1 and Their Relative Roles in Particle Release. *J. Virol.* 78, 6636-6648.
- Hermida-Matsumoto,L. and Resh,M.D. (2000). Localization of Human Immunodeficiency Virus Type 1 Gag and Env at the Plasma Membrane by Confocal Imaging. *J. Virol.* 74, 8670-8679.
- Hill,C.P., Worthylake,D., Bancroft,D.P., Christensen,A.M., and Sundquist,W.I. (1996). Crystal structures of the trimeric human immunodeficiency virus type 1 matrix protein: Implications for membrane association and assembly. *PNAS* 93, 3099-3104.
- Hill,M.K., Shehu-Xhilaga,M., Crowe,S.M., and Mak,J. (2002). Proline Residues within Spacer Peptide p1 Are Important for Human Immunodeficiency Virus Type 1 Infectivity, Protein Processing, and Genomic RNA Dimer Stability. *J. Virol.* 76, 11245-11253.
- Ho,D.D. (1995). Time to Hit HIV, Early and Hard. *N Engl J Med* 333, 450-451.
- Hofmann,W., Reichart,B., Ewald,A., Muller,E., Schmitt,I., Stauber,R.H., Lottspeich,F., Jockusch,B.M., Scheer,U., Hauber,J., and Dabauvalle,M.C. (2001). Cofactor Requirements for Nuclear Export of Rev Response Element (RRE)- and Constitutive Transport Element (CTE)-containing Retroviral RNAs: An Unexpected Role for Actin. *J. Cell Biol.* 152, 895-910.
- Hong,S., Choi,G., Park,S., Chung,A.S., Hunter,E., and Rhee,S.S. (2001). Type D Retrovirus Gag Polyprotein Interacts with the Cytosolic Chaperonin TRiC. *J. Virol.* 75, 2526-2534.
- Hu,C.D., Chinenov,Y., and Kerppola,T.K. (2002). Visualization of Interactions among bZIP and Rel Family Proteins in Living Cells Using Bimolecular Fluorescence Complementation. *Molecular Cell* 9, 789-798.
- Hu,C.D. and Kerppola,T.K. (2003). Simultaneous visualization of multiple protein interactions in living cells using multicolor fluorescence complementation analysis. *Nat Biotech* 21, 539-545.

- Huang, M., Orenstein, J.M., Martin, M.A., and Freed, E.O. (1995). p6Gag is required for particle production from full-length human immunodeficiency virus type 1 molecular clones expressing protease. *J. Virol.* 69, 6810-6818.
- Hurley, J.H. and Emr, S.D. (2006). THE ESCRT COMPLEXES: Structure and Mechanism of a Membrane-Trafficking Network. *Annual Review of Biophysics and Biomolecular Structure* 35, 277-298.
- Hynes, T.R., Mervine, S.M., Yost, E.A., Sabo, J.L., and Berlot, C.H. (2004a). Live Cell Imaging of Gs and the  $\beta$ 2-Adrenergic Receptor Demonstrates That Both  $\alpha$ s and  $\beta$ 1  $\gamma$ 7 Internalize upon Stimulation and Exhibit Similar Trafficking Patterns That Differ from That of the  $\beta$ 2-Adrenergic Receptor. *J. Biol. Chem.* 279, 44101-44112.
- Hynes, T.R., Tang, L., Mervine, S.M., Sabo, J.L., Yost, E.A., Devreotes, P.N., and Berlot, C.H. (2004b). Visualization of G Protein  $\beta$   $\gamma$  Dimers Using Bimolecular Fluorescence Complementation Demonstrates Roles for Both  $\beta$  and  $\gamma$  in Subcellular Targeting. *J. Biol. Chem.* 279, 30279-30286.
- Iyengar, S., Hildreth, J.E.K., and Schwartz, D.H. (1998). Actin-Dependent Receptor Colocalization Required for Human Immunodeficiency Virus Entry into Host Cells. *J. Virol.* 72, 5251-5255.
- Jager, S., Gottwein, E., and Krausslich, H.G. (2007). Ubiquitination of Human Immunodeficiency Virus Type 1 Gag Is Highly Dependent on Gag Membrane Association. *J. Virol.* 81, 9193-9201.
- Jares-Erijman, E.A. and Jovin, T.M. (2003). FRET imaging. *Nat Biotech* 21, 1387-1395.
- Jares-Erijman, E.A. and Jovin, T.M. (2006). Imaging molecular interactions in living cells by FRET microscopy. *Current Opinion in Chemical Biology* 10, 409-416.
- Jimenez-Baranda, S., Gomez-Mouton, C., Rojas, A., Martinez-Prats, L., Mira, E., Ana Lacalle, R., Valencia, A., Dimitrov, D.S., Viola, A., Delgado, R., Martinez, A., and Manes, S. (2007). Filamin-A regulates actin-dependent clustering of HIV receptors. *Nat Cell Biol* 9, 838-846.
- Jin, J., Sturgeon, T., Chen, C., Watkins, S.C., Weisz, O.A., and Montelaro, R.C. (2007). Distinct intracellular trafficking of EIAV and HIV-1 gag during viral assembly and budding revealed by bimolecular fluorescence complementation assays. *J. Virol.* 81, 11226-35.
- Johnson, M.C., Scobie, H.M., Ma, Y.M., and Vogt, V.M. (2002). Nucleic Acid-Independent Retrovirus Assembly Can Be Driven by Dimerization. *J. Virol.* 76, 11177-11185.
- Johnsson, N. and Varshavsky, A. (1994). Split Ubiquitin as a Sensor of Protein Interactions In vivo. *PNAS* 91, 10340-10344.

- Jolly,C., Kashefi,K., Hollinshead,M., and Sattentau,Q.J. (2004). HIV-1 Cell to Cell Transfer across an Env-induced, Actin-dependent Synapse. *J. Exp. Med.* 199, 283-293.
- Jolly,C., Mitar,I., and Sattentau,Q.J. (2007). Requirement for an Intact T-Cell Actin and Tubulin Cytoskeleton for Efficient Assembly and Spread of Human Immunodeficiency Virus Type 1. *J. Virol.* 81, 5547-5560.
- Jouvenet,N., Neil,S.J.D., Bess,C., Johnson,M.C., Virgen,C.A., Simon,S.M., and Bieniasz,P.D. (2006). Plasma Membrane Is the Site of Productive HIV-1 Particle Assembly. *PLoS Biology* 4, e435.
- Katzmann,D.J., Odorizzi,G., and Emr,S.D. (2002). RECEPTOR DOWNREGULATION AND MULTIVESICULAR-BODY SORTING. *Nat Rev Mol Cell Biol* 3, 893-905.
- Kerppola,T.K. (2006). Visualization of molecular interactions by fluorescence complementation. *Nat Rev Mol Cell Biol* 7, 449-456.
- Khorchid,A., Halwani,R., Wainberg,M.A., and Kleiman,L. (2002). Role of RNA in Facilitating Gag/Gag-Pol Interaction. *J. Virol.* 76, 4131-4137.
- Kikonyogo,A., Bouamr,F., Vana,M.L., Xiang,Y., Aiyar,A., Carter,C., and Leis,J. (2001). Proteins related to the Nedd4 family of ubiquitin protein ligases interact with the L domain of Rous sarcoma virus and are required for gag budding from cells. *PNAS* 98, 11199-11204.
- Kim,W., Tang,Y., Okada,Y., Torrey,T.A., Chattopadhyay,S.K., Pfliederer,M., Falkner,F.G., Dorner,F., Choi,W., Hirokawa,N., and Morse,H.C., III (1998). Binding of Murine Leukemia Virus Gag Polyproteins to KIF4, a Microtubule-Based Motor Protein. *J. Virol.* 72, 6898-6901.
- Klimkait,T., Strebel,K., Hoggan,M.D., Martin,M.A., and Orenstein,J.M. (1990). The human immunodeficiency virus type 1-specific protein vpu is required for efficient virus maturation and release. *J. Virol.* 64, 621-629.
- Komano,J., Miyauchi,K., Matsuda,Z., and Yamamoto,N. (2004). Inhibiting the Arp2/3 Complex Limits Infection of Both Intracellular Mature Vaccinia Virus and Primate Lentiviruses. *Mol. Biol. Cell* 15, 5197-5207.
- Krausslich,H.G., Facke,M., Heuser,A.M., Konvalinka,J., and Zentgraf,H. (1995). The spacer peptide between human immunodeficiency virus capsid and nucleocapsid proteins is essential for ordered assembly and viral infectivity. *J. Virol.* 69, 3407-3419.
- Kusumi,A., Koyama-Honda,I., and Suzuki,K. (2004). Molecular Dynamics and Interactions for Creation of Stimulation-Induced Stabilized Rafts from Small Unstable Steady-State Rafts. *Traffic* 5, 213-230.
- Lakadamyali,M., Rust,M.J., Babcock,H.P., and Zhuang,X. (2003). Visualizing infection of individual influenza viruses. *PNAS* 100, 9280-9285.

- Larson,L., Arnaudeau,S., Gibson,B., Li,W., Krause,R., Hao,B., Bamburg,J.R., Lew,D.P., Demaurex,N., and Southwick,F. (2005). Gelsolin mediates calcium-dependent disassembly of *Listeria* actin tails. *PNAS* 102, 1921-1926.
- Le Blanc,I., Prevost,M.C., Dokhlar,M.C., and Rosenberg,A.R. (2002). The PPPY Motif of Human T-Cell Leukemia Virus Type 1 Gag Protein Is Required Early in the Budding Process. *J. Virol.* 76, 10024-10029.
- Lee,E. and De Camilli,P. (2002). From the Cover: Dynamin at actin tails. *PNAS* 99, 161-166.
- Lee,S., Joshi,A., Nagashima,K., Freed,E.O., and Hurley,J.H. (2007a). Structural basis for viral late-domain binding to Alix. *Nat Struct Mol Biol* 14, 194-199.
- Lee,S.K., Boyko,V., and Hu,W.S. (2007b). Capsid is an important determinant for functional complementation of murine leukemia virus and spleen necrosis virus Gag proteins. *Virology* 360, 388-397.
- Lee,Y.M., Liu,B., and Yu,X.F. (1999). Formation of Virus Assembly Intermediate Complexes in the Cytoplasm by Wild-Type and Assembly-Defective Mutant Human Immunodeficiency Virus Type 1 and Their Association with Membranes. *J. Virol.* 73, 5654-5662.
- Lee,Y.M. and Yu,X.F. (1998). Identification and Characterization of Virus Assembly Intermediate Complexes in HIV-1-Infected CD4+T Cells. *Virology* 243, 78-93.
- Lehmann,M.J., Sherer,N.M., Marks,C.B., Pypaert,M., and Mothes,W. (2005). Actin- and myosin-driven movement of viruses along filopodia precedes their entry into cells. *J. Cell Biol.* 170, 317-325.
- Leung,J., Yueh,A., Appah,F.J., Yuan B, de los Santos,K., and Goff,S. (2006). Interaction of Moloney murine leukemia virus matrix protein with IQGAP. *EMBO J.* 25, 2155-2166.
- Levesque,K., Halvorsen,M., Abrahamyan,L., Chatel-Chaix,L., Poupon,V., Gordon,H., DesGroseillers,L., Gatignol,A., and Mouland,A.J. (2006). Trafficking of HIV-1 RNA is Mediated by Heterogeneous Nuclear Ribonucleoprotein A2 Expression and Impacts on Viral Assembly. *Traffic* 7, 1177-1193.
- Li,F., Goila-Gaur,R., Salzwedel,K., Kilgore,N.R., Reddick,M., Matallana,C., Castillo,A., Zoumplis,D., Martin,D.E., Orenstein,J.M., Allaway,G.P., Freed,E.O., and Wild,C.T. (2003). PA-457: A potent HIV inhibitor that disrupts core condensation by targeting a late step in Gag processing. *PNAS* 100, 13555-13560.
- Li,F. and Wild,C.T. (2005). HIV-1 assembly and budding as targets for drug discovery. *Curr. Opin. Investig. Drugs.* 6, 148-154.
- Li,F., Chen,C., Puffer,B.A., and Montelaro,R.C. (2002). Functional Replacement and Positional Dependence of Homologous and Heterologous L Domains in Equine Infectious Anemia Virus Replication. *J. Virol.* 76, 1569-1577.

- Li,F., Zoumplis,D., Matallana,C., Kilgore,N.R., Reddick,M., Yunus,A.S., Adamson,C.S., Salzwedel,K., Martin,D.E., Allaway,G.P., Freed,E.O., and Wild,C.T. Determinants of activity of the HIV-1 maturation inhibitor PA-457. *Virology* 356, 217-224.
- Lindwasser,O.W. and Resh,M.D. (2001). Multimerization of Human Immunodeficiency Virus Type 1 Gag Promotes Its Localization to Barges, Raft-Like Membrane Microdomains. *J. Virol.* 75, 7913-7924.
- Lindwasser,O.W. and Resh,M.D. (2002). Myristoylation as a target for inhibiting HIV assembly: Unsaturated fatty acids block viral budding. *PNAS* 99, 13037-13042.
- Liu,B., Dai,R., Tian,C.J., Dawson,L., Gorelick,R., and Yu,X.F. (1999). Interaction of the Human Immunodeficiency Virus Type 1 Nucleocapsid with Actin. *J. Virol.* 73, 2901-2908.
- Magliery,T.J., Wilson,C.G.M., Pan,W., Mishler,D., Ghosh,I., Hamilton,A.D., and Regan,L. (2005). Detecting Protein-Protein Interactions with a Green Fluorescent Protein Fragment Reassembly Trap: Scope and Mechanism. *J. Am. Chem. Soc.* 127, 146-157.
- Maldarelli,F., King,N.J., and Yagi,M. (1987). Effects of cytoskeleton disrupting agents on mouse mammary tumor virus replication. *Virus Research* 7, 281-295.
- Mann,R., Mulligan,R.C., and Baltimore,D. (1983). Construction of a retrovirus packaging mutant and its use to produce helper-free defective retrovirus. *Cell* 33, 153-159.
- Mariani,R., Rutter,G., Harris,M.E., Hope,T.J., Krausslich,H.G., and Landau,N.R. (2000). A Block to Human Immunodeficiency Virus Type 1 Assembly in Murine Cells. *J. Virol.* 74, 3859-3870.
- Martin-Serrano,J., Yarovoy,A., Perez-Caballero,D., and Bieniasz,P.D. (2003a). Divergent retroviral late-budding domains recruit vacuolar protein sorting factors by using alternative adaptor proteins. *PNAS* 100, 12414-12419.
- Martin-Serrano,J., Zang,T., and Bieniasz,P.D. (2003b). Role of ESCRT-I in Retroviral Budding. *J. Virol.* 77, 4794-4804.
- Massiah,M.A., Starich,M.R., Paschall,C., Summers,M.F., Christensen,A.M., and Sundquist,W.I. (1994). Three-dimensional Structure of the Human Immunodeficiency Virus Type 1 Matrix Protein. *Journal of Molecular Biology* 244, 198-223.
- Mayo,K., Huseby,D., McDermott,J., Arvidson,B., Finlay,L., and Barklis,E. (2003). Retrovirus Capsid Protein Assembly Arrangements. *Journal of Molecular Biology* 325, 225-237.
- McDonald,D., Wu,L., Bohks,S.M., KewalRamani,V.N., Unutmaz,D., and Hope,T.J. (2003). Recruitment of HIV and Its Receptors to Dendritic Cell-T Cell Junctions. *Science* 300, 1295-1297.
- McLaughlin,S. and Murray,D. (2005). Plasma membrane phosphoinositide organization by protein electrostatics. *Nature* 438, 605-611.

- Merrifield,C.J. (2004). Seeing is believing: imaging actin dynamics at single sites of endocytosis. *Trends in Cell Biology* 14, 352-358.
- Merz,A.J. and Higgs,H.N. (2003). Listeria Motility: Biophysics Pushes Things Forward. *Current Biology* 13, R302-R304.
- Miller,J.P., Lo,R.S., Ben Hur,A., Desmarais,C., Stagljar,I., Noble,W.S., and Fields,S. (2005). Large-scale identification of yeast integral membrane protein interactions. *PNAS* 102, 12123-12128.
- Miyawaki,A. (2003). Visualization of the Spatial and Temporal Dynamics of Intracellular Signaling. *Developmental Cell* 4, 295-305.
- Momany,C., Kovari,L., Prongay,A., Keller,W., Gitti,R., Lee,B., Gorbalenya,A., Tong,L., McClure,J., Ehrlich,L.S., Summers,M.F., Carter,C.A., and Rossmann,M. (1996). Crystal structure of dimeric HIV-1 capsid protein. *Nat Struct Biol* 3, 763-770.
- Morita,E. and Sundquist,W.I. (2004). RETROVIRUS BUDDING. *Annual Review of Cell and Developmental Biology* 20, 395-425.
- Mortara,R. and Koch,G. (1986). Analysis of pseudopodial structure and assembly with viral projections. *J Cell Sci Suppl* 5, 129-144.
- Mukhopadhyay,D. and Riezman,H. (2007). Proteasome-Independent Functions of Ubiquitin in Endocytosis and Signaling. *Science* 315, 201-205.
- Munshi,U.M., Kim,J., Nagashima,K., Hurley,J.H., and Freed,E.O. (2007). An Alix Fragment Potently Inhibits HIV-1 Budding: CHARACTERIZATION OF BINDING TO RETROVIRAL YPXL LATE DOMAINS. *J. Biol. Chem.* 282, 3847-3855.
- Muriaux,D., De Rocquigny,H., Roques,B.P., and Paoletti,J. (1996). NCp7 Activates HIV-1Lai RNA Dimerization by Converting a Transient Loop-Loop Complex into a Stable Dimer. *J. Biol. Chem.* 271, 33686-33692.
- Muriaux,D., Mirro,J., Harvin,D., and Rein,A. (2001). RNA is a structural element in retrovirus particles. *PNAS* 98, 5246-5251.
- Muriaux,D., Mirro,J., Nagashima,K., Harvin,D., and Rein,A. (2002). Murine Leukemia Virus Nucleocapsid Mutant Particles Lacking Viral RNA Encapsidate Ribosomes. *J. Virol.* 76, 11405-11413.
- Nasioulas,G., Hughes,S.H., Felber,B.K., and Whitcomb,J.M. (1995). Production of Avian Leukosis Virus Particles in Mammalian Cells Can be Mediated by the Interaction of the Human Immunodeficiency Virus Protein Rev and the Rev-Responsive Element. *PNAS* 92, 11940-11944.

- Neil,S.J.D., Eastman,S.W., Jouvenet,N., and Bieniasz,P.D. (2006). HIV-1 Vpu Promotes Release and Prevents Endocytosis of Nascent Retrovirus Particles from the Plasma Membrane. *PLoS Pathogens* 2, e39.
- Newman,J.L., Butcher,E.W., Patel,D.T., Mikhaylenko,Y., and Summers,M.F. (2004). Flexibility in the P2 domain of the HIV-1 Gag polyprotein. *Protein Sci* 13, 2101-2107.
- Nguyen,D.G., Booth,A., Gould,S.J., and Hildreth,J.E.K. (2003). Evidence That HIV Budding in Primary Macrophages Occurs through the Exosome Release Pathway. *J. Biol. Chem.* 278, 52347-52354.
- Nguyen,D.H. and Hildreth,J.E.K. (2000). Evidence for Budding of Human Immunodeficiency Virus Type 1 Selectively from Glycolipid-Enriched Membrane Lipid Rafts. *J. Virol.* 74, 3264-3272.
- Niu,T.K., Pfeifer,A.C., Lippincott-Schwartz,J., and Jackson,C.L. (2005). Dynamics of GBF1, a Brefeldin A-Sensitive Arf1 Exchange Factor at the Golgi. *Mol. Biol. Cell* 16, 1213-1222.
- Nydegger,S., Foti,M., Derdowski,A., Spearman,P., and Thali,M. (2003). HIV-1 Egress is Gated Through Late Endosomal Membranes. *Traffic* 4, 902-910.
- Nyfeler,B., Michnick,S.W., and Hauri,H.P. (2005). Capturing protein interactions in the secretory pathway of living cells. *PNAS* 102, 6350-6355.
- Ono,A., Ablan,S.D., Lockett,S.J., Nagashima,K., and Freed,E.O. (2004). Phosphatidylinositol (4,5) bisphosphate regulates HIV-1 Gag targeting to the plasma membrane. *PNAS* 101, 14889-14894.
- Ono,A. and Freed,E.O. (1999). Binding of Human Immunodeficiency Virus Type 1 Gag to Membrane: Role of the Matrix Amino Terminus. *J. Virol.* 73, 4136-4144.
- Ono,A. and Freed,E.O. (2001). Plasma membrane rafts play a critical role in HIV-1 assembly and release. *PNAS* 98, 13925-13930.
- Ono,A. and Freed,E.O. (2004). Cell-Type-Dependent Targeting of Human Immunodeficiency Virus Type 1 Assembly to the Plasma Membrane and the Multivesicular Body. *J. Virol.* 78, 1552-1563.
- Ono,A. and Freed,E.O. (2005). Role of Lipid Rafts in Virus Replication. In *Advances in Virus Research. Virus Structure and Assembly*, R.Polly, ed. Academic Press), pp. 311-358.
- Ono,A., Waheed,A.A., and Freed,E.O. (2007). Depletion of cellular cholesterol inhibits membrane binding and higher-order multimerization of human immunodeficiency virus type 1 Gag. *Virology* 360, 27-35.
- Otero,G.C., Harris,M.E., Donello,J.E., and Hope,T.J. (1998). Leptomycin B Inhibits Equine Infectious Anemia Virus Rev and Feline Immunodeficiency Virus Rev Function but Not

- the Function of the Hepatitis B Virus Posttranscriptional Regulatory Element. *J. Virol.* 72, 7593-7597.
- Ott,D.E., Coren,L.V., Kane,B.P., Busch,L.K., Johnson,D.G., Sowder,R.C., Chertova,E.N., Arthur,L.O., and Henderson,L.E. (1996). Cytoskeletal proteins inside human immunodeficiency virus type 1 virions. *J. Virol.* 70, 7734-7743.
- Ott,D.E., Coren,L.V., Copeland,T.D., Kane,B.P., Johnson,D.G., Sowder,R.C., II, Yoshinaka,Y., Oroszlan,S., Arthur,L.O., and Henderson,L.E. (1998). Ubiquitin Is Covalently Attached to the p6Gag Proteins of Human Immunodeficiency Virus Type 1 and Simian Immunodeficiency Virus and to the p12Gag Protein of Moloney Murine Leukemia Virus. *J. Virol.* 72, 2962-2968.
- Ott,D.E., Coren,L.V., Johnson,D.G., Kane,B.P., Sowder,R.C., Kim,Y.D., Fisher,R.J., Zhou,X.Z., Lu,K.P., and Henderson,L.E. (2000). Actin-Binding Cellular Proteins inside Human Immunodeficiency Virus Type 1. *Virology* 266, 42-51.
- Ott,D. (2002). Potential roles of cellular proteins in HIV-1. *Rev Med Virol* 12, 359-374.
- Owens,R.J., Dubay,J.W., Hunter,E., and Compans,R.W. (1991). Human Immunodeficiency Virus Envelope Protein Determines the Site of Virus Release in Polarized Epithelial Cells. *PNAS* 88, 3987-3991.
- Pan,S., Wang,R., Zhou,X., He,G., Koomen,J., Kobayashi,R., Sun,L., Corvera,J., Gallick,G.E., and Kuang,J. (2006). Involvement of the Conserved Adaptor Protein Alix in Actin Cytoskeleton Assembly. *J. Biol. Chem.* 281, 34640-34650.
- Parent,L.J., Bennett,R.P., Craven,R.C., Nelle,T.D., Krishna,N.K., Bowzard,J.B., Wilson,C.B., Puffer,B.A., Montelaro,R.C., and Wills,J.W. (1995). Positionally independent and exchangeable late budding functions of the Rous sarcoma virus and human immunodeficiency virus Gag proteins. *J. Virol.* 69, 5455-5460.
- Patnaik,A., Chau,V., Li,F., Montelaro,R.C., and Wills,J.W. (2002). Budding of Equine Infectious Anemia Virus Is Insensitive to Proteasome Inhibitors. *J. Virol.* 76, 2641-2647.
- Patnaik,A., Chau,V., and Wills,J.W. (2000). Ubiquitin is part of the retrovirus budding machinery. *PNAS* 97, 13069-13074.
- Pelchen-Matthews,A., Kramer,B., and Marsh,M. (2003). Infectious HIV-1 assembles in late endosomes in primary macrophages. *J. Cell Biol.* 162, 443-455.
- Pelletier,J.N., Campbell-Valois,F.X., and Michnick,S.W. (1998). Oligomerization domain-directed reassembly of active dihydrofolate reductase from rationally designed fragments. *PNAS* 95, 12141-12146.
- Perez-Caballero,D., Hatzioannou,T., Martin-Serrano,J., and Bieniasz,P.D. (2004). Human Immunodeficiency Virus Type 1 Matrix Inhibits and Confers Cooperativity on Gag Precursor-Membrane Interactions. *J. Virol.* 78, 9560-9563.

- Perlman, M. and Resh, M.D. (2006). Identification of an Intracellular Trafficking and Assembly Pathway for HIV-1 Gag. *Traffic* 7, 731-745.
- Pettit, S.C., Moody, M.D., Wehbie, R.S., Kaplan, A.H., Nantermet, P.V., Klein, C.A., and Swanstrom, R. (1994). The p2 domain of human immunodeficiency virus type 1 Gag regulates sequential proteolytic processing and is required to produce fully infectious virions. *J. Virol.* 68, 8017-8027.
- Pietschmann, T., Heinkelein, M., Heldmann, M., Zentgraf, H., Rethwilm, A., and Lindemann, D. (1999). Foamy Virus Capsids Require the Cognate Envelope Protein for Particle Export. *J. Virol.* 73, 2613-2621.
- Pontow, S.E., Heyden, N.V., Wei, S., and Ratner, L. (2004). Actin Cytoskeletal Reorganizations and Coreceptor-Mediated Activation of Rac during Human Immunodeficiency Virus-Induced Cell Fusion. *J. Virol.* 78, 7138-7147.
- Poole, E., Strappe, P., Mok, H., Hicks, R., and Lever, A. (2005). HIV-1 Gag-RNA Interaction Occurs at a Perinuclear/Centrosomal Site; Analysis by Confocal Microscopy and FRET. *Traffic* 6, 741-755.
- Pope, B.J., Gooch, J.T., and Weeds, A.G. (1997). Probing the Effects of Calcium on Gelsolin. *Biochemistry* 36, 15848-15855.
- Pornillos, O., Alam, S.L., Davis, D.R., and Sundquist, W.I. (2002). Structure of the Tsg101 UEV domain in complex with the PTAP motif of the HIV-1 p6 protein. *Nat Struct Mol Biol* 9, 812-817.
- Provitera, P., Bouamr, F., Murray, D., Carter, C., and Scarlata, S. (2000). Binding of equine infectious anemia virus matrix protein to membrane bilayers involves multiple interactions. *Journal of Molecular Biology* 296, 887-898.
- Puffer, B.A., Parent, L.J., Wills, J.W., and Montelaro, R.C. (1997). Equine infectious anemia virus utilizes a YXXL motif within the late assembly domain of the Gag p9 protein. *J. Virol.* 71, 6541-6546.
- Puffer, B.A., Watkins, S.C., and Montelaro, R.C. (1998). Equine Infectious Anemia Virus Gag Polyprotein Late Domain Specifically Recruits Cellular AP-2 Adapter Protein Complexes during Virion Assembly. *J. Virol.* 72, 10218-10221.
- Putterman, D., Pepinsky, R., and Vogt, V.M. (1990). Ubiquitin in avian leukosis virus particles. *Virology* 176, 633-637.
- Rackham, O. and Brown, C. (2004). Visualization of RNA-protein interactions in living cells: FMRP and IMP1 interact on mRNAs. *EMBO J.* 23, 3355.
- Rajaram, N. and Kerppola, T.K. (2004). Synergistic Transcription Activation by Maf and Sox and Their Subnuclear Localization Are Disrupted by a Mutation in Maf That Causes Cataract. *Mol. Cell. Biol.* 24, 5694-5709.

- Raposo,G., Moore,M., Innes,D., Leijendekker,R., Leigh-Brown,A., Benaroch,P., and Geuze,H. (2002). Human Macrophages Accumulate HIV-1 Particles in MHC II Compartments. *Traffic* 3, 718-729.
- Raymond,C.K., Howald-Stevenson,I., Vater,C.A., and Stevens,T.H. (1992). Morphological classification of the yeast vacuolar protein sorting mutants: evidence for a prevacuolar compartment in class E vps mutants. *Mol. Biol. Cell* 3, 1389-1402.
- Reil H, Bukovsky AA, Gelderblom HR, and Gottlinger,H. (1998). Efficient HIV-1 replication can occur in the absence of the viral matrix protein. *EMBO J.* 17, 2699-2708.
- Rein,A., Henderson,L.E., and Levin,J.G. (1998). Nucleic-acid-chaperone activity of retroviral nucleocapsid proteins: significance for viral replication. *Trends in Biochemical Sciences* 23, 297-301.
- Remy,I. and Michnick,S.W. (2004a). A cDNA library functional screening strategy based on fluorescent protein complementation assays to identify novel components of signaling pathways. *Methods* 32, 381-388.
- Remy,I. and Michnick,S.W. (2004b). Regulation of Apoptosis by the Ft1 Protein, a New Modulator of Protein Kinase B/Akt. *Mol. Cell. Biol.* 24, 1493-1504.
- Remy,I., Montmarquette,A., and Michnick,S.W. (2004). PKB/Akt modulates TGF- $\beta$  signalling through a direct interaction with Smad3. *Nat Cell Biol* 6, 358-365.
- Rey,O.S.V.A., Canon,J.U.D.E., and Krogstad,P.A.U.L. (1996). HIV-1 Gag Protein Associates with F-actin Present in Microfilaments. *Virology* 220, 530-534.
- Roberts,M.M. and Oroszlan,S. (1989). The preparation and biochemical characterization of intact capsids of equine infectious anemia virus. *Biochemical and Biophysical Research Communications* 160, 486-494.
- Rossi,F., Charlton,C.A., and Blau,H.M. (1997). Monitoring protein-protein interactions in intact eukaryotic cells by beta-galactosidase complementation. *PNAS* 94, 8405-8410.
- Rudner,L., Nydegger,S., Coren,L.V., Nagashima,K., Thali,M., and Ott,D.E. (2005). Dynamic Fluorescent Imaging of Human Immunodeficiency Virus Type 1 Gag in Live Cells by Biarsenical Labeling. *J. Virol.* 79, 4055-4065.
- Ryzhova,E.V., Vos,R.M., Albright,A.V., Harrist,A.V., Harvey,T., and Gonzalez-Scarano,F. (2006). Annexin 2: a Novel Human Immunodeficiency Virus Type 1 Gag Binding Protein Involved in Replication in Monocyte-Derived Macrophages. *J. Virol.* 80, 2694-2704.
- Saad,J.S., Miller,J., Tai,J., Kim,A., Ghanam,R.H., and Summers,M.F. (2006). From the Cover: Structural basis for targeting HIV-1 Gag proteins to the plasma membrane for virus assembly. *PNAS* 103, 11364-11369.

- Sandefur,S., Smith,R.M., Varthakavi,V., and Spearman,P. (2000). Mapping and Characterization of the N-Terminal I Domain of Human Immunodeficiency Virus Type 1 Pr55Gag. *J. Virol.* 74, 7238-7249.
- Sandrin,V. and Cosset,F.L. (2005). Intracellular vs. cell surface assembly of retroviral pseudotypes is determined by the cellular localization of the viral glycoprotein, its capacity to interact with Gag and the expression of the Nef protein. *J. Biol. Chem.* M506070200.
- Sasaki,H., Nakamura,M., Ohno,T., Matsuda,Y., Yuda,Y., and Nonomura,Y. (1995). Myosin-Actin Interaction Plays an Important Role in Human Immunodeficiency Virus Type 1 Release From Host Cells. *PNAS* 92, 2026-2030.
- Sasaki,H., Ozaki,H., Karaki,H., and Nonomura,Y. (2004). Actin filaments play an essential role for transport of nascent HIV-1 proteins in host cells. *Biochem Biophys Res Commun* 316, 588-593.
- Scarлата,S. and Carter,C. (2003). Role of HIV-1 Gag domains in viral assembly. *Biochimica et Biophysica Acta (BBA) - Biomembranes* 1614, 62-72.
- Schmitt,A.P. and Lamb,R.A. (2005). Influenza Virus Assembly and Budding at the Viral Budozone. In *Advances in Virus Research (Virus Structure and Assembly, R.Polly, ed. Academic Press)*, pp. 383-416.
- Schubert,U., Ott,D.E., Chertova,E.N., Welker,R., Tessmer,U., Princiotta,M.F., Bennink,J.R., Krausslich,H.G., and Yewdell,J.W. (2000). Proteasome inhibition interferes with Gag polyprotein processing, release, and maturation of HIV-1 and HIV-2. *PNAS* 97, 13057-13062.
- Sfakianos,J.N. and Hunter,E. (2003). M-PMV Capsid Transport Is Mediated by Env/Gag Interactions at the Pericentriolar Recycling Endosome. *Traffic* 4, 671-680.
- Sfakianos,J.N., LaCasse,R.A., and Hunter,E. (2003). The M-PMV Cytoplasmic Targeting-Retention Signal Directs Nascent Gag Polypeptides to a Pericentriolar Region of the Cell. *Traffic* 4, 660-670.
- Shaner,N.C., Steinbach,P.A., and Tsien,R.Y. (2005). A guide to choosing fluorescent proteins. *Nat Meth* 2, 905-909.
- Shehu-Xhilaga,M., Ablan,S., Demirov,D.G., Chen,C., Montelaro,R.C., and Freed,E.O. (2004). Late Domain-Dependent Inhibition of Equine Infectious Anemia Virus Budding. *J. Virol.* 78, 724-732.
- Sherer,N.M., Lehmann,M.J., Jimenez-Soto,L.F., Ingmundson,A., Horner,S.M., Cicchetti,G., Allen,P.G., Pypaert,M., Cunningham,J.M., and Mothes,W. (2003). Visualization of Retroviral Replication in Living Cells Reveals Budding into Multivesicular Bodies. *Traffic* 4, 785-801.

- Shyu, Y.J., Liu, H., Deng, X., and Hu, C.D. (2006). Identification of new fluorescent protein fragments for bimolecular fluorescence complementation analysis under physiological conditions. *Biotechniques* 40, 61-66.
- Simon, V., Ho, D.D., and Abdool Karim, Q. (2006). HIV/AIDS epidemiology, pathogenesis, prevention, and treatment. *The Lancet* 368, 489-504.
- Simons, K. and Toomre, D. (2000). Lipid rafts and signal transduction. *Nat Rev Mol Cell Biol* 1, 31-39.
- Simons, K. and Vaz, W.L.C. (2004). MODEL SYSTEMS, LIPID RAFTS, AND CELL MEMBRANES1. *Annual Review of Biophysics and Biomolecular Structure* 33, 269-295.
- Sodeik, B. (2000). Mechanisms of viral transport in the cytoplasm. *Trends in Microbiology* 8, 465-472.
- Spearman, P., Horton, R., Ratner, L., and Kuli-Zade, I. (1997). Membrane binding of human immunodeficiency virus type 1 matrix protein in vivo supports a conformational myristyl switch mechanism. *J. Virol.* 71, 6582-6592.
- Spearman, P., Wang, J.J., Vander Heyden, N., and Ratner, L. (1994). Identification of human immunodeficiency virus type 1 Gag protein domains essential to membrane binding and particle assembly. *J. Virol.* 68, 3232-3242.
- Stains, C.I., Porter, J.R., Ooi, A.T., Segal, D.J., and Ghosh, I. (2005). DNA Sequence-Enabled Reassembly of the Green Fluorescent Protein. *J. Am. Chem. Soc.* 127, 10782-10783.
- Stanke, N., Stange, A., Luftenegger, D., Zentgraf, H., and Lindemann, D. (2005). Ubiquitination of the Prototype Foamy Virus Envelope Glycoprotein Leader Peptide Regulates Subviral Particle Release. *J. Virol.* 79, 15074-15083.
- Sticht, J., Humbert, M., Findlow, S., Bodem, J., Muller, B., Dietrich, U., Werner, J., and Krausslich, H.G. (2005). A peptide inhibitor of HIV-1 assembly in vitro. *Nat Struct Mol Biol* 12, 671-677.
- Strack, B., Calistri, A., Craig, S., Popova, E., and Gottlinger, H.G. (2003). AIP1/ALIX Is a Binding Partner for HIV-1 p6 and EIAV p9 Functioning in Virus Budding. *Cell* 114, 689-699.
- Strack, B., Calistri, A., and Gottlinger, H.G. (2002). Late Assembly Domain Function Can Exhibit Context Dependence and Involves Ubiquitin Residues Implicated in Endocytosis. *J. Virol.* 76, 5472-5479.
- Stray, S.J., Bourne, C.R., Punna, S., Lewis, W.G., Finn, M.G., and Zlotnick, A. (2005). A heteroaryldihydropyrimidine activates and can misdirect hepatitis B virus capsid assembly. *PNAS* 102, 8138-8143.

- Stray,S.J., Johnson,J.M., Kopek,B.G., and Zlotnick,A. (2006). An in vitro fluorescence screen to identify antivirals that disrupt hepatitis B virus capsid assembly. *Nat Biotech* 24, 358-362.
- Suomalainen,M. (2002). Lipid Rafts and Assembly of Enveloped Viruses. *Traffic* 3, 705-709.
- Swanson,C.M. and Malim,M.H. (2006). Retrovirus RNA Trafficking: From Chromatin to Invasive Genomes. *Traffic* 7, 1440-1450.
- Swanson,C.M., Puffer,B.A., Ahmad,K.M., Doms,R.W., and Malim,M.H. (2004). Retroviral mRNA nuclear export elements regulate protein function and virion assembly. *EMBO J.* 23, 2632-2640.
- Takahashi,K.i., Baba,S., Koyanagi,Y., Yamamoto,N., Takaku,H., and Kawai,G. (2001). Two Basic Regions of NCp7 Are Sufficient for Conformational Conversion of HIV-1 Dimerization Initiation Site from Kissing-loop Dimer to Extended-duplex Dimer. *J. Biol. Chem.* 276, 31274-31278.
- Tang,C., Loeliger,E., Kinde,I., Kyere,S., Mayo,K., Barklis,E., Sun,Y., Huang,M., and Summers,M.F. (2003). Antiviral Inhibition of the HIV-1 Capsid Protein. *Journal of Molecular Biology* 327, 1013-1020.
- Tang,C., Loeliger,E., Luncsford,P., Kinde,I., Beckett,D., and Summers,M.F. (2004). From the Cover: Entropic switch regulates myristate exposure in the HIV-1 matrix protein. *PNAS* 101, 517-522.
- Tang,C., Ndassa,Y., and Summers,M.F. (2002). Structure of the N-terminal 283-residue fragment of the immature HIV-1 Gag polyprotein. *Nat Struct Mol Biol* 9, 537-543.
- Tang,Y., Winkler,U., Freed,E.O., Torrey,T.A., Kim,W., Li,H., Goff,S.P., and Morse,H.C., III (1999). Cellular Motor Protein KIF-4 Associates with Retroviral Gag. *J. Virol.* 73, 10508-10513.
- Tanzi,G.O., Piefer,A.J., and Bates,P. (2003). Equine Infectious Anemia Virus Utilizes Host Vesicular Protein Sorting Machinery during Particle Release. *J. Virol.* 77, 8440-8447.
- Tritel,M. and Resh,M.D. (2000). Kinetic Analysis of Human Immunodeficiency Virus Type 1 Assembly Reveals the Presence of Sequential Intermediates. *J. Virol.* 74, 5845-5855.
- Tritel,M. and Resh,M.D. (2001). The Late Stage of Human Immunodeficiency Virus Type 1 Assembly Is an Energy-Dependent Process. *J. Virol.* 75, 5473-5481.
- Ullmann,A., Perrin,D., Jacob,F., and Monod,J. (1996). Identification, by in vitro complementation and purification, of a peptide fraction of Escherichia coli beta-galactosidase. *Journal of Molecular Biology* 12, 918-923.
- Vale,R.D. (2003). The Molecular Motor Toolbox for Intracellular Transport. *Cell* 112, 467-480.

- Vallee,H. and Carre,H. (1904). Sur la nature infectieuse de l'anemie du cheval. C. R. Hebd. Seances Acad. Sci. Ser. D Sci. Nat. 139, 333.
- van Rheene,J., Achame,E., Janssen,H., Calafat,J., and Jalink K (2005). PIP2 signaling in lipid domains: a critical re-evaluation. *EMBO J.* 24, 1664-1673.
- Varthakavi,V., Smith,R.M., Bour,S.P., Strebel,K., and Spearman,P. (2003). Viral protein U counteracts a human host cell restriction that inhibits HIV-1 particle production. *PNAS* 100, 15154-15159.
- VerPlank,L., Bouamr,F., LaGrassa,T.J., Agresta,B., Kikonyogo,A., Leis,J., and Carter,C.A. (2001). Tsg101, a homologue of ubiquitin-conjugating (E2) enzymes, binds the L domain in HIV type 1 Pr55Gag. *PNAS* 98, 7724-7729.
- Vogt,V.M. (2000). Ubiquitin in retrovirus assembly: Actor or bystander? *PNAS* 97, 12945-12947.
- von Schwedler,U.K., Stuchell,M., Muller,B., Ward,D.M., Chung,H.Y., Morita,E., Wang,H.E., Davis,T., He,G.P., Cimborra,D.M., Scott,A., Krausslich,H.G., Kaplan,J., Morham,S.G., and Sundquist,W.I. (2003). The Protein Network of HIV Budding. *Cell* 114, 701-713.
- Welsch,S., Habermann,A., Jager,S., Muller,B., Krijnse-Locker,J., and Krausslich,H.G. (2006). Ultrastructural Analysis of ESCRT Proteins Suggests a Role for Endosome-Associated Tubular-Vesicular Membranes in ESCRT Function. *Traffic* 7, 1551-1566.
- Welsch,S., Keppler,O.T., Habermann,A., Allespach,I., Krijnse-Locker,J., and Krausslich,H.G. (2007). HIV-1 Buds Predominantly at the Plasma Membrane of Primary Human Macrophages. *PLoS Pathogens* 3, e36.
- Wieggers,K., Rutter,G., Kottler,H., Tessmer,U., Hohenberg,H., and Krausslich,H.G. (1998). Sequential Steps in Human Immunodeficiency Virus Particle Maturation Revealed by Alterations of Individual Gag Polyprotein Cleavage Sites. *J. Virol.* 72, 2846-2854.
- Wolffe,E.J., Katz,E., Weisberg,A., and Moss,B. (1997). The A34R glycoprotein gene is required for induction of specialized actin-containing microvilli and efficient cell-to-cell transmission of vaccinia virus. *J. Virol.* 71, 3904-3915.
- Xiang,Y., Cameron,C.E., Wills,J.W., and Leis,J. (1996). Fine mapping and characterization of the Rous sarcoma virus Pr76gag late assembly domain. *J. Virol.* 70, 5695-5700.
- Yasuda,J. and Hunter,E. (1998). A Proline-Rich Motif (PPPY) in the Gag Polyprotein of Mason-Pfizer Monkey Virus Plays a Maturation-Independent Role in Virion Release. *J. Virol.* 72, 4095-4103.
- Yasuda,J., Hunter,E., Nakao,M., and Shida,H. (2002). Functional involvement of a novel Nedd4-like ubiquitin. *EMBO reports* 3, 636-640.

- Yuan,B., Li,X., and Goff,S. (1999). Mutations altering the moloney murine leukemia virus p12 Gag protein affect virion production and early events of the virus life cycle. *EMBO J.* 18, 4700-4710.
- Zang,W.Q. and Benedict Yen,T.S. (1999). Distinct Export Pathway Utilized by the Hepatitis B Virus Posttranscriptional Regulatory Element. *Virology* 259, 299-304.
- Zeinalipour-Loizidou,E., Nicolaou,C., Nicolaidis,A., and Kostrikis,L. (2007). HIV-1 integrase: from biology to chemotherapeutics. *Current HIV Research* 5, 365-388.
- Zhang,J., Campbell,R.E., Ting,A.Y., and Tsien,R.Y. (2002). Creating new fluorescent probes for cell biology. *Nat Rev Mol Cell Biol* 3, 906-918.
- Zhou,W., Parent,L.J., Wills,J.W., and Resh,M.D. (1994). Identification of a membrane-binding domain within the amino-terminal region of human immunodeficiency virus type 1 Gag protein which interacts with acidic phospholipids. *J. Virol.* 68, 2556-2569.
- Zhou,W. and Resh,M.D. (1996). Differential membrane binding of the human immunodeficiency virus type 1 matrix protein. *J. Virol.* 70, 8540-8548.
- Zimmerman,C., Klein,K.C., Kiser,P.K., Singh,A.R., Firestein,B.L., Riba,S.C., and Lingappa,J.R. (2002). Identification of a host protein essential for assembly of immature HIV-1 capsids. *Nature* 415, 88-92.